



## **Appendix A.1**

### **CASTOR V/21 CASK**

#### **GENERAL DESCRIPTION**

The GNSI CASTOR V/21 cask is a thick-walled nodular cast iron cylinder that is approximately 4.9 meters high (192.4 in.), 2.40 meters (94.5 in.) in diameter with fins, and weighs (empty) 92.3 metric tons (101.8 tons). The side wall thickness without fins is about 379 mm (14.9 in.). The cask has a cylindrical cask cavity which holds a fuel basket which is designed to accommodate 21 PWR fuel assemblies. The loaded weight of the cask is about 106 metric tons (116.9 tons).

The cask is sealed with two lids installed one on top of the other. Both lids are sealed with multiple seals consisting of metal seals and elastomer o-rings. The primary lid is constructed of stainless steel. The overall thickness is 290 mm (11.4 in.). The secondary lid is also made of stainless steel. The overall thickness is 90 mm (3.5 in.). The lids are fastened to the body with bolts.

For neutron shielding, two concentric rows of axial holes in the wall of the cask body are filled with polyethylene rods. The bottom and the secondary cover each have a slab of the same material inserted for the same purpose. The cast iron wall of the cask provides gamma radiation shielding.

In the area of the fuel assemblies, the body has cooling fins on the outside. Four trunnions are bolted on, two at the head end and two at the bottom end of the body.

#### **A.1/3.1.1 Materials to be Stored**

The structural evaluations of the CASTOR V/21 are provided in Chapters 4 and 8 of the Topical Report. These evaluations used a fuel assembly weight of 1442 lb, but the possible combinations of Surry Units 1 and 2 fuel assemblies containing a burnable poison rod assembly (BPRA) or thimble plugging device (TPD) could weigh up to 1525 lb. An evaluation has been performed by GNSI to evaluate the effect of the increased weight of the fuel assembly from 1442 lb to 1525 lb. This evaluation concluded that the calculated stresses at all locations in the cask and basket were less than the allowable stresses. At one location, credit was taken in the evaluation for the actual basket temperature.

An evaluation has also been performed on the effect to the cask surface dose rates as a result of placing BPRAs or TPDs in the fuel stored in the CASTOR V/21. This evaluation confirmed that the calculated surface dose rates for the CASTOR V/21 remained less than the design basis dose rates used to calculate doses at the ISFSI perimeter and to the nearest resident.

An evaluation has been performed on the effect on criticality control from the storage of BPRAs or TPDs in the fuel stored in the CASTOR V/21. BPRA rods will displace water (a

moderator) in the fuel assembly thimble tubes, therefore, even the use of depleted BPRAs will reduce reactivity in a cask. TPDs are short and do not displace water in the thimble tubes, therefore, their use will not affect reactivity.

The CASTOR V/21 is designed for a maximum internal pressure under accident conditions, and helium buildup or pre-pressurization in BPRAs will affect this analysis. The confinement analysis for the CASTOR V/21 has been reanalyzed for twenty-one 20-finger BPRAs, and this reanalysis shows that the maximum pressure under accident conditions would be 3.4 bars absolute, when the design basis for this cask is 8 bars absolute. The impact of TPDs on the confinement analysis is bounded by the impact of BPRAs.

To account for the additional decay heat from BPRAs and TPDs, fuel assembly decay heat estimates must include an estimate for the decay heat from the actual component in each fuel assembly. Therefore, the combined decay heat from the fuel assembly and its component must be less than the limit for a fuel assembly in the CASTOR V/21.

Based on these evaluations, the storage of fuel assemblies with BPRAs or TPDs is acceptable for the CASTOR V/21.

#### **A.1/7.3.2.1 Cask Surface Dose Rates**

The assumptions used in calculating the GNSI CASTOR V/21 cask surface dose rates and energy spectra are provided in Sections 3.3.5 and 7.3.2.2 of the GNSI Topical Report (Reference 1). This analysis was performed using these same assumptions except that the values for fuel enrichment and burnup were increased to 3.7 weight percent  $U^{235}$  and 40,000 MWD/MTU, respectively.

Neutron and gamma source terms for the stored spent fuel were generated using OREST (ORIGEN II). Typical results from these runs are shown in Surry ISFSI SAR Tables 7.2-1, 7.2-2, 7.2-3, and 7.2-4. ANISN (Reference 4) and DOT (Reference 10) were used by GNSI to calculate the cask surface fluxes. Flux-to-dose rate conversion factors, as shown in Tables 7.2-2 and 7.2-3 of the *GNSI CASTOR V/21 Topical Report* (Reference 1), were then used to obtain the surface dose rates for the cask. The GNSI cask average surface dose rates for 5-year-old fuel are 9.5 mrem/hour neutron and 27.8 mrem/hour gamma for the side and 29.7 mrem/hour neutron and 0.7 mrem/hour gamma for the top. When these dose rates are combined, the side and top average surface dose rates are 37.3 mrem/hour and 30.4 mrem/hour, respectively. These dose rates are bounded by the total average surface dose rates of 224 mrem/hour for the side and 76 mrem/hour for the top reported in the Surry ISFSI SAR, Section 7.3.2.1.

Figure A.1/7.3-2 shows the normalized surface dose rates on the GNSI CASTOR V/21 cask versus age of spent fuel for both gamma and neutron radiation.

### A.1/7.3.2.2 Dose Rate Versus Distance

The cask surface dose rates discussed in Section A.1/7.3.2.1 result in the dose rates at various distances as shown on Figures A.1/7.3-7a through A.1/7.3-10. The neutron transport results shown on these figures were generated using a series of adjoint (References 2 & 3) ANISN (Reference 4) runs. These calculations were performed with a BUGLE-80 (Reference 5) cross-section set for an infinite-air medium. As explained in References 2 and 3, the adjoint method is the preferred analytical technique when more than one set of sources must be evaluated at a given detector location for a response of interest. For the adjoint analyses reported here, the adjoint source is the flux-to-dose conversion factor reported in Reference 9. Four separate ANISN analyses were performed at distances of 50, 460, 1500, and 2460 meters. The resulting adjoint fluxes are presented in Tables A.1/7.3-3 and A.1/7.3-4. These adjoint fluxes were then folded with the cask surface leakage spectra supplied by GNSI over the area of the cask's top and side, respectively. Cask surface neutron leakage data are provided in Table A.1/7.3-2. (The 84-group structure in the GNSI cask's leakage spectrum for the side of the cask was collapsed to the 47-group BUGLE structure prior to folding the data.)

The resultant neutron dose rates were then used to construct the dose rate versus distance curves presented on Figures A.1/7.3-7a, A.1/7.3-8a and A.1/7.3-9a.

For the gamma-ray transport, simple point kernel calculations using infinite medium dose rate buildup factors in dry air were performed. Using a point source model and References 6 and 7, air-to-void correction factors were developed and applied to the gamma dose rates in void based on Reference 8. The gamma dose rates for the casks are shown on Figures A.1/7.3-7b, A.1/7.3-8b and A.1/7.3-9b.

For Figure A.1/7.3-10, decay factors have been used assuming that four casks are placed in the ISFSI each year for 21 years and each new group of four casks has a minimum of 5 years decay of the fuel. As shown on Figure A.1/7.3-10, the design basis dose rate for the ISFSI bounds the dose rate for the ISFSI filled to capacity with 84 GNSI CASTOR V/21 casks.

### A.1/7.3.5 References

1. *Topical Safety Analysis Report for the GNSI CASTOR X Cask for an Independent Spent Fuel Storage Installation (Dry Storage)*, General Nuclear Systems, Inc., June 1988.
2. V. R. Cain, *The Use of Discrete Ordinates Adjoint Calculations*, A Review of the Discrete Ordinates 5 Method for Radiation Transport Calculations, ORNL-RSIC-19, March 1968, pp. 85-94.
3. G. I. Bell, S. Glasstone, *Nuclear Reactor Theory*, Chapter 6.1 - *The Adjoint Function and Its Applications*, Van Nostrand Reinhold Company, New York, 1970.
4. W. W. Engle, Jr., *A User's Manual for ANISN, A One-Dimensional Discrete Ordinates Transport Code with Anisotropic Scattering*, K-1643, Union Carbide Corporation, Nuclear Division, June 1973.

5. *BUGLE-80, Coupled 47-Neutron, 20-Gamma-Ray, P3, Cross-Section Library for LWR Shielding Calculations*, DLC-75, R. W. Roussin, ORNL, June 1980.
6. Warkentin, J. K., *Polynomial Coefficients for Dose Buildup in Air*, Radiation Research Associates, Inc., August 15, 1975, RRA-N7511.
7. Hubbell, L. H., *Photon Cross-Sections, Attenuation Coefficients, and Energy Absorption Coefficients from 10 KeV to 100 GeV*, National Bureau of Standards, August 1969, NSRDS-NBS29.
8. Spacetrans II, *Dose Calculations at Detectors at Various Distances from the Surface of a Cylinder*, Neutron Physics Division of Oak Ridge National Laboratory, September 1973, ORNL-TM-2592.
9. ANSI/ANS-6.1.1-1977, *American National Standard - Neutron and Gamma Ray Flux to Dose Rate Factors*, American Nuclear Society, March 17, 1977.
10. Mynatt, F. R., Rhodes, W. A., et al., *The DOT-II Two Dimensional Discrete Ordinates Transport Code*, ORNL-TM-4280.
11. [Deleted]

Table A.1/7.3-2 (SHEET 1 OF 2)  
 CASTOR V/21 CASK SURFACE NEUTRON LEAKAGES

| Neutron Group | Upper <sup>a</sup> Energy (ev) | Cask Surface<br>Leakage Spectra<br>(n/cm <sup>2</sup> - sec) |          |
|---------------|--------------------------------|--|----------|
|               |                                | Side   | Top      |
| 1             | 1.7E+07                        | 1.10E-03   | 1.49E-04 |
| 2             | 1.4E+07                        | 3.06E-03   | 4.14E-04 |
| 3             | 1.2E+07                        | 1.55E-02   | 1.86E-03 |
| 4             | 1.0E+07                        | 2.67E-02   | 2.79E-03 |
| 5             | 8.6E+06                        | 3.80E-02   | 3.56E-03 |
| 6             | 7.4E+06                        | 7.11E-02   | 6.76E-03 |
| 7             | 6.1E+06                        | 1.17E-01   | 1.18E-02 |
| 8             | 5.0E+06                        | 2.68E-01   | 3.37E-02 |
| 9             | 3.7E+06                        | 2.21E-01   | 3.31E-02 |
| 10            | 3.0E+06                        | 2.44E-01   | 4.70E-02 |
| 11            | 2.7E+06                        | 2.26E-01   | 4.53E-02 |
| 12            | 2.5E+06                        | 1.35E-01   | 2.69E-02 |
| 13            | 2.4E+06                        | 3.00E-02   | 5.99E-03 |
| 14            | 2.3E+06                        | 2.95E-01   | 7.25E-02 |
| 15            | 2.2E+06                        | 7.63E+01   | 1.87E-01 |
| 16            | 1.9E+06                        | 1.67E+00   | 6.22E-01 |
| 17            | 1.6E+06                        | 2.43E+00   | 9.47E-01 |
| 18            | 1.4E+06                        | 6.90E+00   | 9.40E+00 |
| 19            | 1.0E+06                        | 8.07E+00   | 1.41E+01 |
| 20            | 8.2E+05                        | 3.51E+00   | 6.13E+00 |
| 21            | 7.4E+05                        | 6.09E+00   | 1.06E+01 |
| 22            | 6.1E+05                        | 1.31E+01   | 5.44E+02 |
| 23            | 5.0E+05                        | 2.59E+01   | 1.24E+02 |
| 24            | 3.7E+05                        | 1.46E+01   | 6.90E+01 |
| 25            | 3.0E+05                        | 2.30E+01   | 1.09E+02 |
| 26            | 1.8E+05                        | 1.46E+01   | 6.90E+01 |
| 27            | 1.1E+05                        | 2.28E+01   | 6.76E+01 |
| 28            | 6.7E+04                        | 1.39E+01   | 4.11E+01 |
| 29            | 5.0E+04                        | 4.76E+00   | 1.41E+01 |
| 30            | 3.2E+04                        | 2.98E+00   | 8.83E+00 |
| 31            | 2.6E+04                        | 9.90E-01   | 2.94E+00 |
| 32            | 2.4E+04                        | 1.21E+00   | 3.56E+00 |
| 33            | 2.2E+04                        | 3.60E+00   | 1.07E+01 |
| 34            | 1.5E+04                        | 4.13E+00   | 1.22E+01 |

Table A.1/7.3-2 (SHEET 2 OF 2)  
 CASTOR V/21 CASK SURFACE NEUTRON LEAKAGES

| Neutron Group | Upper <sup>a</sup> Energy (ev) | Cask Surface<br>Leakage Spectra<br>(n/cm <sup>2</sup> - sec) |          |
|---------------|--------------------------------|--|----------|
|               |                                | Side   | Top      |
| 35            | 7.1E+03                        | 1.96E+00   | 5.80E+00 |
| 36            | 3.4E+03                        | 7.76E+00   | 1.77E+01 |
| 37            | 1.6E+03                        | 6.96E+00   | 1.50E+01 |
| 38            | 4.5E+02                        | 4.71E+00   | 9.05E+00 |
| 39            | 2.1E+02                        | 2.25E+00   | 4.32E+00 |
| 40            | 1.0E+02                        | 6.87E+00   | 9.47E+00 |
| 41            | 3.7E+01                        | 5.84E+00   | 7.87E+00 |
| 42            | 1.1E+01                        | 3.97E+00   | 4.21E+00 |
| 43            | 5.0E+00                        | 3.46E+00   | 3.14E+00 |
| 44            | 1.8E+00                        | 1.81E+00   | 1.34E+00 |
| 45            | 8.8E-01                        | 1.19E+00   | 7.33E-01 |
| 46            | 4.1E-01                        | 3.01E-01   | 1.36E-01 |
| 47            | 1.0E-01                        | 8.63E-02   | 3.91E-02 |

Note: CASTOR V/21 Cask Surface Area: 400,000 cm<sup>2</sup> (side),  
 47,000 cm<sup>2</sup> (top).

a. Reference 5.

Table A.1/7.3-3 (SHEET 1 OF 2)  
 SIDE OF GNSI CASTOR V/21 CASK ADJOINT FLUXES<sup>a</sup>  
 FOR A SOURCE OF 1 n/sec PER GROUP

| Neutron Group | SIDE OF CASK<br>(rem/hr per n/sec) |            |             |             |
|---------------|------------------------------------|------------|-------------|-------------|
|               | 50 Meters                          | 460 Meters | 1500 Meters | 2460 Meters |
| 1             | 1.0E-12                            | 6.8E-15    | 1.1E-17     | 4.7E-20     |
| 2             | 9.6E-13                            | 6.4E-15    | 1.1E-17     | 4.4E-20     |
| 3             | 8.4E-13                            | 6.4E-15    | 1.2E-17     | 5.2E-20     |
| 4             | 8.0E-13                            | 6.9E-15    | 1.4E-17     | 6.4E-20     |
| 5             | 8.1E-13                            | 6.8E-15    | 1.2E-17     | 5.0E-20     |
| 6             | 8.1E-13                            | 6.7E-15    | 1.2E-17     | 4.7E-20     |
| 7             | 8.6E-13                            | 6.2E-15    | 8.3E-18     | 2.2E-20     |
| 8             | 8.2E-13                            | 5.5E-15    | 4.8E-18     | 7.2E-21     |
| 9             | 8.0E-13                            | 6.3E-15    | 4.3E-18     | 5.4E-21     |
| 10            | 7.9E-13                            | 6.9E-15    | 4.6E-18     | 6.0E-21     |
| 11            | 7.8E-13                            | 7.3E-15    | 4.4E-18     | 5.4E-21     |
| 12            | 7.9E-13                            | 7.4E-15    | 4.0E-18     | 4.4E-21     |
| 13            | 7.9E-13                            | 7.4E-15    | 3.9E-18     | 4.2E-21     |
| 14            | 7.9E-13                            | 6.9E-15    | 2.6E-18     | 1.7E-21     |
| 15            | 8.1E-13                            | 6.5E-15    | 1.6E-18     | 6.9E-22     |
| 16            | 8.5E-13                            | 5.4E-15    | 6.2E-19     | 9.7E-23     |
| 17            | 8.5E-13                            | 4.7E-15    | 3.9E-19     | 4.7E-23     |
| 18            | 8.6E-13                            | 4.0E-15    | 2.3E-19     | 2.3E-23     |
| 19            | 7.7E-13                            | 2.9E-15    | 1.1E-19     | 7.4E-24     |
| 20            | 7.1E-13                            | 2.3E-15    | 4.3E-20     | 1.4E-24     |
| 21            | 6.4E-13                            | 1.7E-15    | 2.2E-20     | 4.9E-25     |
| 22            | 5.9E-13                            | 1.3E-15    | 8.9E-21     | 1.2E-25     |
| 23            | 5.0E-13                            | 7.7E-16    | 1.3E-21     | 1.7E-27     |
| 24            | 3.9E-13                            | 6.3E-16    | 8.1E-22     | 9.1E-28     |
| 25            | 3.1E-13                            | 5.2E-16    | 4.8E-22     | 4.5E-28     |
| 26            | 2.0E13                             | 3.2E-16    | 7.6E-23     | 1.3E-29     |
| 27            | 1.4E-13                            | 2.2E-16    | 1.2E-23     | 3.2E-31     |
| 28            | 9.8E-14                            | 1.6E-16    | 2.4E-24     | 1.1E-32     |
| 29            | 7.4E-14                            | 1.3E-16    | 6.8E-25     | 1.0E-33     |
| 30            | 6.5E-14                            | 1.1E-16    | 4.6E-25     | 6.0E-34     |
| 31            | 6.1E-14                            | 1.0E-16    | 3.6E-25     | 4.4E-34     |
| 32            | 5.9E-14                            | 1.0E-16    | 3.3E-25     | 3.9E-34     |
| 33            | 5.6E-14                            | 9.3E-17    | 2.7E-25     | 3.0E-34     |
| 34            | 5.1E-14                            | 7.9E-17    | 1.6E-25     | 1.6E-34     |
| 35            | 5.2E-14                            | 5.6E-17    | 5.0E-26     | 2.9E-35     |

Table A.1/7.3-3 (SHEET 2 OF 2)  
 SIDE OF GNSI CASTOR V/21 CASK ADJOINT FLUXES<sup>a</sup>  
 FOR A SOURCE OF 1 n/sec PER GROUP

| Neutron Group | SIDE OF CASK<br>(rem/hr per n/sec) |            |             |             |
|---------------|------------------------------------|------------|-------------|-------------|
|               | 50 Meters                          | 460 Meters | 1500 Meters | 2460 Meters |
| 36            | 5.4E-14                            | 3.8E-17    | 1.5E-26     | 6.1E-36     |
| 37            | 5.5E-14                            | 2.7E-17    | 6.4E-27     | 2.3E-36     |
| 38            | 5.6E-14                            | 1.4E-17    | 4.1E-28     | 0.0E+00     |
| 39            | 5.5E-14                            | 8.8E-18    | 1.5E-28     | 0.0E+00     |
| 40            | 5.4E-14                            | 5.7E-18    | 6.0E-29     | 0.0E+00     |
| 41            | 5.2E-14                            | 2.8E-18    | 1.3E-29     | 0.0E+00     |
| 42            | 4.6E-14                            | 8.6E-19    | 2.2E-31     | 0.0E+00     |
| 43            | 4.2E-14                            | 4.2E-19    | 5.5E-32     | 0.0E+00     |
| 44            | 3.5E-14                            | 1.1E-19    | 1.2E-33     | 0.0E+00     |
| 45            | 2.8E-14                            | 4.0E-20    | 1.6E-34     | 0.0E+00     |
| 46            | 2.2E-14                            | 1.3E-20    | 2.7E-35     | 0.0E+00     |
| 47            | 1.4E-14                            | 2.6E-21    | 2.1E-36     | 0.0E+00     |

Note: Enveloping factor of three is not included.

a. Reference 4.

Table A.1/7.3-4 (SHEET 1 OF 2)  
 TOP OF GNSI CASTOR V/21 CASK ADJOINT FLUXES<sup>a</sup>  
 FOR A SOURCE OF 1 n/sec PER GROUP

| Neutron<br>Group | TOP OF CASK<br>(rem/hr per n/sec) |            |             |             |
|------------------|-----------------------------------|------------|-------------|-------------|
|                  | 50 Meters                         | 460 Meters | 1500 Meters | 2460 Meters |
| 1                | 1.0E-12                           | 6.8E-15    | 1.1E-17     | 4.7E-20     |
| 2                | 9.6E-13                           | 6.4E-15    | 1.1E-17     | 4.4E-20     |
| 3                | 8.4E-13                           | 6.4E-15    | 1.2E-17     | 5.2E-20     |
| 4                | 8.0E-13                           | 6.8E-15    | 1.3E-17     | 5.8E-20     |
| 5                |                                   |            |             |             |
| 6                |                                   |            |             |             |
| 7                |                                   |            |             |             |
| 8                | 8.3E-13                           | 6.2E-15    | 7.7E-18     | 2.2E-20     |
| 9                |                                   |            |             |             |
| 10               |                                   |            |             |             |
| 11               |                                   |            |             |             |
| 12               |                                   |            |             |             |
| 13               |                                   |            |             |             |
| 14               | 8.2E-13                           | 5.7E-15    | 1.6E-18     | 1.5E-21     |
| 15               |                                   |            |             |             |
| 16               |                                   |            |             |             |
| 17               |                                   |            |             |             |
| 18               |                                   |            |             |             |
| 19               |                                   |            |             |             |
| 20               |                                   |            |             |             |
| 21               | 6.5E-13                           | 1.9E-15    | 4.2E-20     | 2.4E-24     |
| 22               |                                   |            |             |             |
| 23               |                                   |            |             |             |
| 24               |                                   |            |             |             |
| 25               | 2.8E-13                           | 4.7E-16    | 3.9E-22     | 3.9E-28     |
| 26               |                                   |            |             |             |
| 27               |                                   |            |             |             |
| 28               |                                   |            |             |             |
| 29               | 8.8E-14                           | 1.5E-16    | 1.8E-24     | 0           |
| 30               |                                   |            |             |             |
| 31               |                                   |            |             |             |
| 32               | 6.1E-14                           | 9.7E-17    | 3.0E-25     | 0           |
| 33               |                                   |            |             |             |
| 34               | 5.2E-14                           | 7.2E-17    | 1.3E-25     | 0           |
| 35               |                                   |            |             |             |

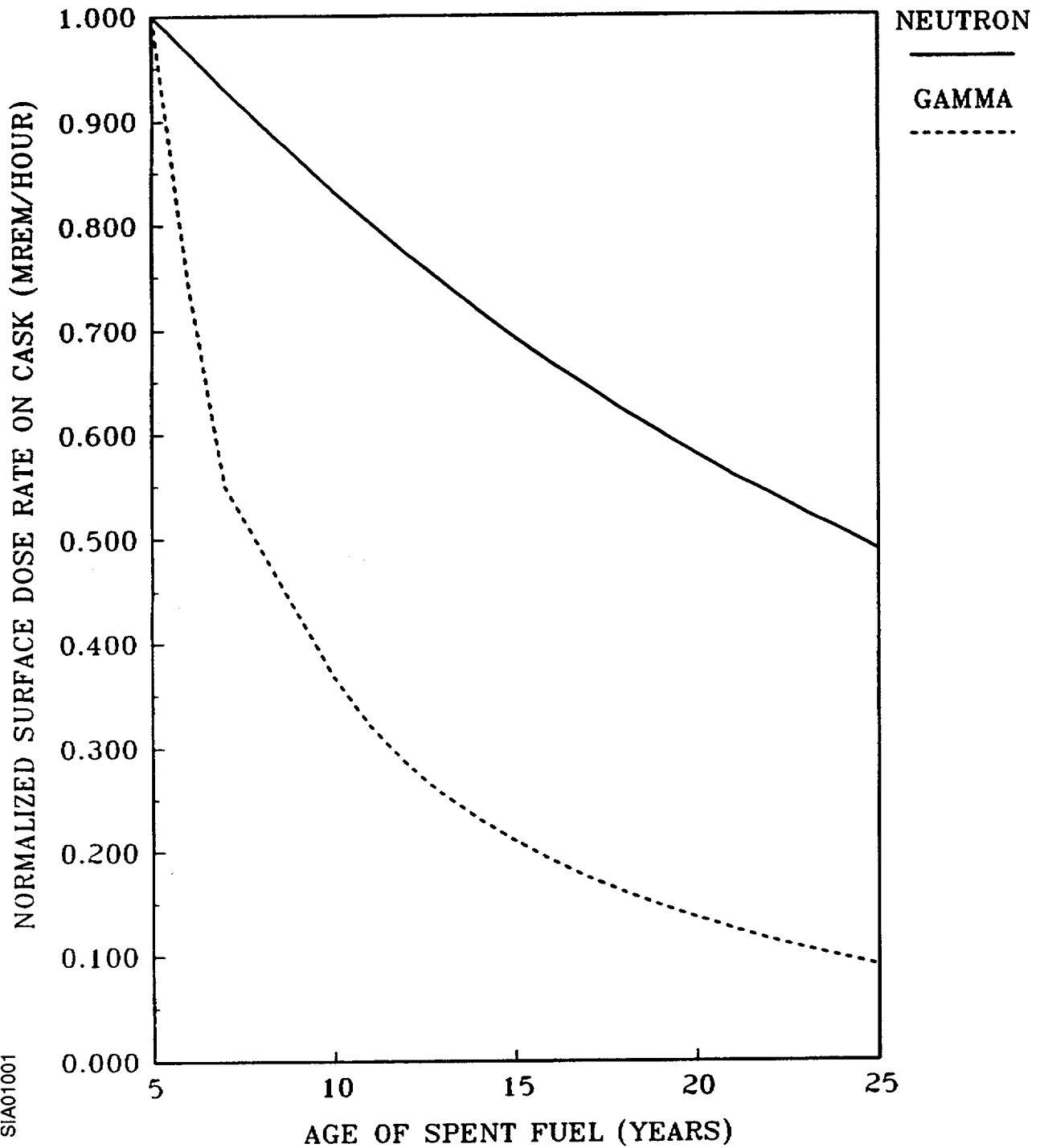
Table A.1/7.3-4 (SHEET 2 OF 2)  
 TOP OF GNSI CASTOR V/21 CASK ADJOINT FLUXES<sup>a</sup>  
 FOR A SOURCE OF 1 n/sec PER GROUP

| Neutron<br>Group | TOP OF CASK<br>(rem/hr per n/sec) |            |             |             |
|------------------|-----------------------------------|------------|-------------|-------------|
|                  | 50 Meters                         | 460 Meters | 1500 Meters | 2460 Meters |
| 36               | 5.4E-14                           | 3.8E-17    | 1.5E-26     | 0           |
| 37               | 5.5E-14                           | 2.5E-17    | 6.8E-27     | 0           |
| 38               |                                   |            |             |             |
| 39               | 5.5E-14                           | 7.7E-18    | 2.1E-28     | 0           |
| 40               |                                   |            |             |             |
| 41               |                                   |            |             |             |
| 42               | 5.0E-14                           | 2.3E-18    | 1.3E-29     | 0           |
| 43               |                                   |            |             |             |
| 44               |                                   |            |             |             |
| 45               |                                   |            |             |             |
| 46               | 3.0E-14                           | 7.1E-20    | 1.4E-33     | 0           |
| 47               |                                   |            |             |             |

Note: Enveloping factor of three is not included.

a. Reference 4.

Figure A.1/7.3-2  
NORMALIZED SURFACE DOSE RATE ON GNSI CASTOR V/21  
CASK VERSUS AGE OF SPENT FUEL



SIA01001

Figure A.1/7.3-3a  
[DELETED]

|

Figure A.1/7.3-3b  
[DELETED]

Figure A.1/7.3-4a  
[DELETED]

|

Figure A.1/7.3-4b  
[DELETED]

|

Figure A.1/7.3-5a  
[DELETED]

|

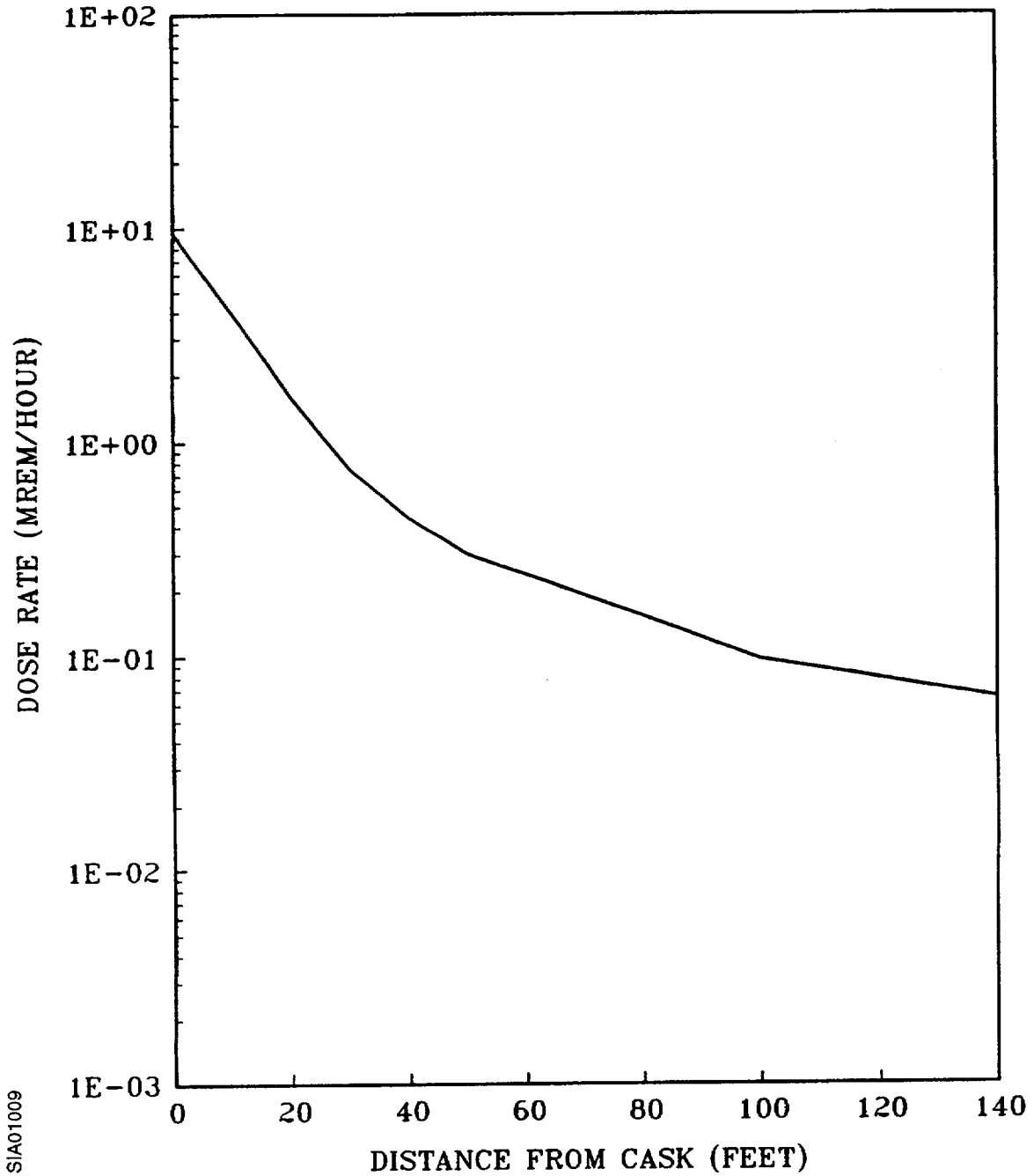
Figure A.1/7.3-5b  
[DELETED]

|

Figure A.1/7.3-6  
[DELETED]

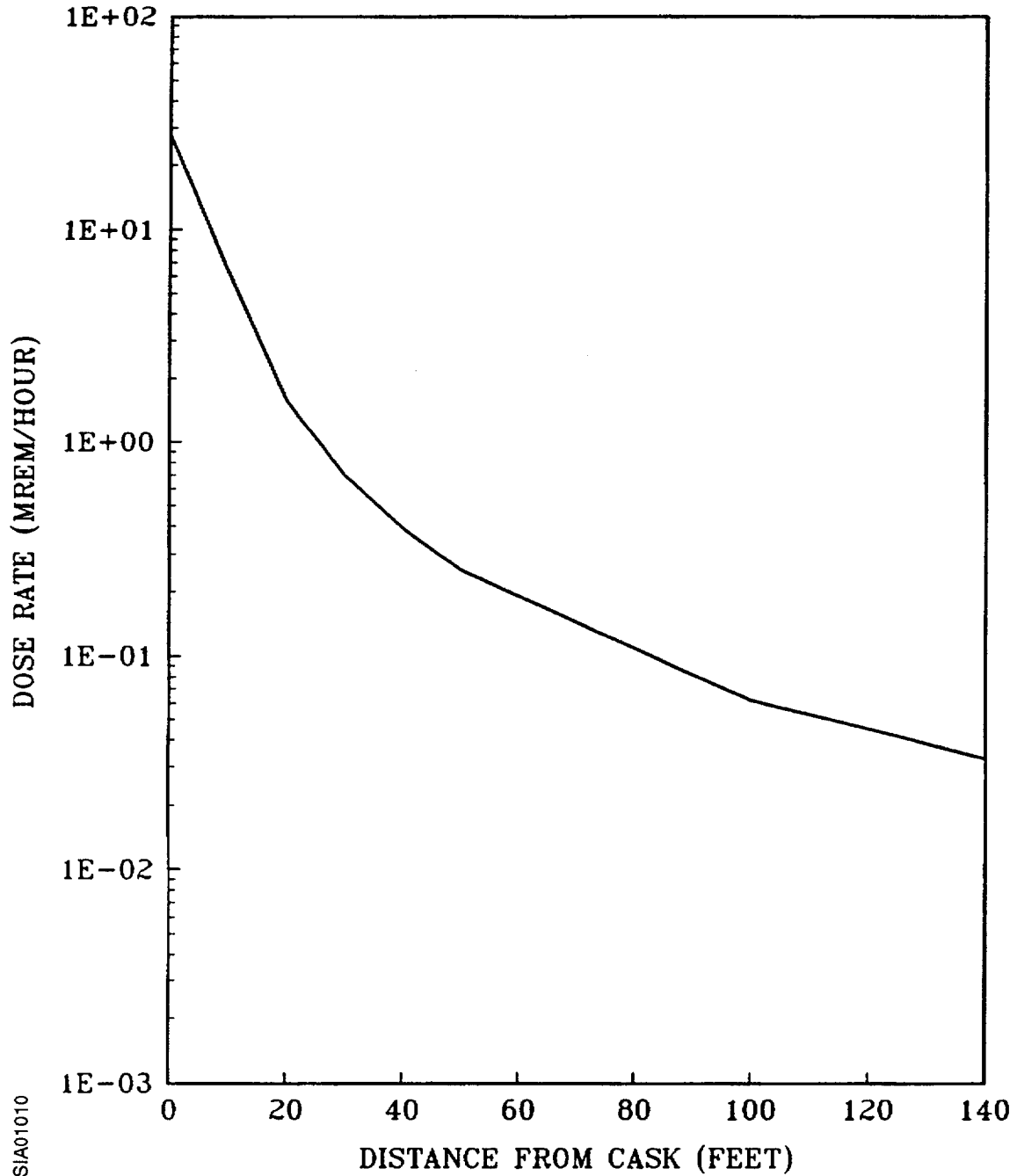
|

Figure A.1/7.3-7a  
GNSI CASTOR V/21 NEUTRON DOSE RATE  
FROM ONE CASK VS. DISTANCE  
(0-140 FEET)



SIA01009

Figure A.1/7.3-7b  
GNSI CASTOR V/21 GAMMA DOSE RATE  
FROM ONE CASK VS. DISTANCE  
(0-140 FEET)



SIA01010

Figure A.1/7.3-8a  
GNSI CASTOR V/21 NEUTRON DOSE RATE  
FROM ONE CASK VS. DISTANCE  
(0-700 FEET)

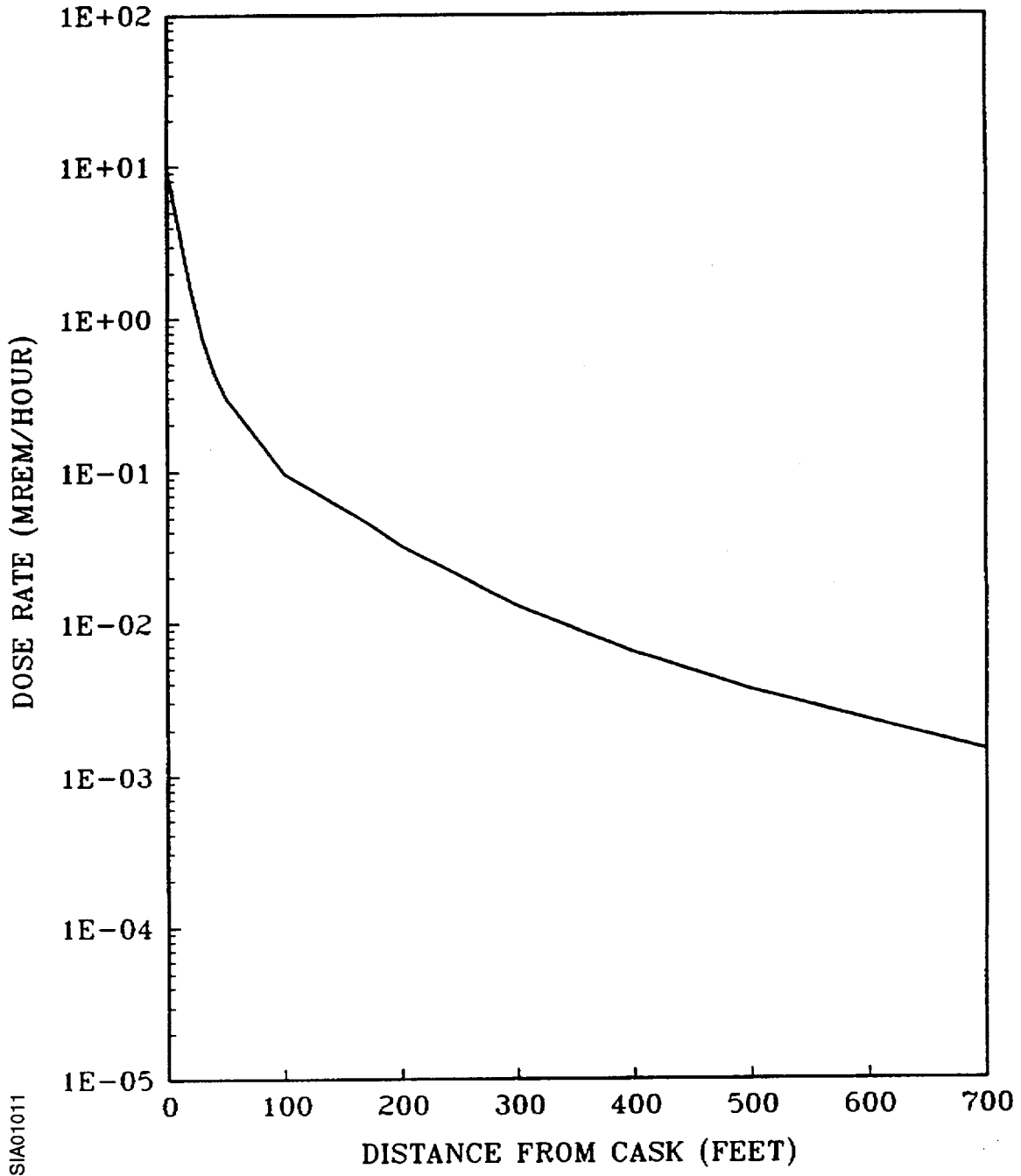
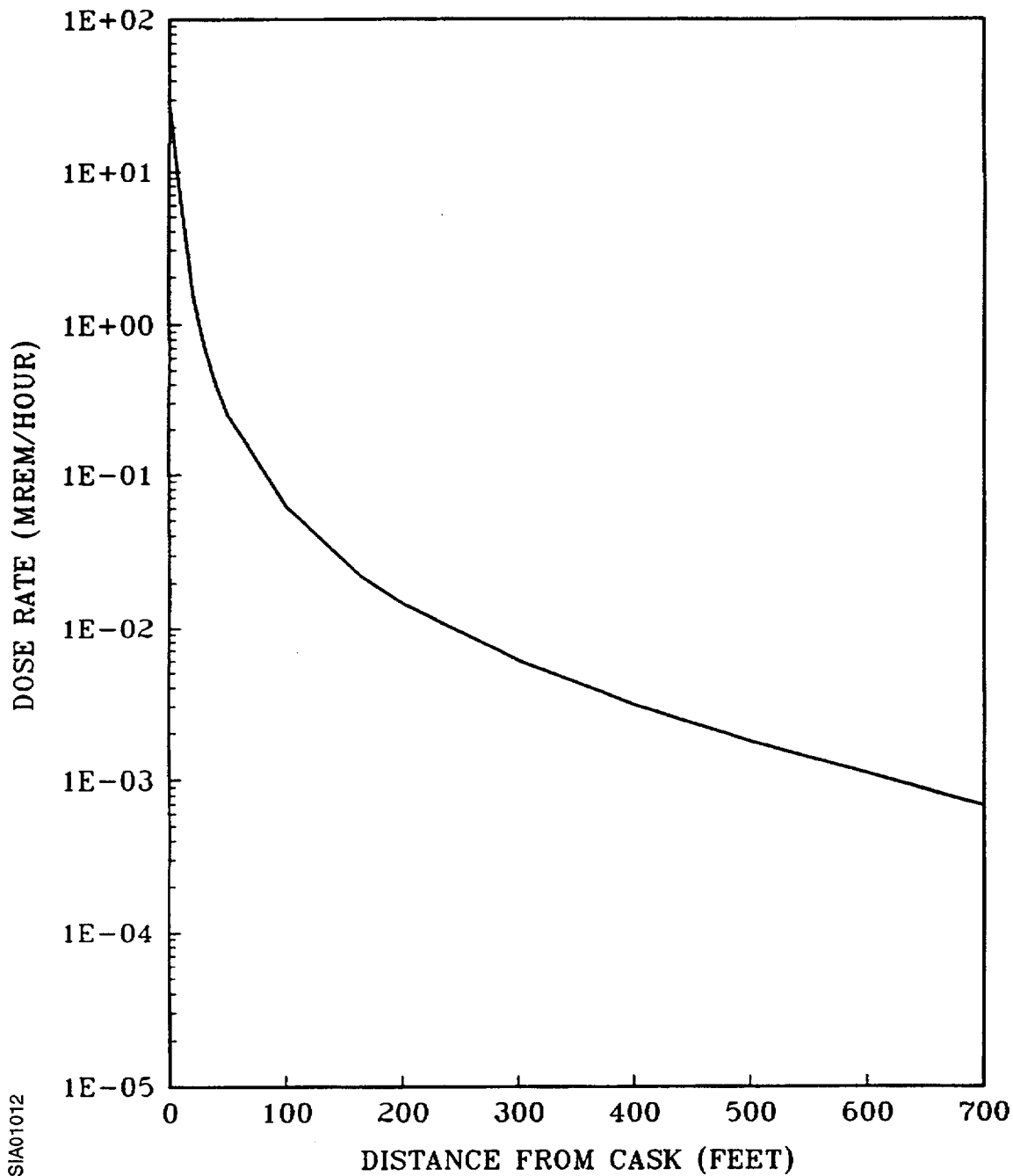
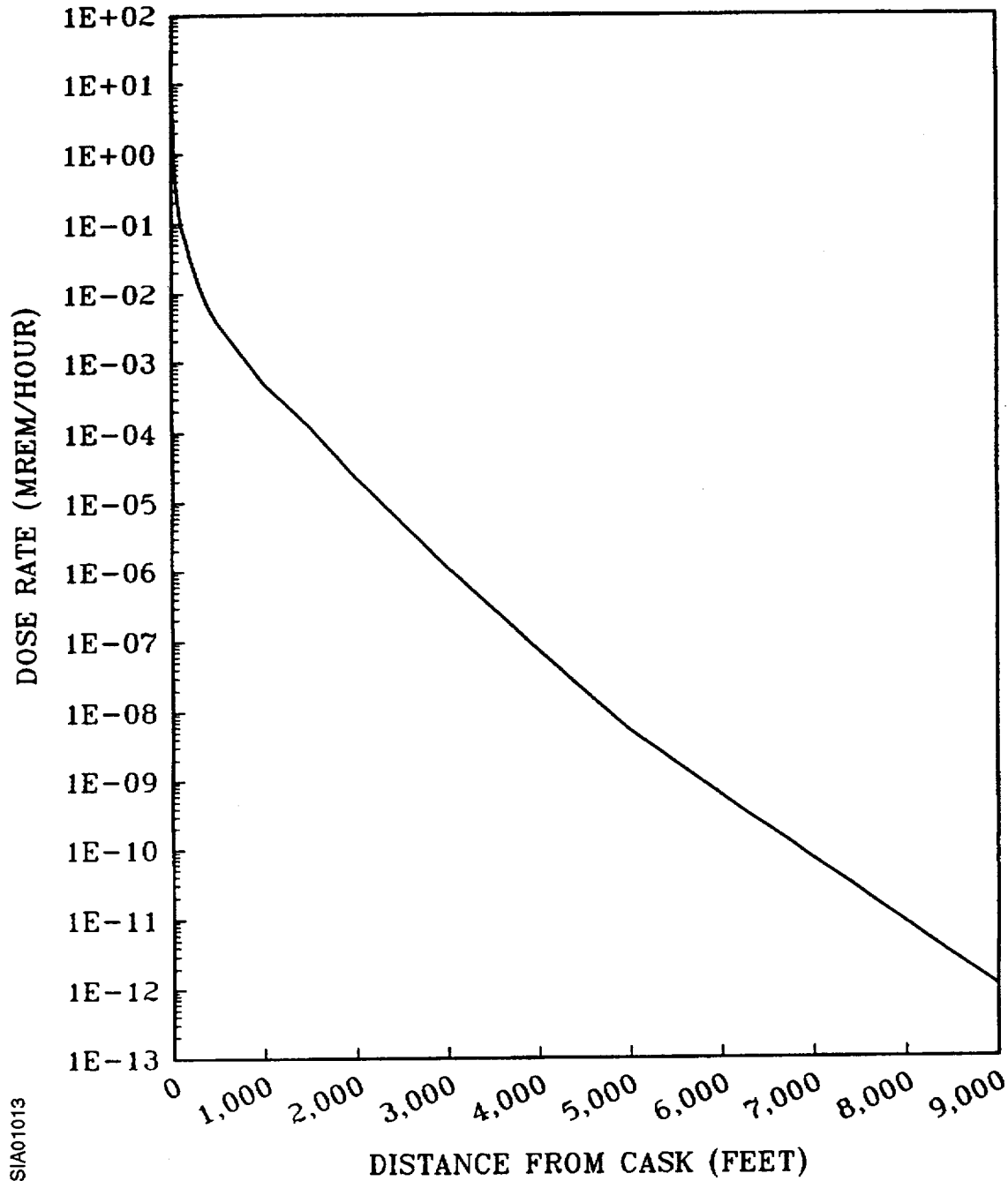


Figure A.1/7.3-8b  
GNSI CASTOR V/21 GAMMA DOSE RATE  
FROM ONE CASK VS. DISTANCE  
(0-700 FEET)



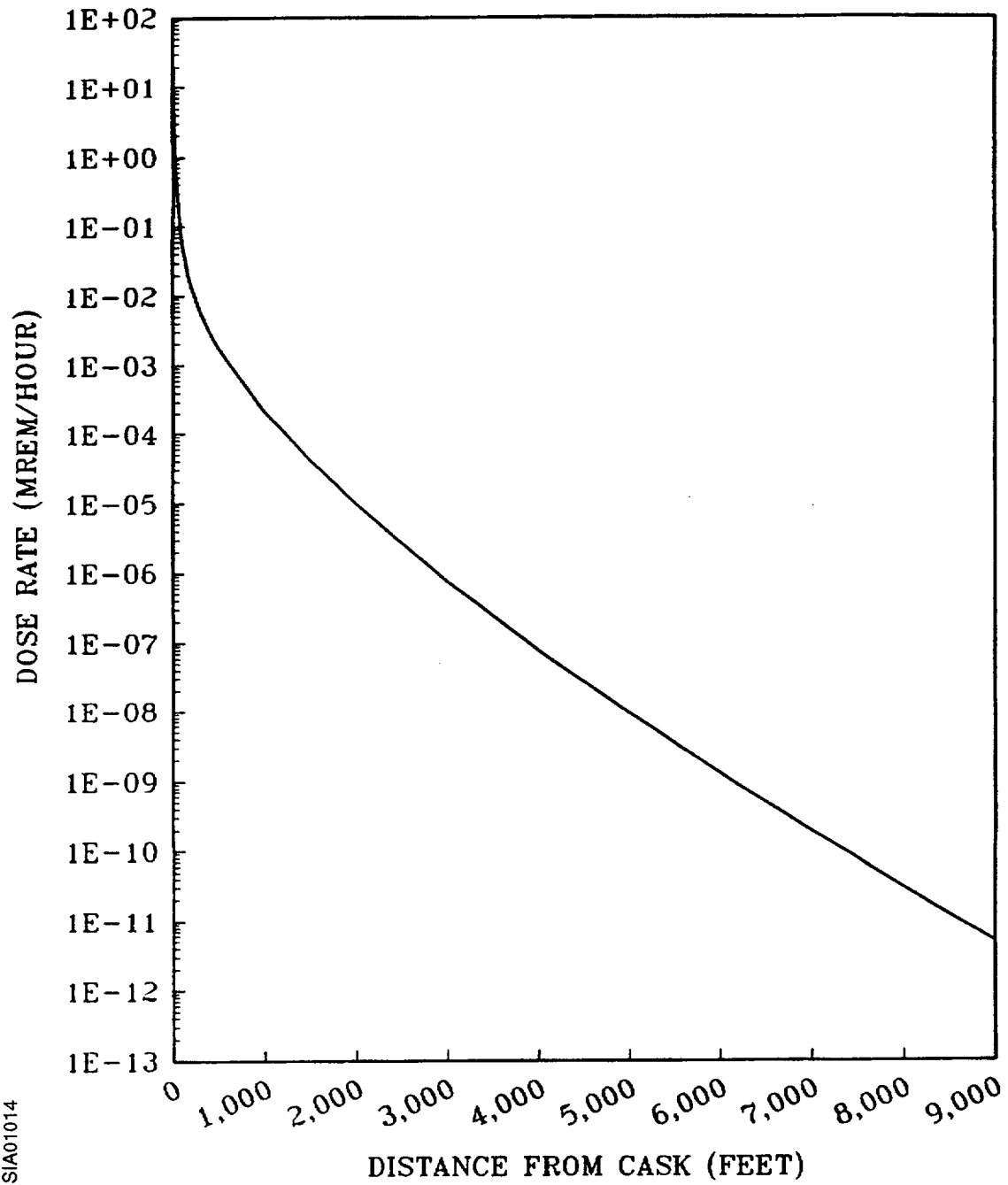
SIA01012

Figure A.1/7.3-9a  
GNSI CASTOR V/21 NEUTRON DOSE RATE  
FROM ONE CASK VS. DISTANCE  
(0-9000 FEET)



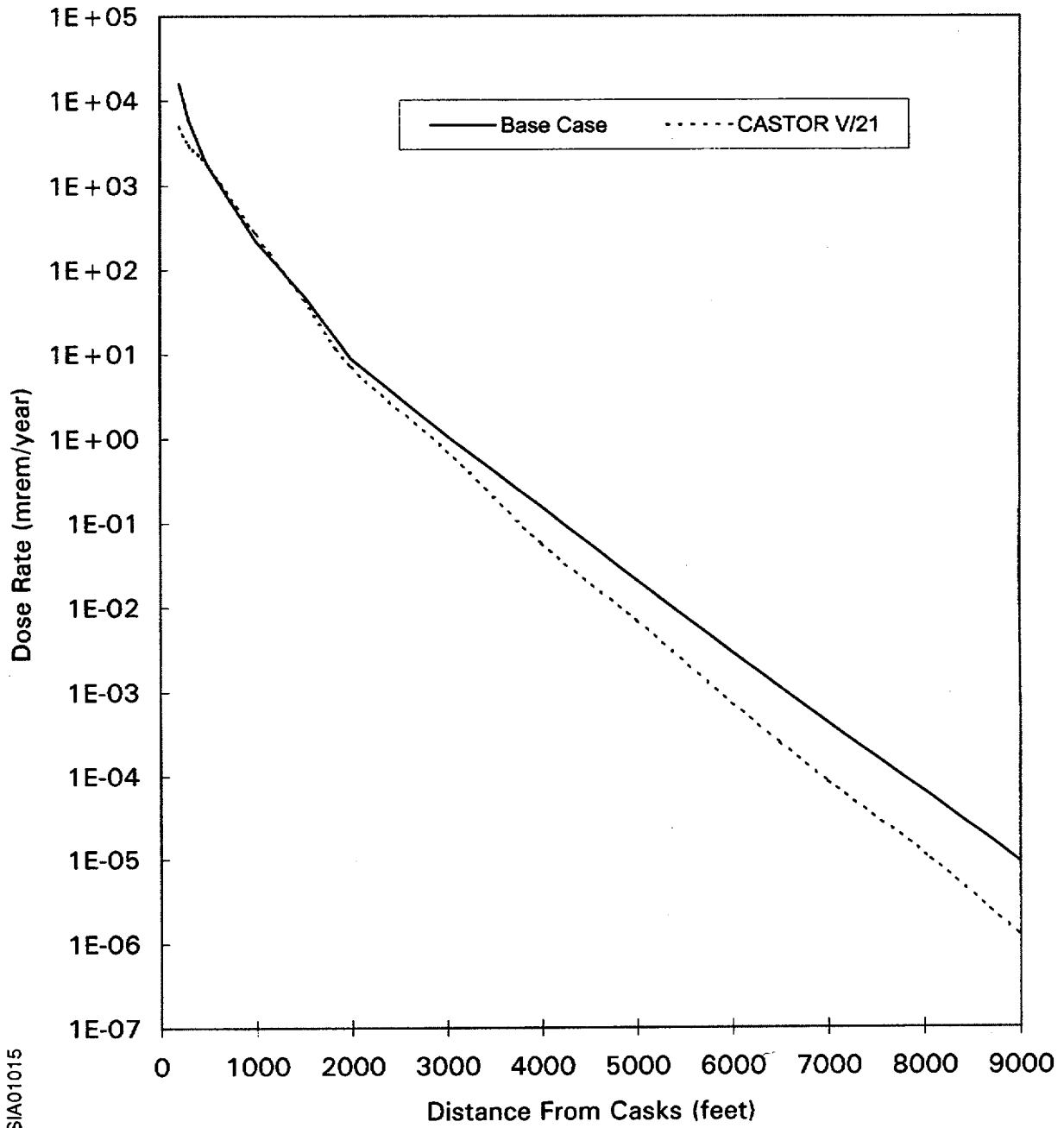
SIA01013

Figure A.1/7.3-9b  
GNSI CASTOR V/21 GAMMA DOSE RATE  
FROM ONE CASK VS. DISTANCE  
(0-9000 FEET)



SIA01014

Figure A.1/7.3-10  
DOSE RATE FOR 84 CASTOR V/21 CASKS VERSUS  
DISTANCE COMPARED TO ISFSI BASE CASE DOSE RATE VERSUS DISTANCE



SIA01015

**A.1/8.2.2 Extreme Wind**

The effects and consequences of extreme winds on the GNSI cask are presented in Section 8.2.1.2.1 of the GNSI Topical Report. The GNSI analysis demonstrates that extreme winds are not capable of overturning their cask nor of producing leakage from it. Since no radioactivity would be released, no resultant doses would occur.

**A.1/8.2.5 Fire**

The ability of the GNSI cask to withstand postulated fires is presented in Section 8.2.1.2.7 of the GNSI Topical Report. As concluded in Surry ISFSI SAR Section 8.2.5, no fires other than small electrical fires are credible at the ISFSI slab. Based on the GNSI analyses referenced above, since no radioactivity would be released, no resultant doses would occur.

**A.1/8.2.8 Loss of Neutron Shield**

As discussed in Section 1.2.4 of the GNSI Topical Report, the neutron absorbing material for the GNSI cask includes polyethylene rods inserted into the cask wall. Thus, no loss of neutron shield is postulated.

*Appendix A.2*  
*Westinghouse MC-10 Cask*

## **Appendix A.2**

### **WESTINGHOUSE MC-10 CASK**

#### **GENERAL DESCRIPTION**

The Westinghouse MC-10 cask is a low alloy steel shielded container which is approximately 88 inches in diameter and 188 inches long. The forged steel walls and bottom are approximately 10 inches thick and 11 inches thick, respectively, to provide radiation (gamma) shielding and structural integrity. Three covers are provided to seal the top end of the cask cylinder. A low alloy steel cover, approximately 9 inches thick, with a metallic o-ring provides initial seal and gamma shielding following fuel loading. A carbon steel cover, approximately 3.5 inches thick, with a dual-seal elastomer o-ring and metallic ring provides primary containment seal. The third cover, providing support for neutron absorbing material, may be welded over the first two covers to provide seal redundancy. The outside surfaces of the cask wall and bottom are jacketed with neutron absorbing materials.

The cask contains a basket assembly which consists of 24 storage locations utilizing a honeycomb-type basket structure. The stainless steel basket structure maintains the subcritical array of storage locations, provides lateral structural integrity, and conducts fuel assembly decay heat to the cask wall.

The exterior coating system employed on the MC-10 cask at the Surry ISFSI differs from the specific coating system identified on page 4.2-124 of the MC-10 TSAR. The coating system employed at Surry consists of a polyamide epoxy primer and epoxy enamel topcoat which provides a decontaminable finish and exterior corrosion protection, and is consistent with the surface emissivity referenced on page 4.2-19 of the MC-10 TSAR.

#### **A.2/3.1.1 Materials to be Stored**

The structural evaluations of the MC-10 are provided in Chapters 4 and 8 of the Topical Report. These evaluations used a fuel weight of 1442 lb, but the maximum weight of Surry Units 1 and 2 fuel assemblies containing a burnable poison rod assembly (BPRA) or thimble plugging device (TPD) in the one MC-10 at the Surry ISFSI is 1490 lb. An evaluation has been performed by Westinghouse to evaluate the effect of the increased weight of the fuel assembly from 1442 lb to 1490 lb. The Westinghouse evaluation concluded that the calculated stresses at all locations in the cask and basket were less than the allowable stresses.

An evaluation has also been performed on the effect to the cask surface dose rates as a result of placing BPRAs or TPDs in the fuel stored in the MC-10. This evaluation confirmed that the calculated surface dose rates for the MC-10 remained less than the design basis dose rates used to calculate doses at the ISFSI perimeter and to the nearest resident.

An evaluation has been performed on the effect on criticality control from the storage of BPRAs or TPDs in the fuel stored in the MC-10. BPRA rods will displace water (a moderator) in

the fuel assembly thimble tubes, therefore, even the use of depleted BPRAs will reduce reactivity in a cask. TPDs are short and do not displace water in the thimble tubes, therefore, their use will not affect reactivity.

The MC-10 is designed for a maximum internal pressure under normal and accident conditions, and helium buildup or pre-pressurization in BPRAs will affect this analysis. The confinement analysis for the MC-10 has been reanalyzed for twenty-four 20-finger BPRAs, and this reanalysis shows that the maximum pressure under normal conditions is 1.7 atm., when the design basis for this cask is 2.5 atm. The maximum pressure under accident conditions would be 3.4 atm. absolute, when the design basis for this cask is 3.5 atm. absolute. This analysis assumed that the maximum fuel rod internal pressure was 90 bars, instead of the 134.4 bars assumed in the MC-10 TSAR. This lower 90 bars limit must be applied for any fuel assembly containing BPRAs that is placed in the MC-10 cask. The impact of TPDs on the confinement analysis is bounded by the impact of BPRAs.

To account for the additional decay heat from BPRAs and TPDs, fuel assembly decay heat estimates must include an estimate for the decay heat from the actual component in each fuel assembly. Therefore, the combined decay heat from the fuel assembly and its component must be less than the limit for a fuel assembly in the MC-10.

Based on these evaluations, the storage of fuel assemblies with BPRAs or TPDs is acceptable for the MC-10.

#### **A.2/7.3.2.1 Cask Surface Dose Rates**

The Westinghouse MC-10 cask is evaluated for fuel with an initial enrichment of 3.7 wt.% U-235 and burnup of 35,000 MWD/MTU

The assumptions used in calculating the Westinghouse MC-10 cask surface dose rates and energy spectra are provided in Section 7.3.2.2 of the Westinghouse Topical Report (Reference 1).

Neutron and gamma source terms for the stored spent fuel were generated using OREST (ORIGEN II). Typical results from these runs are shown in Surry ISFSI SAR Tables 7.2-1, 7.2-2, 7.2-3, and 7.2-4. ANISN-W (Reference 10) and DOT-IIW (Reference 11) were used by Westinghouse to calculate the cask surface fluxes. Flux-to-dose rate conversion factors, as shown in Table 7.3-6 of the Westinghouse Topical Report (Reference 1), were then used to obtain the average surface dose rates for the cask. The Westinghouse cask average surface dose rates for 10-year-old fuel are 9.96 mrem/hour neutron and 23.05 mrem/hour gamma for the side and 2.62 mrem/hour neutron and 2.46 mrem/hour gamma for the top. When these dose rates are combined, the side and top average surface dose rates are 33.01 mrem/hour and 5.08 mrem/hour, respectively. These dose rates are bounded by the total average surface dose rates of 224 mrem/hour for the side and 76 mrem/hour for the top reported in the Surry ISFSI SAR, Section 7.3.2.1.

Figure A.2/7.3-2 shows the normalized surface dose rates on a Westinghouse cask versus age of spent fuel for both gamma and neutron radiation.

#### **A.2/7.3.2.2 Dose Rate Versus Distance**

The cask surface dose rates discussed in Section A.2/7.3.2.1 result in the dose rates at various distances as shown on Figures A.2/7.3-3a through A.2/7.3-6. The neutron transport results shown on these figures were generated using a series of adjoint (References 2 & 3) ANISN (Reference 4) runs. These calculations were performed with a BUGLE-80 (Reference 5) cross-section set for an infinite-air medium. As explained in References 2 and 3, the adjoint method is the preferred analytical technique when more than one set of sources must be evaluated at a given detector location for a response of interest. For the adjoint analyses reported here, the adjoint source is the flux-to-dose conversion factor reported in Reference 9. Four separate ANISN analyses were performed at distances of 50, 460, 1500, and 2460 meters. The resulting adjoint fluxes are presented in Table A.1/7.3-3. These adjoint fluxes were then folded with the cask surface leakage spectra supplied by Westinghouse over the area of the cask's top and side. Cask surface neutron leakage data are provided in Table A.2/7.3-2.

The resultant neutron dose rates were then used to construct the dose rate versus distance curves presented on Figures A.2/7.3-3a, A.2/7.3-4a, and A.2/7.3-5a.

For the gamma-ray transport, simple point kernel calculations using infinite medium dose rate buildup factors in dry air were performed. Using a point source model and References 6 and 7, air-to-void correction factors were developed and applied to the gamma dose rates in void based on Reference 8. The gamma dose rates for the casks are shown on Figures A.2/7.3-3b, A.2/7.3-4b, and A.2/7.3-5b.

For Figure A.2/7.3-6, decay factors have been used assuming that four Westinghouse MC-10 casks are placed in the ISFSI each year for 18.5 years and each new group of four casks has a minimum of 10 years decay of the fuel. As shown on Figure A.2/7.3-6, the design basis dose rate for the ISFSI bounds the dose rate for the ISFSI filled to capacity with Westinghouse MC-10 casks.

#### **A.2/7.3.5 References**

1. *Topical Safety Analysis Report for the Westinghouse MC-10 Cask for an Independent Spent Fuel Storage Installation (Dry Storage)*, Proprietary and Nonproprietary Version WCAPs 10740 and 10741, Revision 2-A, Westinghouse Nuclear Energy Systems, November 1987.
2. V. R. Cain, *The Use of Discrete Ordinates Adjoint Calculations, A Review of the Discrete Ordinates 5 Method for Radiation Transport Calculations*, ORNL-RSIC-19, March 1968, pp. 85-94.
3. G. I. Bell, S. Glasstone, *Nuclear Reactor Theory*, Chapter 6.1 - The Adjoint Function and Its Applications, Van Nostrand Reinhold Company, New York, 1970.

4. W. W. Engle, Jr., *A User's Manual for ANISN, A One-Dimensional Discrete Ordinates Transport Code with Anisotropic Scattering*, K-1643, Union Carbide Corporation, Nuclear Division, June 1973.
5. *BUGLE-80, Coupled 47-Neutron, 20-Gamma-Ray, P3, Cross-Section Library for LWR Shielding Calculations*, DLC-75, R. W. Roussin, ORNL, June 1980.
6. Warkentin, J. K., *Polynomial Coefficients for Dose Buildup in Air*, Radiation Research Associates, Inc., August 15, 1975, RRA-N7511.
7. Hubbell, L. H., *Photon Cross-Sections, Attenuation Coefficients, and Energy Absorption Coefficients from 10 KeV to 100 GeV*, National Bureau of Standards, August 1969, NSRDS-NBS29.
8. *Spacetrans II, Dose Calculations at Detectors at Various Distances from the Surface of a Cylinder*, Neutron Physics Division of Oak Ridge National Laboratory, September 1973, ORNL-TM-2592.
9. ANSI/ANS-6.1.1-1977, *American National Standard - Neutron and Gamma Ray Flux to Dose Rate Factors*, American Nuclear Society, March 17, 1977.
10. CCC-255, *ANISN-W, A One Dimensional Discrete Ordinates Transport Computer Program*, Contributed by Westinghouse Advanced Reactors Division, Madison, Pennsylvania; ORNL Radiation Shielding Information Center, Oak Ridge, Tennessee, 1971.
11. CCC-89, *DOT-IIW, A Two Dimensional Discrete Ordinates Transport Computer Program*, Contributed by the Westinghouse Advance Reactors Division, Madison, Pennsylvania; ORNL Radiation Shielding Information Center, 1980. (DOT-IIW is an unpublished enhancement of DOT-IIW for the CRAY-IS computer).
12. [Deleted]

Table A.2/7.3-2  
WESTINGHOUSE MC-10 CASK SURFACE NEUTRON LEAKAGE

| Neutron Group | Upper <sup>a</sup> Energy (ev) | Cask Surface<br>Leakage Spectra<br>(n/cm <sup>2</sup> - sec) |        |
|---------------|--------------------------------|--|--------|
|               |                                | Side   | Top    |
| 1             | 1.7E+7                         | 5.64-4   | 8.10-5 |
| 2             | 1.4E+7                         | 2.04-3   | 2.88-4 |
| 3             | 1.2E+7                         | 6.86-3   | 9.56-4 |
| 4             | 1.0E+7                         | 1.23-2   | 1.70-3 |
| 5             | 8.6E+6                         | 2.02-2   | 2.78-3 |
| 6             | 7.4E+6                         | 4.74-2   | 6.52-3 |
| 7             | 6.1E+6                         | 7.09-2   | 9.70-3 |
| 8             | 5.0E+6                         | 1.61-1   | 2.21-2 |
| 9             | 3.7E+6                         | 1.59-1   | 2.23-2 |
| 10            | 3.0E+6                         | 1.59-1   | 2.28-2 |
| 11            | 2.7E+6                         | 2.00-1   | 2.89-2 |
| 12            | 2.5E+6                         | 1.18-1   | 1.70-2 |
| 13            | 2.4E+6                         | 4.69-2   | 6.98-3 |
| 14            | 2.3E+6                         | 2.06-1   | 3.09-2 |
| 15            | 2.2E+6                         | 4.46-1   | 6.66-2 |
| 16            | 1.9E+6                         | 6.66-1   | 1.04-1 |
| 17            | 1.6E+6                         | 9.27-1   | 1.46-1 |
| 18            | 1.4E+6                         | 2.24   | 3.78-1 |
| 19            | 1.0E+6                         | 1.75   | 3.16-1 |
| 20            | 8.2E+5                         | 9.77-1   | 1.65-1 |
| 21            | 7.4E+5                         | 4.71   | 9.14-1 |
| 22            | 6.1E+5                         | 4.69   | 9.07-1 |
| 23            | 5.0E+5                         | 4.30   | 8.38-1 |
| 24            | 3.7E+5                         | 4.64   | 9.98-1 |
| 25            | 3.0E+5                         | 8.34   | 1.68   |
| 26            | 1.8E+5                         | 7.61   | 1.58   |
| 27            | 1.1E+5                         | 6.50   | 1.32   |
| 28            | 6.7E+4                         | 6.10   | 1.24   |
| 29            | 5.0E+4                         | 2.42   | 4.53-1 |
| 30            | 3.2E+4                         | 1.46   | 2.09-1 |
| 31            | 2.6E+4                         | 1.13   | 3.20-1 |
| 32            | 2.4E+4                         | 1.29   | 3.25-1 |
| 33            | 2.2E+4                         | 4.65   | 1.07   |
| 34            | 1.5E+4                         | 8.52   | 1.72   |
| 35            | 7.1E+3                         | 9.54   | 2.01   |

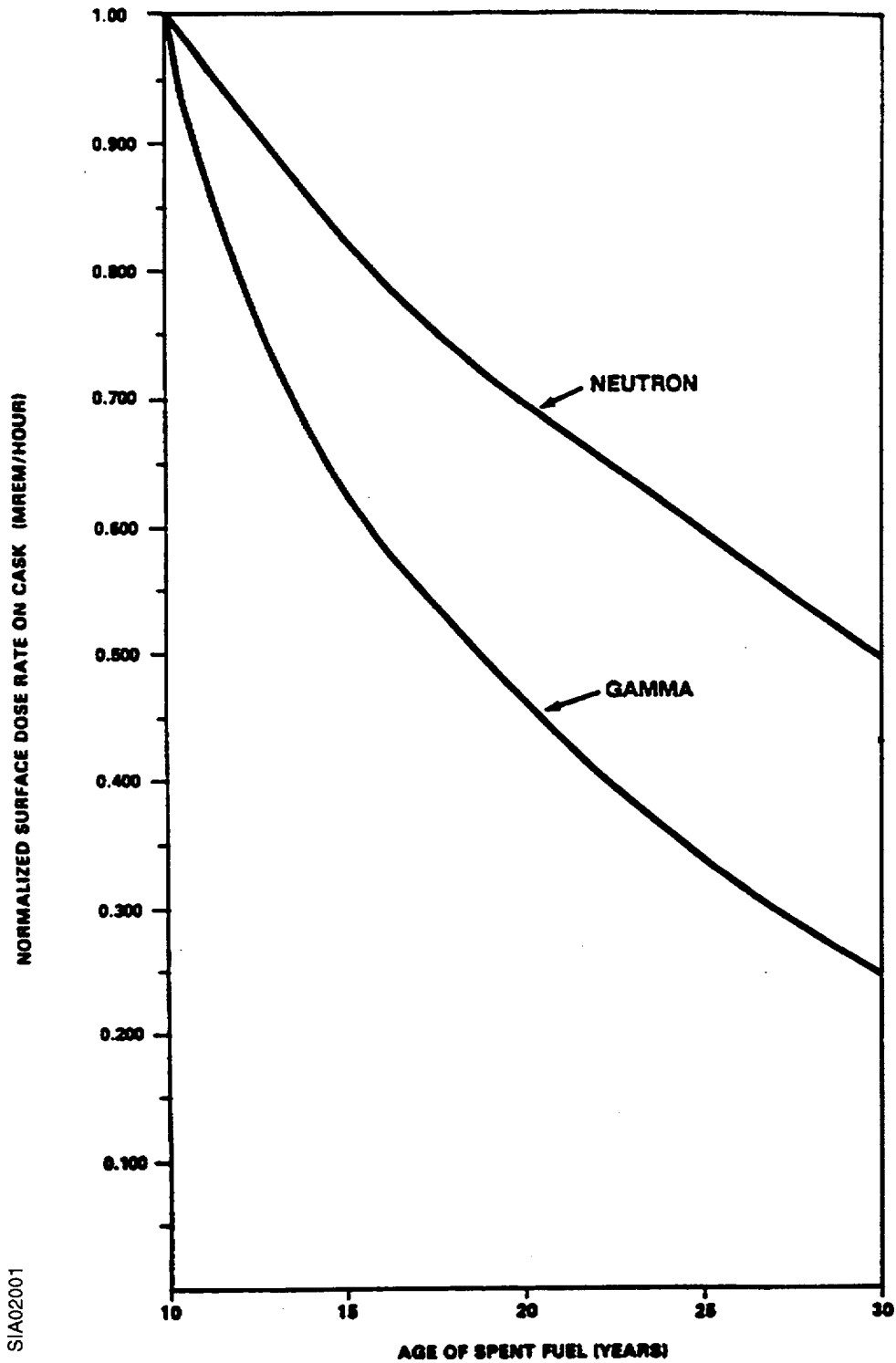
Table A.2/7.3-2  
WESTINGHOUSE MC-10 CASK SURFACE NEUTRON LEAKAGE

| Neutron Group | Upper <sup>a</sup> Energy (ev) | Cask Surface<br>Leakage Spectra<br>(n/cm <sup>2</sup> - sec) |      |
|---------------|--------------------------------|--|------|
|               |                                | Side   | Top  |
| 36            | 3.4E+3                         | 9.77   | 2.02 |
| 37            | 1.6E+3                         | 18.3   | 3.68 |
| 38            | 4.5E+2                         | 11.9   | 2.36 |
| 39            | 2.1E+2                         | 12.6   | 2.48 |
| 40            | 1.0E+2                         | 17.9   | 3.53 |
| 41            | 3.7E+1                         | 23.8   | 4.63 |
| 42            | 1.1E+1                         | 14.1   | 2.69 |
| 43            | 5.0E+0                         | 17.8   | 3.39 |
| 44            | 1.8E+0                         | 12.0   | 2.27 |
| 45            | 8.8E-1                         | 10.4   | 1.93 |
| 46            | 4.1E-1                         | 17.6   | 3.23 |
| 47            | 1.0E-1                         | 6.82   | 1.27 |

Note: Westinghouse MC-10 cask surface area: 3.58+05 cm<sup>2</sup>  
(side), 4.48+04 cm<sup>2</sup> (top).

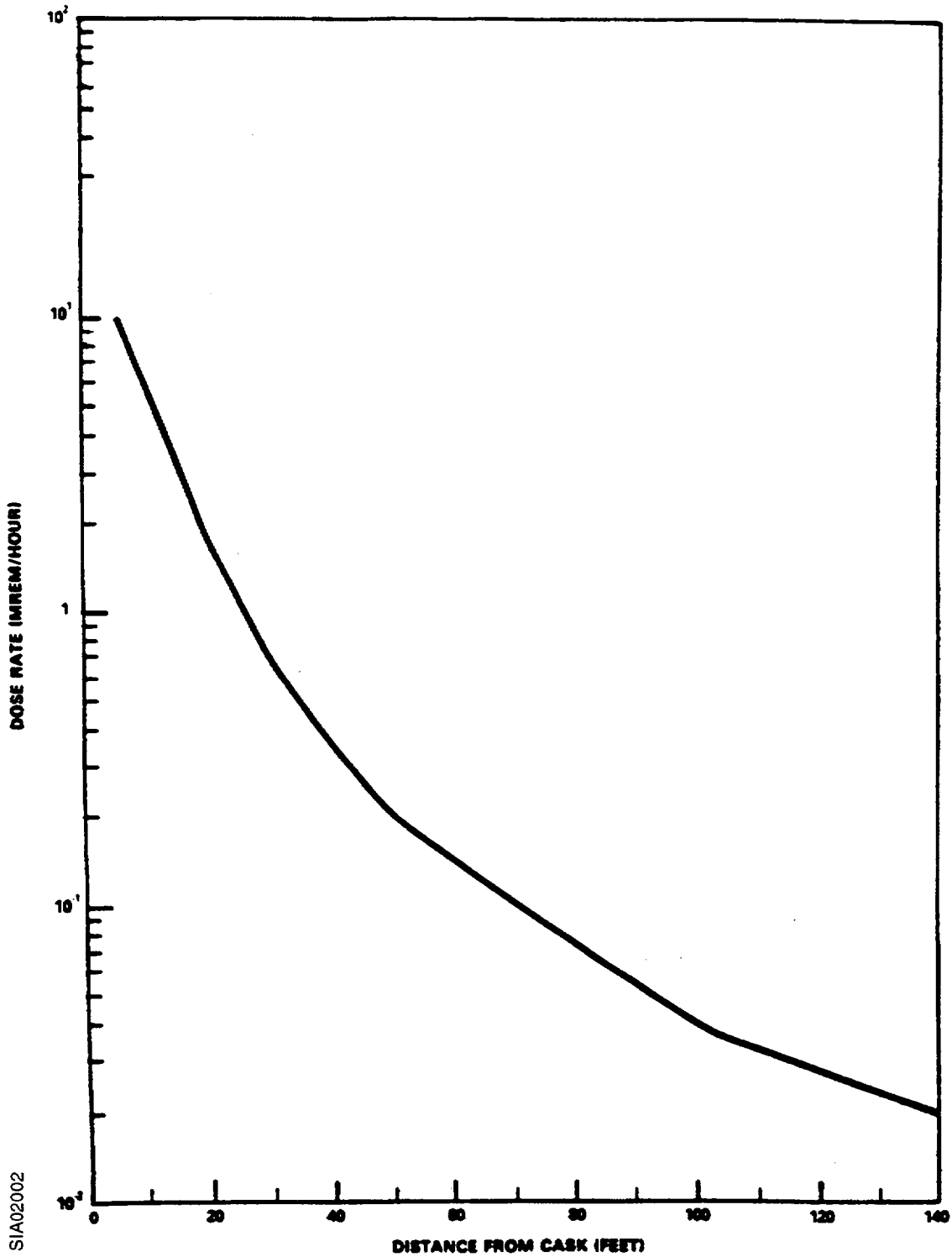
a. Reference 5.

Figure A.2/7.3-2  
NORMALIZED SURFACE DOSE RATE ON  
WESTINGHOUSE MC-10 CASK  
VERSUS AGE OF SPENT FUEL



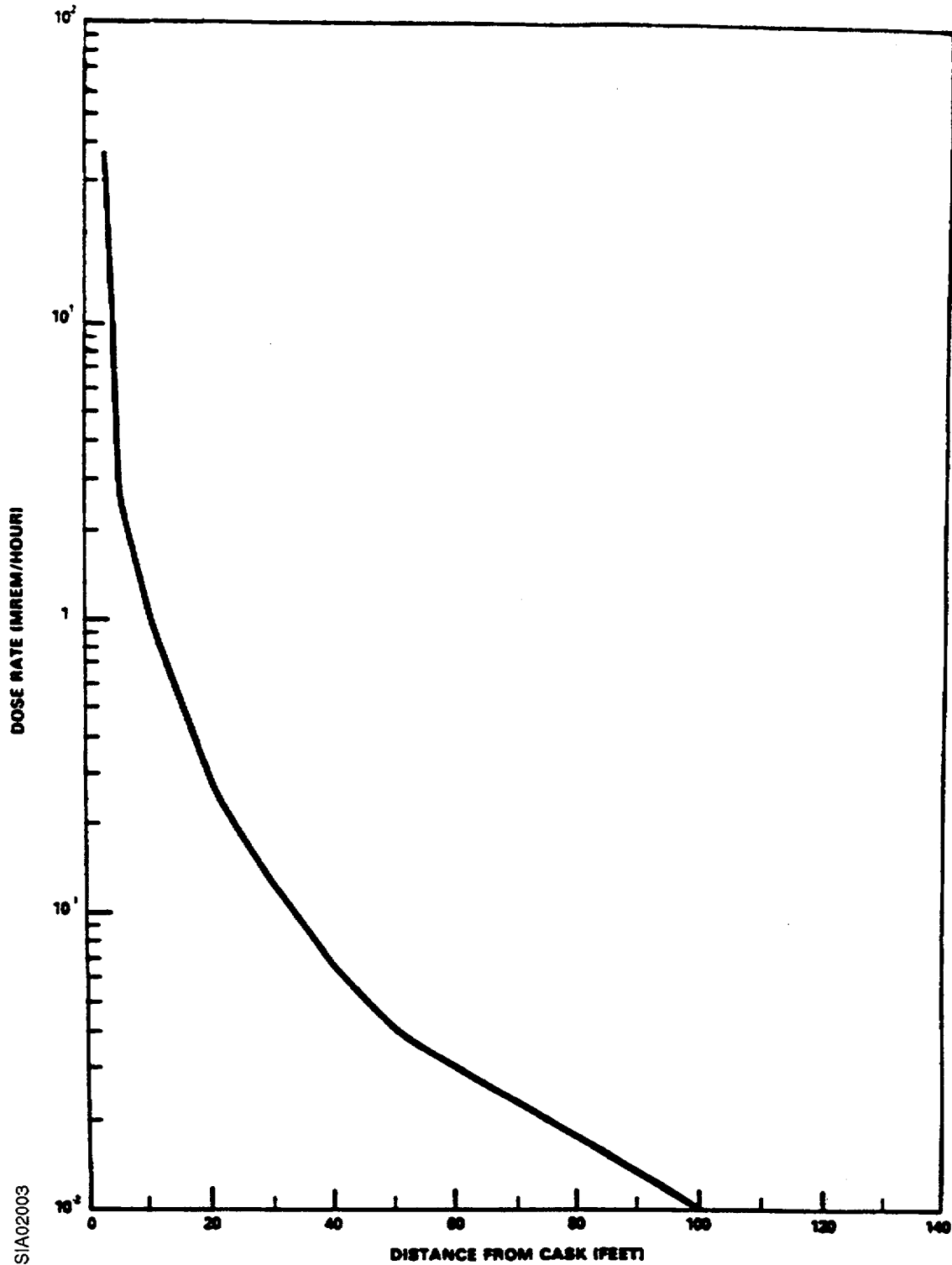
S/A02001

Figure A.2/7.3-3a  
WESTINGHOUSE MC-10  
NEUTRON DOSE RATE FROM ONE CASK  
VERSUS DISTANCE  
(0-140 FEET)



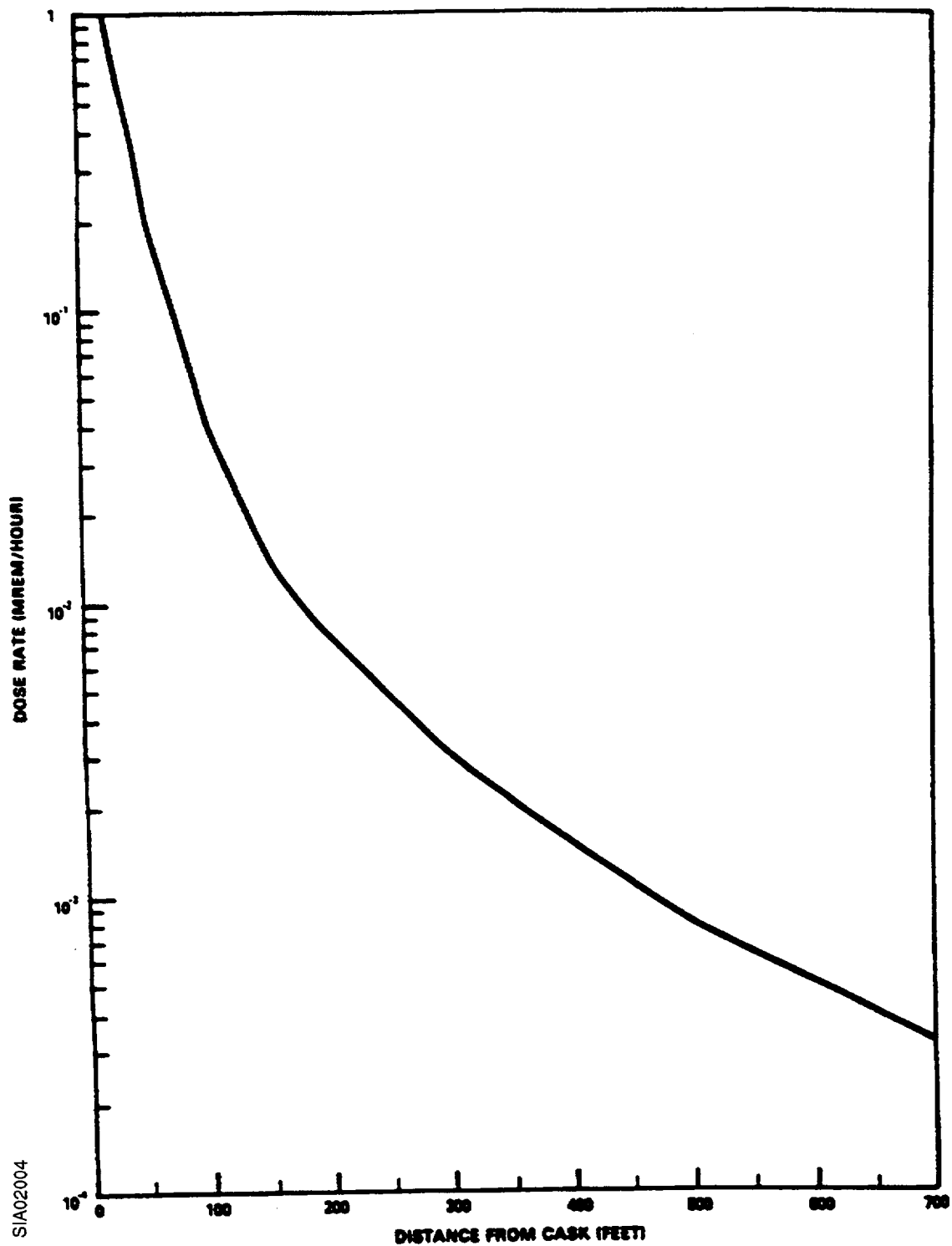
SIA02002

Figure A.2/7.3-3b  
WESTINGHOUSE MC-10  
GAMMA DOSE RATE FROM ONE CASK  
VERSUS DISTANCE  
(0-140 FEET)



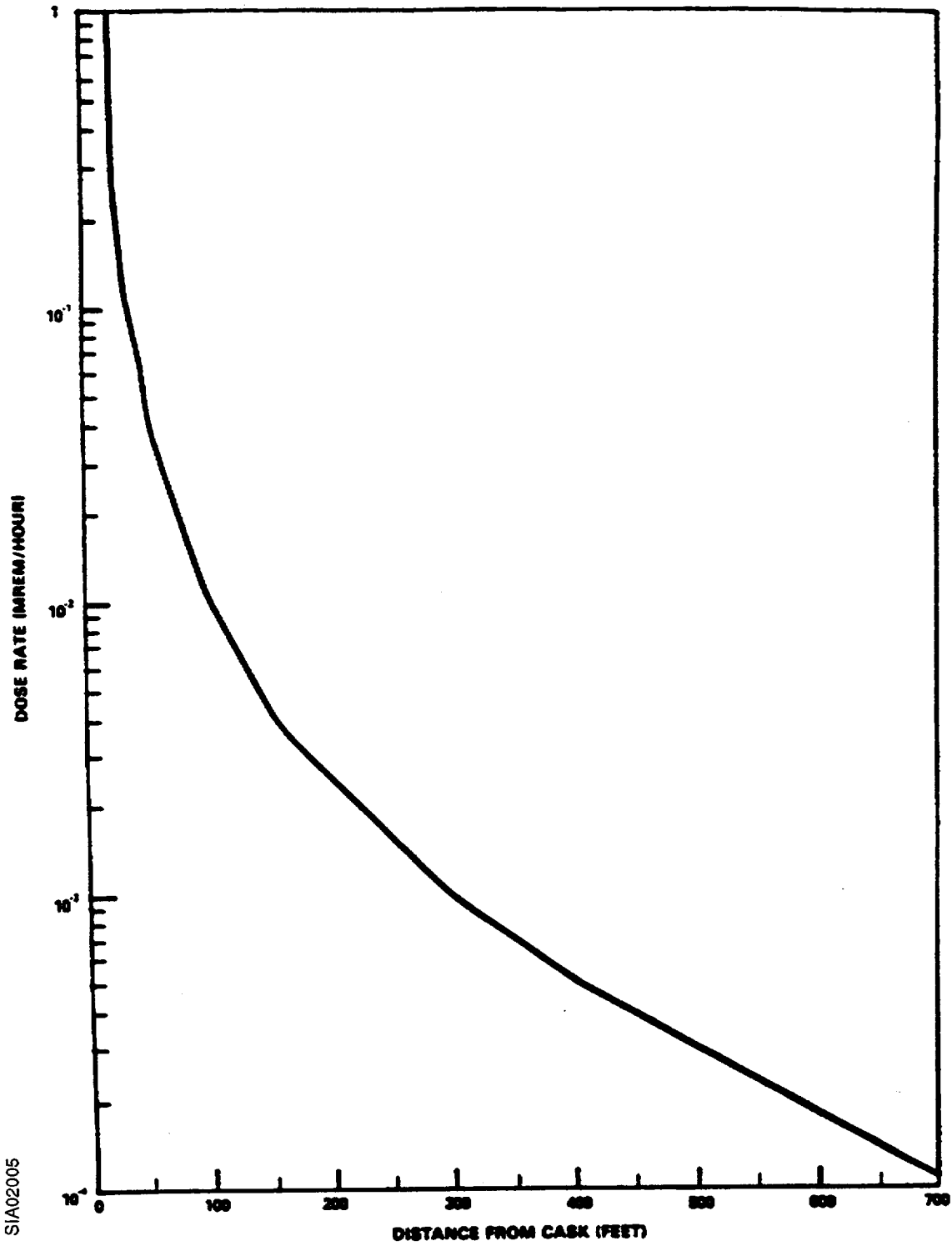
SIA02003

Figure A.2/7.3-4a  
WESTINGHOUSE MC-10  
NEUTRON DOSE RATE FROM ONE CASK  
VERSUS DISTANCE  
(0-700 FEET)



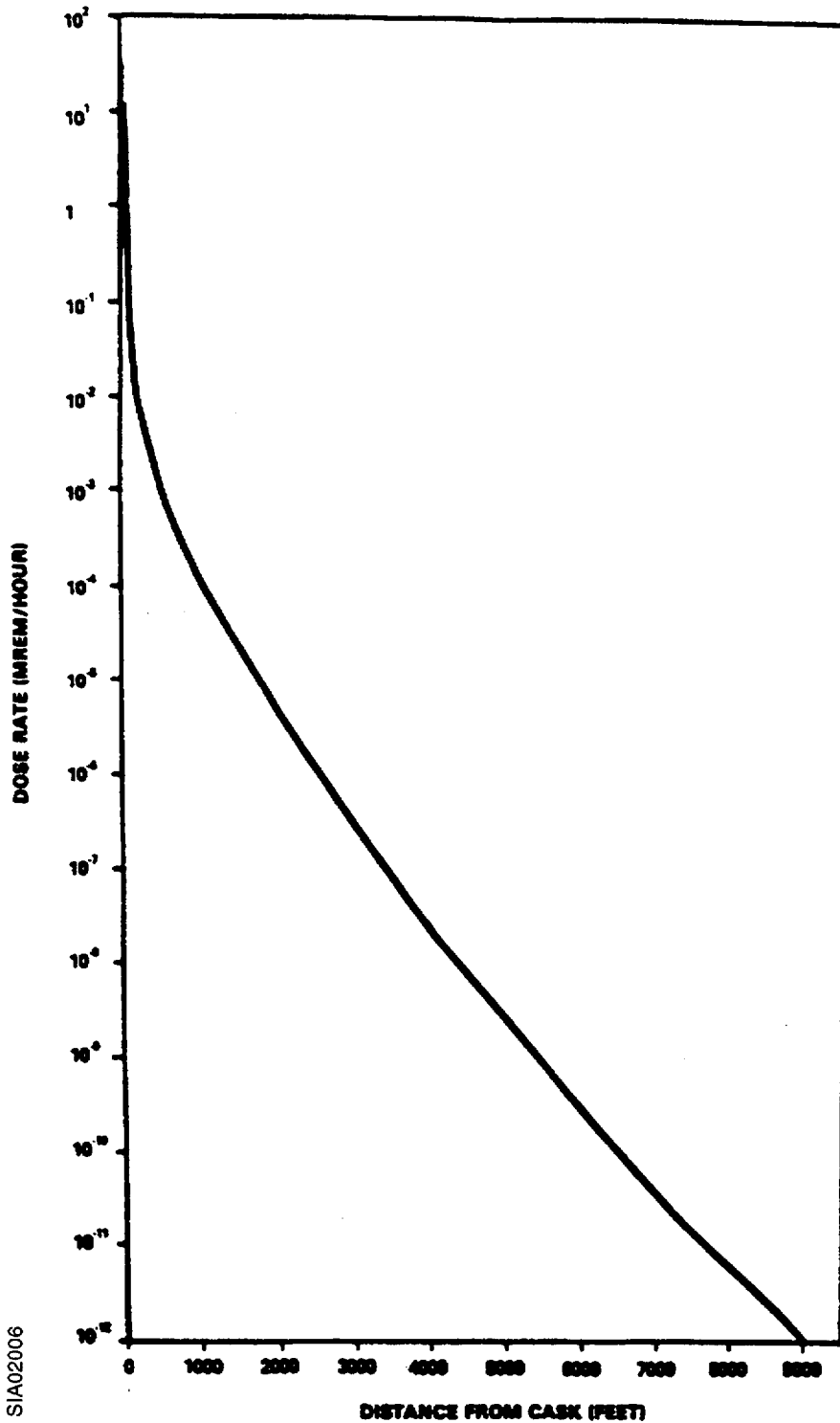
SIA02004

Figure A.2/7.3-4b  
WESTINGHOUSE MC-10  
GAMMA DOSE RATE FROM ONE CASK  
VERSUS DISTANCE  
(0-700 FEET)



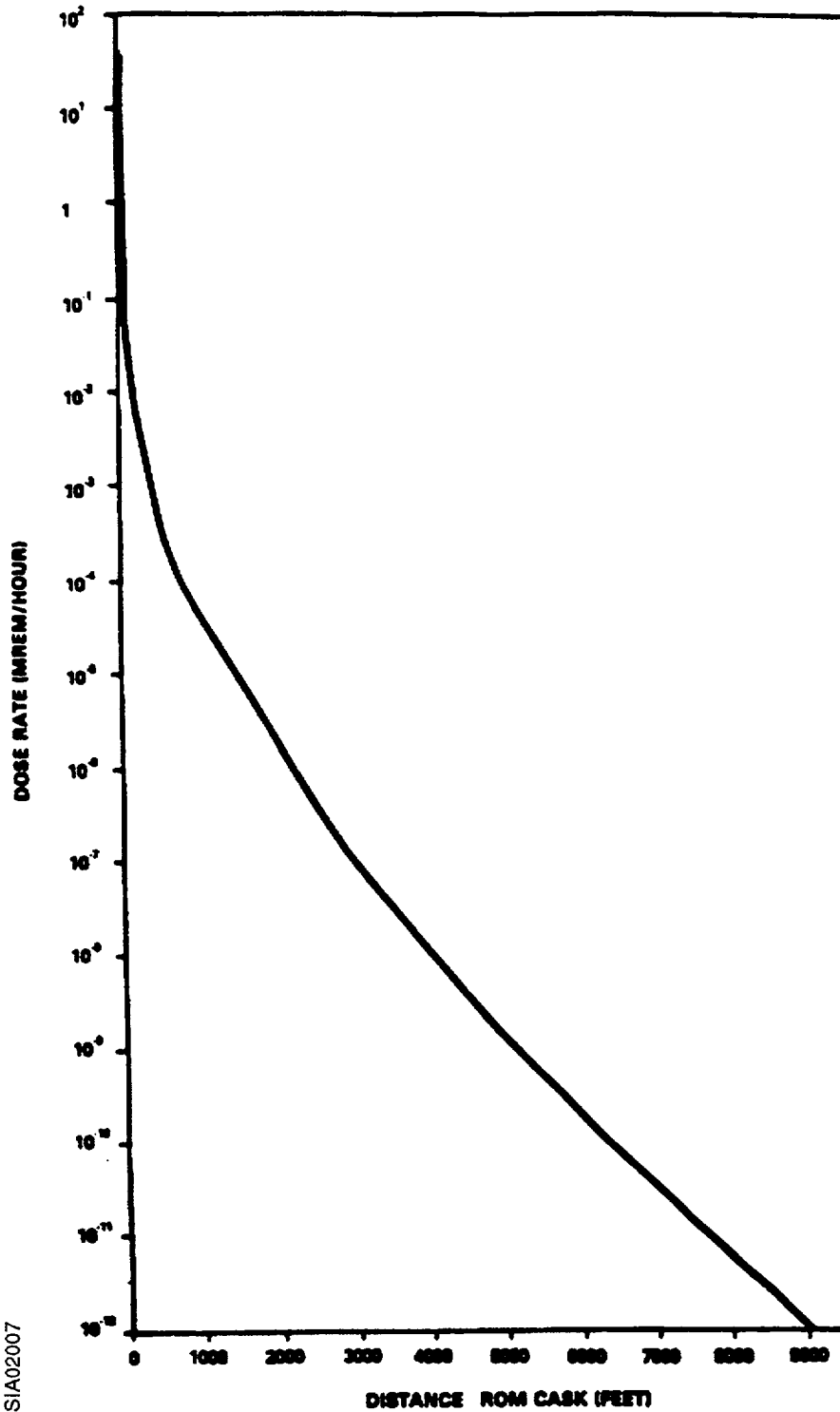
SIA02005

Figure A.2/7.3-5a  
WESTINGHOUSE MC-10  
NEUTRON DOSE RATE FROM ONE CASK  
VERSUS DISTANCE  
(0-9000 FEET)



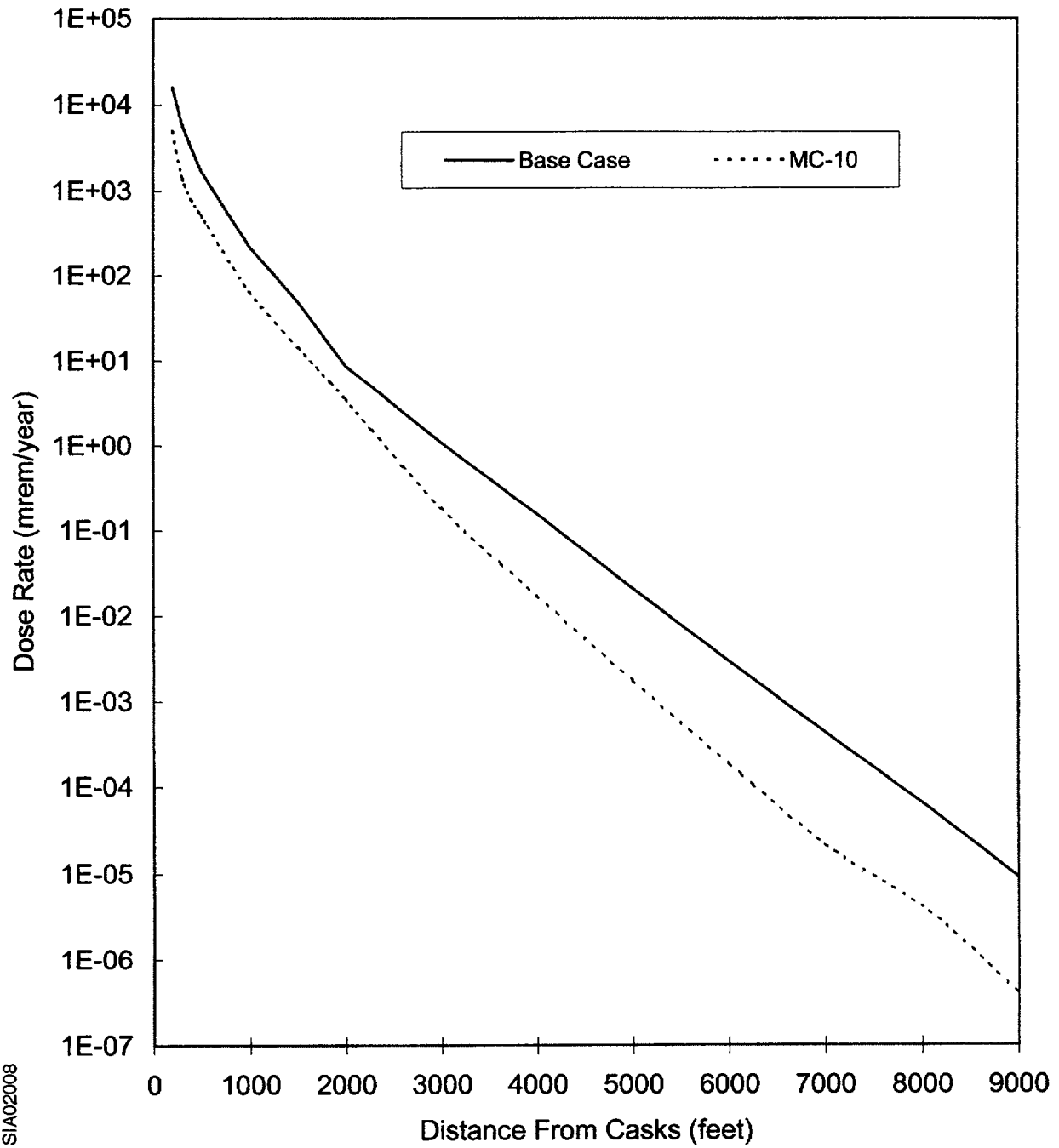
SIA02006

Figure A.2/7.3-5b  
WESTINGHOUSE MC-10  
GAMMA DOSE RATE FROM ONE CASK  
VERSUS DISTANCE  
(0-9000 FEET)



SIA02007

Figure A.2/7.3-6  
DOSE RATE FOR 74 MC-10 CASKS VERSUS DISTANCE  
COMPARED TO ISFSI DESIGN BASIS BASE CASE VERSUS DISTANCE



SIA02008

### **A.2/8.2.2 Extreme Wind**

The effects and consequences of extreme winds on the Westinghouse cask are presented in Section 8.2.7 of the Westinghouse Topical Report. For a 360 mph tornado wind, the Westinghouse analysis concludes that the cask will not topple during the tornado event. If the 360 mph tornado wind is combined with a 3 psi tornado pressure drop, sufficient load will result to topple the cask. The consequences of a postulated cask topple are conservatively bounded by the 5-foot drop accident in Section 8.2.6 of the Westinghouse Topical Report.

### **A.2/8.2.5 Fire**

The ability of the Westinghouse cask to withstand postulated fires is presented in Section 8.2.4 of the Westinghouse Topical Report. As concluded in Surry ISFSI SAR Section 8.2.5, no fires other than small electrical fires are credible at the ISFSI slab. Therefore, consistent with Section 8.2.4.3 of the Westinghouse Topical Report, a total loss of the cask neutron shield due to fire exposure is not a credible event for the Surry ISFSI. See also Section A.2/8.2.8 of this Appendix.

### **A.2/8.2.8 Loss of Neutron Shield**

As discussed in Section 1.3.2 of the Westinghouse Topical Report, the MC-10 cask features an outer shell of neutron absorbing material (BISCO NS-3) which is encapsulated at the cask outer surface between the ribs and at the cask bottom and the top seal cover. The neutron absorbing material also contributes an energy-absorbing feature during a postulated drop accident.

Section 8.2.2 and 8.2.4 of the Westinghouse Topical Report postulate a loss of this outer neutron shielding due to fire. However, no fires other than small electrical fires are credible at the ISFSI slab based on Section 8.2.5 of the Surry ISFSI SAR. Therefore, consistent with the Westinghouse evaluation of this event, a total loss of the cask neutron shield due to fire exposure is not a credible event for the Surry ISFSI.

Should the outer neutron shield be damaged from a postulated fire, cask tip-over, or cask drop event, temporary shielding could be placed external to the cask (e.g., high temperature polyethylene sheets or concrete blocks) until the cask shielding could be repaired. Depending on the extent of damage, Section 8.2.10 of the Surry ISFSI SAR outlines the steps that would be taken to return the cask to the spent fuel pool to facilitate the repair or replacement of the portion of the BISCO NS-3 that was damaged. See also the discussion in Section 8.2.2.3 of the Westinghouse Topical Report.

**Intentionally Blank**

*Appendix A.3*  
*NAC Intact 28 S/T Cask*

2

## **Appendix A.3**

### **NAC INTACT 28 S/T CASK**

#### **GENERAL DESCRIPTION**

The NAC-I28 S/T cask is a smooth right circular cylinder of multiwall construction with a 1.5 inch thick inner shell and a 2.63 inch thick outer shell of austenitic stainless steel separated by 3.2 inches of lead gamma shielding. The inner and outer shells are connected to each other at the ends by an austenitic stainless steel ring and plate. The upper end of the cask is sealed by an austenitic stainless steel bolted closure lid which is 6.5 inches thick in the edge flange region and has a 1-inch inner closure plate and a 5.5-inch outer closure plate. The closure plates are separated by two inches of lead gamma shielding. The closure lid utilizes a double barrier seal system with two metallic o-rings forming the seals. The lower end of the cask is 6 inch thick austenitic stainless steel with a 1 inch outer closure plate. The bottom end closure plates are separated by 1.80 inches of lead gamma shielding. The cask body is approximately 181 inches long and 94 inches in diameter. Neutron emissions from the stored fuel are attenuated by an integral neutron shield located outside the outer shell which contains a 7-inch thickness of borated solid neutron shield material. Neutron emissions from the top of the cask are attenuated during storage by a 3-inch thick solid neutron shield cap encased in stainless steel.

The cask contains a basket assembly which consists of 28 storage locations. The aluminum basket structure provides nuclear criticality control, structural integrity, and heat transfer to the cask cavity wall.

A tipover impact limiter is attached to the top of the cask after the cask is placed at the ISFSI. This impact limiter consists of an annular ring of aluminum honeycomb material enclosed in a thin stainless steel shell with a backing ring, web plates and a bearing ring providing structural support. The impact limiter is bolted to the cask body through eight tabs welded to the top of the bearing ring.

#### **A.3/3.1.1 Materials to be Stored**

The structural evaluations of the NAC-I28 S/T are provided in Chapters 4 and 8 of the Topical Report. These evaluations used a fuel weight of 1440 lb, but the possible combinations of Surry Units 1 and 2 fuel assemblies containing a burnable poison rod assembly (BPRA) or thimble plugging device (TPD) could weigh up to 1525 lb. However, this cask design is also approved for the storage of consolidated fuel canisters weighing up to 2988 lb. Therefore, the use of combined fuel assembly and BPRA or TPD weights of up to 1525 lb is acceptable for the NAC-I28 S/T.

An evaluation has also been performed on the effect to the cask surface dose rates as a result of placing BPRAs or TPDs in the fuel stored in the NAC-I28 S/T. This evaluation confirmed that the calculated surface dose rates for the NAC-I28 S/T remained less than the design basis dose rates used to calculate doses at the ISFSI perimeter and to the nearest resident.

An evaluation has been performed on the effect on criticality control from the storage of BPRAs or TPDs in the fuel stored in the NAC-I28 S/T. BPrA rods will displace water (a moderator) in the fuel assembly thimble tubes, therefore, even the use of depleted BPRAs will reduce reactivity in a cask. TPDs are short and do not displace water in the thimble tubes, therefore, their use will not affect reactivity.

The NAC-I28 S/T is designed for a maximum internal pressure under accident conditions, and helium buildup or pre-pressurization in BPRAs will affect this analysis. The confinement analysis for the NAC-I28 S/T has been reanalyzed for twenty-eight 20-finger BPRAs, and this reanalysis shows that the maximum pressure under accident conditions would be 116.5 psia, when the design basis for this cask is 150 psia. The impact of TPDs on the confinement analysis is bounded by the impact of BPRAs.

To account for the additional decay heat from BPRAs and TPDs, fuel assembly decay heat estimates must include an estimate for the decay heat from the actual component in each fuel assembly. Therefore, the combined decay heat from the fuel assembly and its component must be less than the limit for a fuel assembly in the NAC-I28 S/T.

Based on these evaluations, the storage of fuel assemblies with BPRAs or TPDs is acceptable for the NAC-I28 S/T.

#### **A.3/7.3.2.1 Cask Surface Dose Rates**

The NAC-I28 S/T cask is evaluated for fuel with an initial enrichment of 1.9 wt.% U-235 and burnup of 22,000 MWD/MTU.

The NAC-I28 S/T cask surface dose rates and energy spectra are provided in a supplement (Reference 11) to the NAC Topical Report (Reference 1).

Neutron and gamma source terms for the stored spent fuel were generated using OREST (ORIGEN II). Typical results from these runs are shown in Surry ISFSI SAR Tables 7.2-1, 7.2-2, 7.2-3 and 7.2-4. XSDRNPM-S (Reference 10) was used by NAC to calculate the cask surface fluxes. The NAC-I28 S/T cask average surface dose rates for 10-year-old fuel are 0.30 mrem/hour neutron and 7.88 mrem/hour gamma for the side and 3.56 mrem/hour neutron and 32.91 mrem/hour gamma for the top. When these dose rates are combined, the side and top average surface dose rates are 8.18 mrem/hour and 36.47 mrem/hour, respectively. These dose rates are bounded by the total average surface dose rates of 224 mrem/hour for the side and 76 mrem/hour for the top reported in the Surry ISFSI SAR, Section 7.3.2.1.

Figure A.3/7.3-2 shows the normalized surface dose rates on NAC-I28 S/T cask versus age of spent fuel for both gamma and neutron radiation.

#### **A.3/7.3.2.2 Dose Rate Versus Distance**

The cask surface dose rates discussed in Section A.3/7.3.2.1 result in the dose rates at various distances as shown on Figures A.3/7.3-3a through A.3/7.3-6. The neutron transport results

shown on these figures were generated using a series of adjoint (References 2 & 3) ANISN (Reference 4) runs. These calculations were performed with a BUGLE-80 (Reference 5) cross-section set for an infinite-air medium. As explained in References 2 and 3, the adjoint method is the preferred analytical technique when more than one set of sources must be evaluated at a given detector location for a response of interest. For the adjoint analyses reported here, the adjoint source is the flux-to-dose conversion factor reported in Reference 9. Four separate ANISN analyses were performed at distances of 50, 460, 1500, and 2460 meters. The resulting adjoint fluxes are presented in Table A.1/7.3-3. These adjoint fluxes were then folded with the cask surface leakage spectra supplied by NAC over the area of the cask's top and side. Cask surface neutron leakage data are provided in Table A.3/7.3-2.

The resultant neutron dose rates were then used to construct the dose rate versus distance curves presented on Figures A.3/7.3-3a, A.3/7.3-4a, and A.3/7.3-5a.

For the gamma-ray transport, simple point kernel calculations using infinite medium dose rate buildup factors in dry air were performed. Using a point source model and References 6 and 7, air-to-void correction factors were developed and applied to the gamma dose rates in void based on Reference 8. The gamma dose rates for the casks are shown on Figures A.3/7.3-3b, A.3/7.3-4b, and A.3/7.3-5b.

For Figure A.3/7.3-6, decay factors have been used assuming that 3 NAC-I28 S/T casks are placed in the ISFSI each year for 21 years and each new group of 3 casks has a minimum of 10 years decay of the fuel. As shown on Figure A.3/7.3-6, the design basis dose rate for the ISFSI bounds the dose rate for the ISFSI filled to capacity with NAC-I28 S/T casks.

#### A.3/7.3.5 References

1. *Topical Safety Analysis Report for the NAC Storage/Transport Cask Containing 28 Intact Fuel Assemblies for use at an Independent Spent Fuel Storage Installation*, Nuclear Assurance Corporation, November 1988.
2. V. R. Cain, The Use of Discrete Ordinates Adjoint Calculations, *A Review of the Discrete Ordinates 5 Method for Radiation Transport Calculations*, ORNL-RSIC-19, March 1968, pp. 85-94.
3. G. I. Bell, S. Glasstone, *Nuclear Reactor Theory*, Chapter 6.1 - The Adjoint Function and Its Applications, Van Nostrand Reinhold Company, New York, 1970.
4. W. W. Engle, Jr., *A User's Manual for ANISN, A One-Dimensional Discrete Ordinates Transport Code with Anisotropic Scattering*, K-1643, Union Carbide Corporation, Nuclear Division, June 1973.
5. *BUGLE-80, Coupled 47-Neutron, 20-Gamma-Ray, P3, Cross-Section Library for LWR Shielding Calculations*, DLC-75, R. W. Roussin, ORNL, June 1980.

6. Warkentin, J. K., *Polynomial Coefficients for Dose Buildup in Air*, Radiation Research Associates, Inc., August 15, 1975, RRA-N7511.
7. Hubbell, L. H., *Photon Cross-Sections, Attenuation Coefficients, and Energy Absorption Coefficients from 10 KeV to 100 GeV*, National Bureau of Standards, August 1969, NSRDS-NBS29.
8. Spacetran II, *Dose Calculations at Detectors at Various Distances from the Surface of a Cylinder*, Neutron Physics Division of Oak Ridge National Laboratory, September 1973, ORNL-TM-2592.
9. ANSI/ANS-6.1.1-1977, *American National Standard - Neutron and Gamma Ray Flux to Dose Rate Factors*, American Nuclear Society, March 17, 1977.
10. NUREG/CR-0200, Vol. 2, *XSDRNPM-S: A One-Dimensional Discrete-Ordinates Code for Transport Analysis*, ORNL/NUREG/CSD-2/V2/R1, N. M. Green & L. M. Petrie, ORNL Computer Sciences Division, Oak Ridge, Tennessee, 1983.
11. Letter from Alan H. Wells (NAC) to John P. Roberts (NRC), Docket No. M-54, March 1, 1989.
12. [Deleted]

Table A.3/7.3-2  
 NAC-I28 S/T SURFACE NEUTRON LEAKAGES

| Neutron Group | Upper <sup>a</sup> Energy (ev) | Cask Surface Leakage Spectra<br>(n/cm <sup>2</sup> - sec) |          |
|---------------|--------------------------------|---|----------|
|               |                                | Side  | Top      |
| 1             | 1.7E+7                         | 4.55E-04  | 9.21E-05 |
| 2             | 1.4E+7                         | 1.59E-03  | 3.77E-04 |
| 3             | 1.2E+7                         | 5.84E-03  | 1.69E-03 |
| 4             | 1.0E+7                         | 1.07E-02  | 3.74E-03 |
| 5             | 8.6E+6                         | 1.85E-02  | 7.43E-03 |
| 6             | 7.4E+6                         | 3.94E-02  | 1.88E-02 |
| 7             | 6.1E+6                         | 5.33E-02  | 2.71E-02 |
| 8             | 5.0E+6                         | 9.74E-02  | 5.10E-02 |
| 9             | 3.7E+6                         | 8.10E-02  | 4.90E-02 |
| 10            | 3.0E+6                         | 5.04E-02  | 3.79E-02 |
| 11            | 2.7E+6                         | 5.68E-02  | 4.91E-02 |
| 12            | 2.5E+6                         | 2.96E-02  | 2.69E-02 |
| 13            | 2.4E+6                         | 6.60E-03  | 7.67E-03 |
| 14            | 2.3E+6                         | 3.66E-02  | 4.02E-02 |
| 15            | 2.2E+6                         | 1.12E-01  | 1.18E-01 |
| 16            | 1.9E+6                         | 1.23E-01  | 1.50E-01 |
| 17            | 1.6E+6                         | 1.78E-01  | 2.41E-01 |
| 18            | 1.4E+6                         | 3.12E-01  | 5.81E-01 |
| 19            | 1.0E+6                         | 1.99E-01  | 4.71E-01 |
| 20            | 8.2E+5                         | 9.46E-02  | 2.25E-01 |
| 21            | 7.4E+5                         | 1.94E-01  | 6.92E-01 |
| 22            | 6.1E+5                         | 1.85E-01  | 8.69E-01 |
| 23            | 5.0E+5                         | 2.25E-01  | 1.05E+00 |
| 24            | 3.7E+5                         | 1.56E-01  | 9.29E-01 |
| 25            | 3.0E+5                         | 2.58E-01  | 1.56E+00 |
| 26            | 1.8E+5                         | 2.13E-01  | 1.43E+00 |
| 27            | 1.1E+5                         | 1.58E-01  | 1.11E+00 |
| 28            | 6.7E+4                         | 1.34E-01  | 1.05E+00 |
| 29            | 5.0E+4                         | 5.15E-02  | 4.08E-01 |
| 30            | 3.2E+4                         | 2.41E-02  | 2.07E-01 |
| 31            | 2.6E+4                         | 3.80E-02  | 2.90E-01 |
| 32            | 2.4E+4                         | 2.96E-02  | 2.09E-01 |
| 33            | 2.2E+4                         | 7.54E-02  | 6.12E-01 |
| 34            | 1.5E+4                         | 1.62E-01  | 1.38E+00 |
| 35            | 7.1E+3                         | 1.32E-01  | 1.27E+00 |

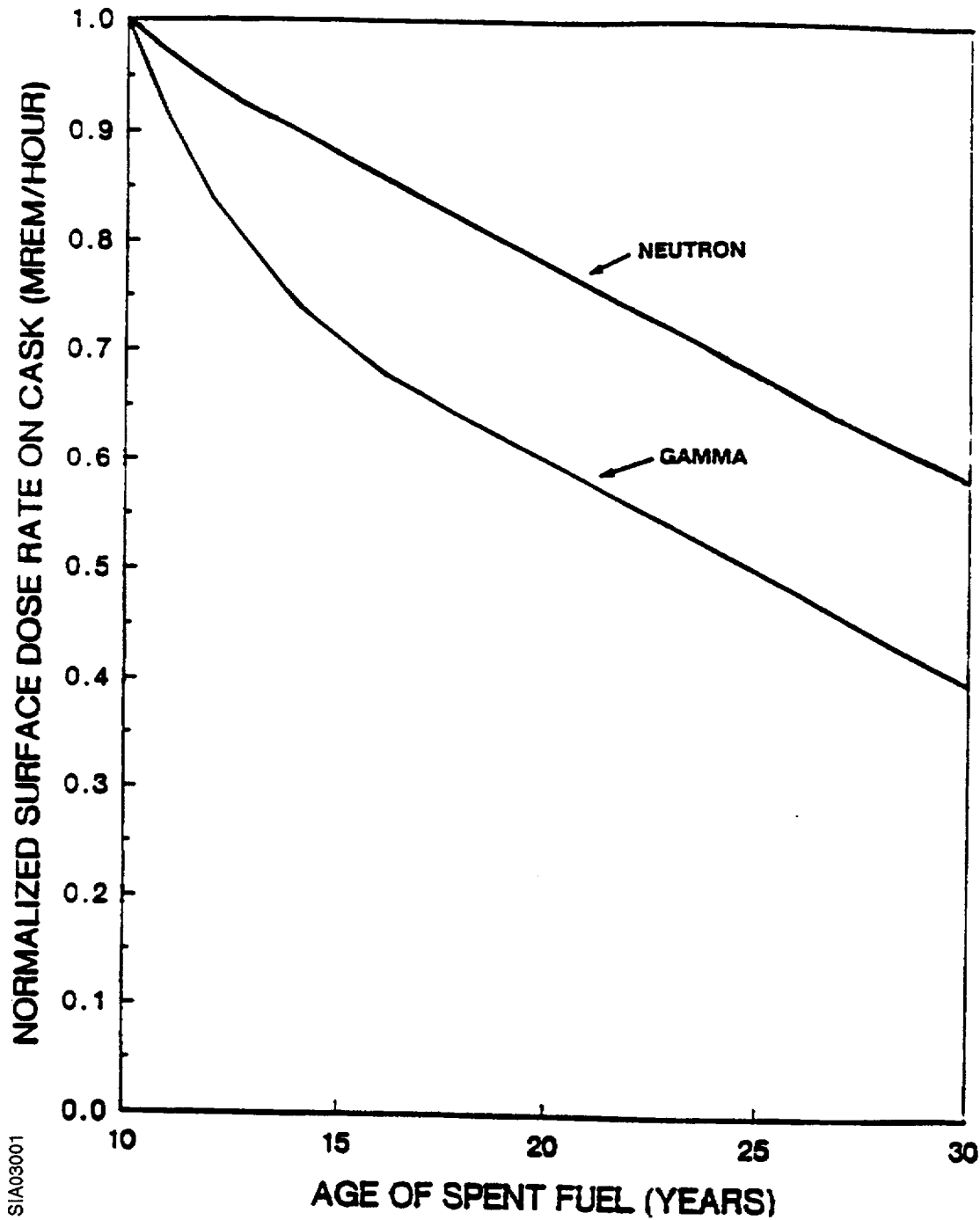
Table A.3/7.3-2  
 NAC-I28 S/T SURFACE NEUTRON LEAKAGES

| Neutron Group | Upper <sup>a</sup> Energy (ev) | Cask Surface<br>Leakage Spectra<br>(n/cm <sup>2</sup> - sec) |          |
|---------------|--------------------------------|--|----------|
|               |                                | Side   | Top      |
| 36            | 3.4E+3                         | 1.41E-01   | 1.46E+00 |
| 37            | 1.6E+3                         | 2.57E-01   | 2.76E+00 |
| 38            | 4.5E+2                         | 1.41E-01   | 1.65E+00 |
| 39            | 2.1E+2                         | 1.49E-01   | 1.83E+01 |
| 40            | 1.0E+2                         | 2.04E-01   | 2.63E+01 |
| 41            | 3.7E+1                         | 2.64E-01   | 3.54E+01 |
| 42            | 1.1E+1                         | 1.62E-01   | 2.23E+01 |
| 43            | 5.0E+0                         | 1.93E-01   | 2.69E+01 |
| 44            | 1.8E+0                         | 1.45E-01   | 2.03E+01 |
| 45            | 8.8E-1                         | 1.36E-01   | 1.92E+01 |
| 46            | 4.1E-1                         | 2.31E-01   | 3.29E+01 |
| 47            | 1.0E-1                         | 1.93E-01   | 2.72E+01 |

Note: NAC-I28 S/T Cask Surface Area: 274,236 cm<sup>2</sup> (side),  
 38,133 cm<sup>2</sup> (top).

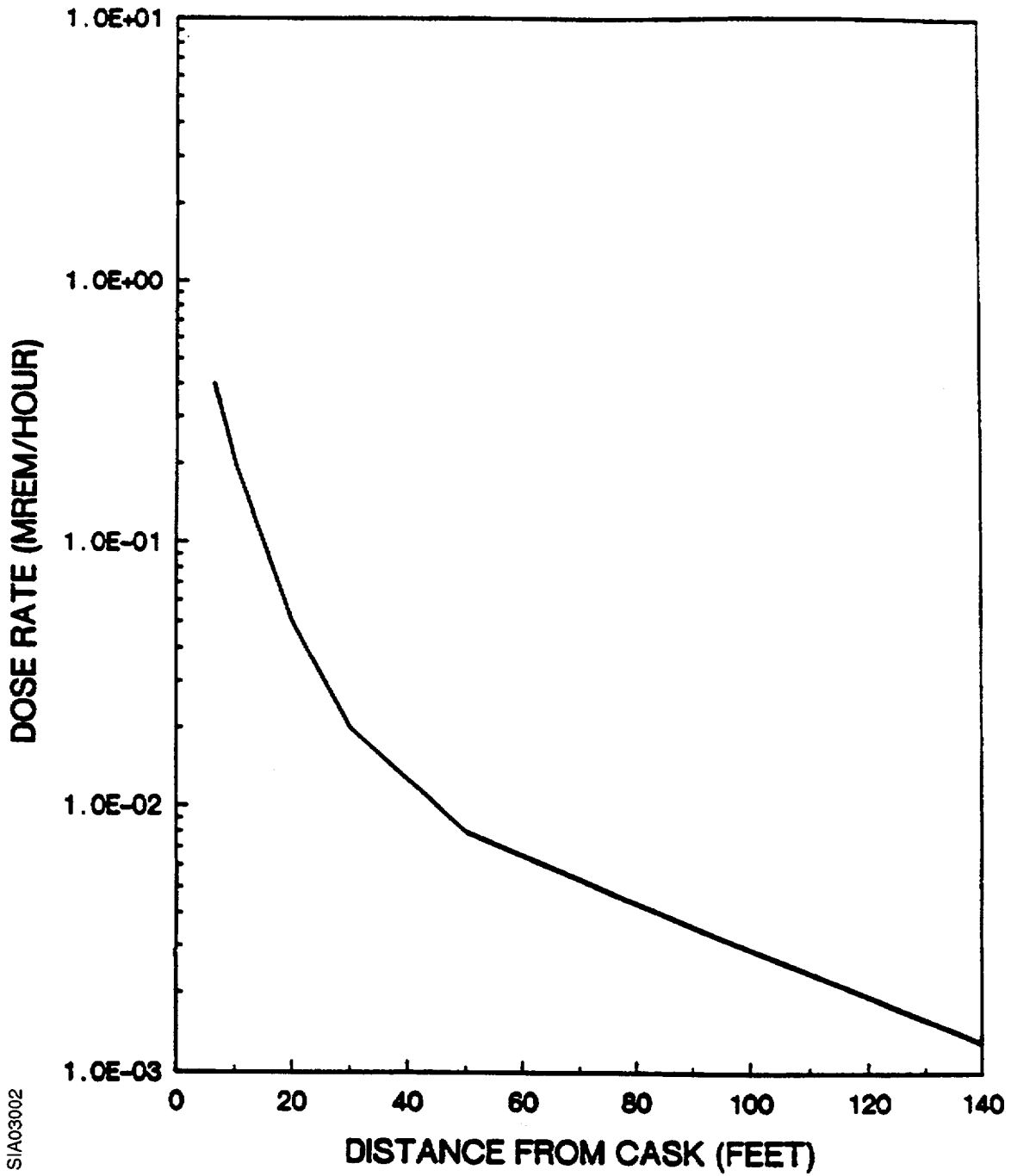
a.Reference 5.

Figure A.3/7.3-2  
NORMALIZED SURFACE DOSE RATE ON  
NAC-I28 S/T CASK  
VERSUS AGE OF SPENT FUEL



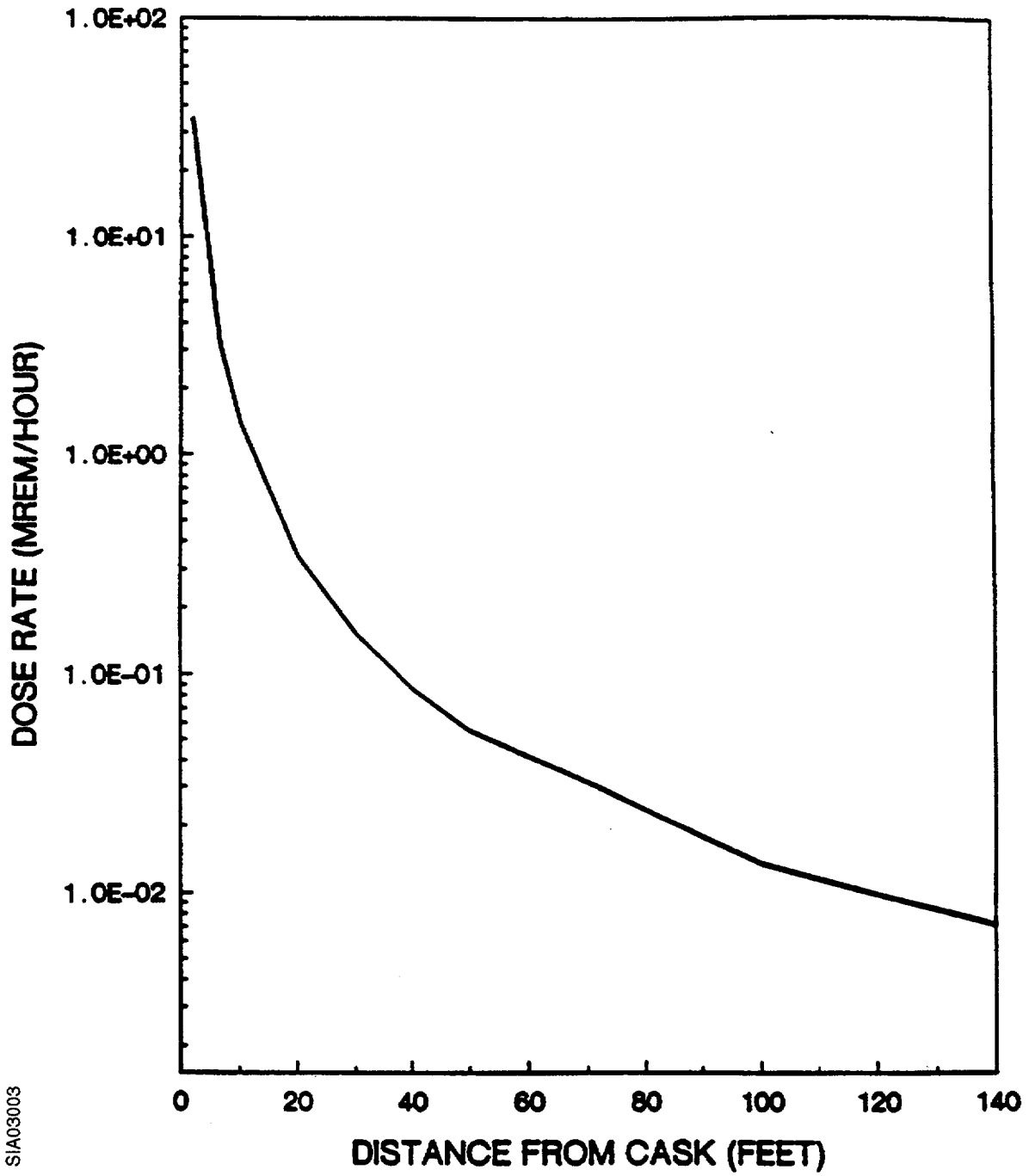
SIA03001

Figure A.3/7.3-3a  
NAC-I28 S/T  
NEUTRON DOSE RATE FROM ONE CASK  
VERSUS DISTANCE  
(0-140 FEET)



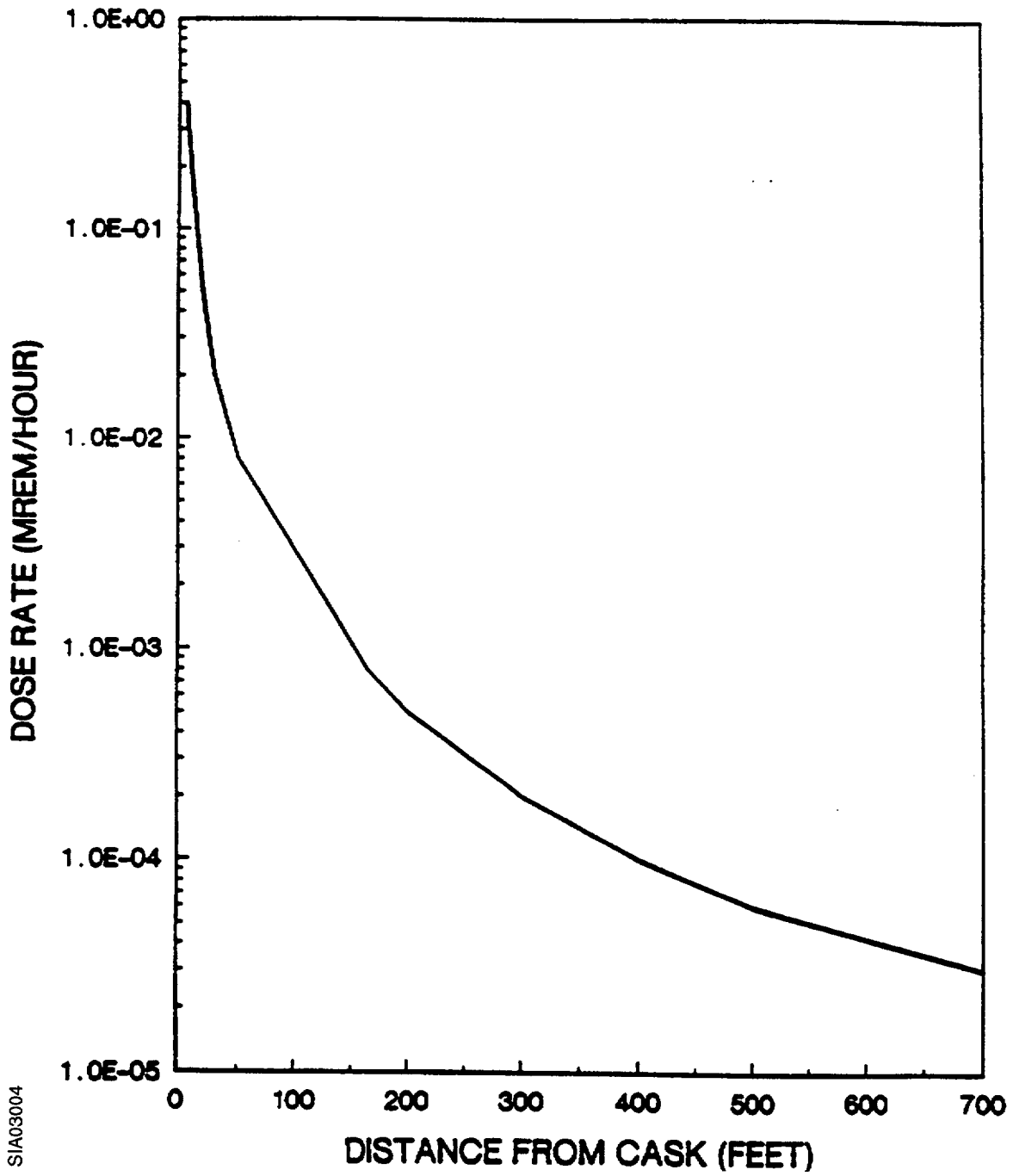
SIA03002

Figure A.3/7.3-3b  
NAC-I28 S/T  
GAMMA DOSE RATE FROM ONE CASK  
VERSUS DISTANCE  
(0-140 FEET)



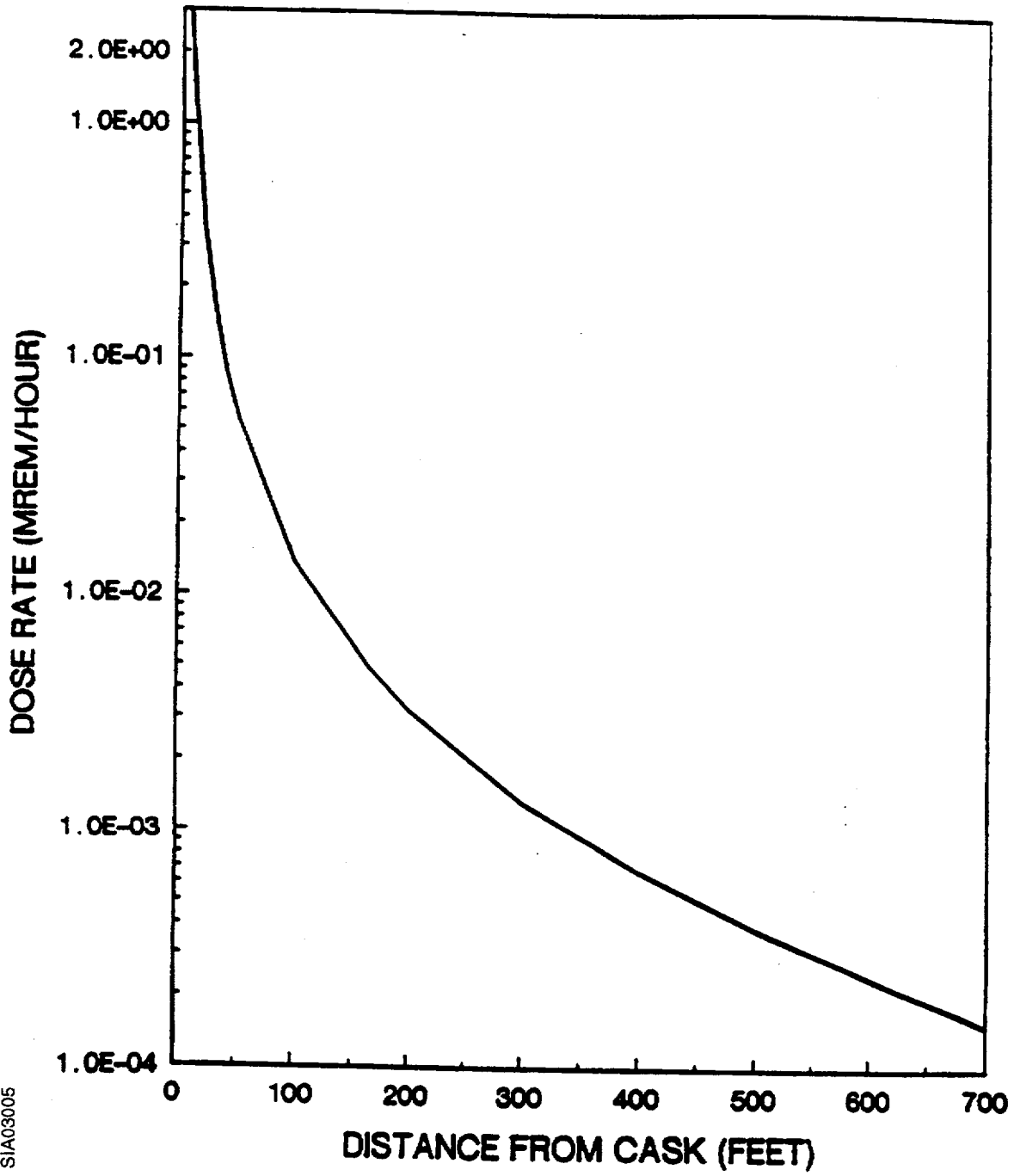
SIA03003

Figure A.3/7.3-4a  
NAC-I28 S/T  
NEUTRON DOSE RATE FROM ONE CASK  
VERSUS DISTANCE  
(0-700 FEET)



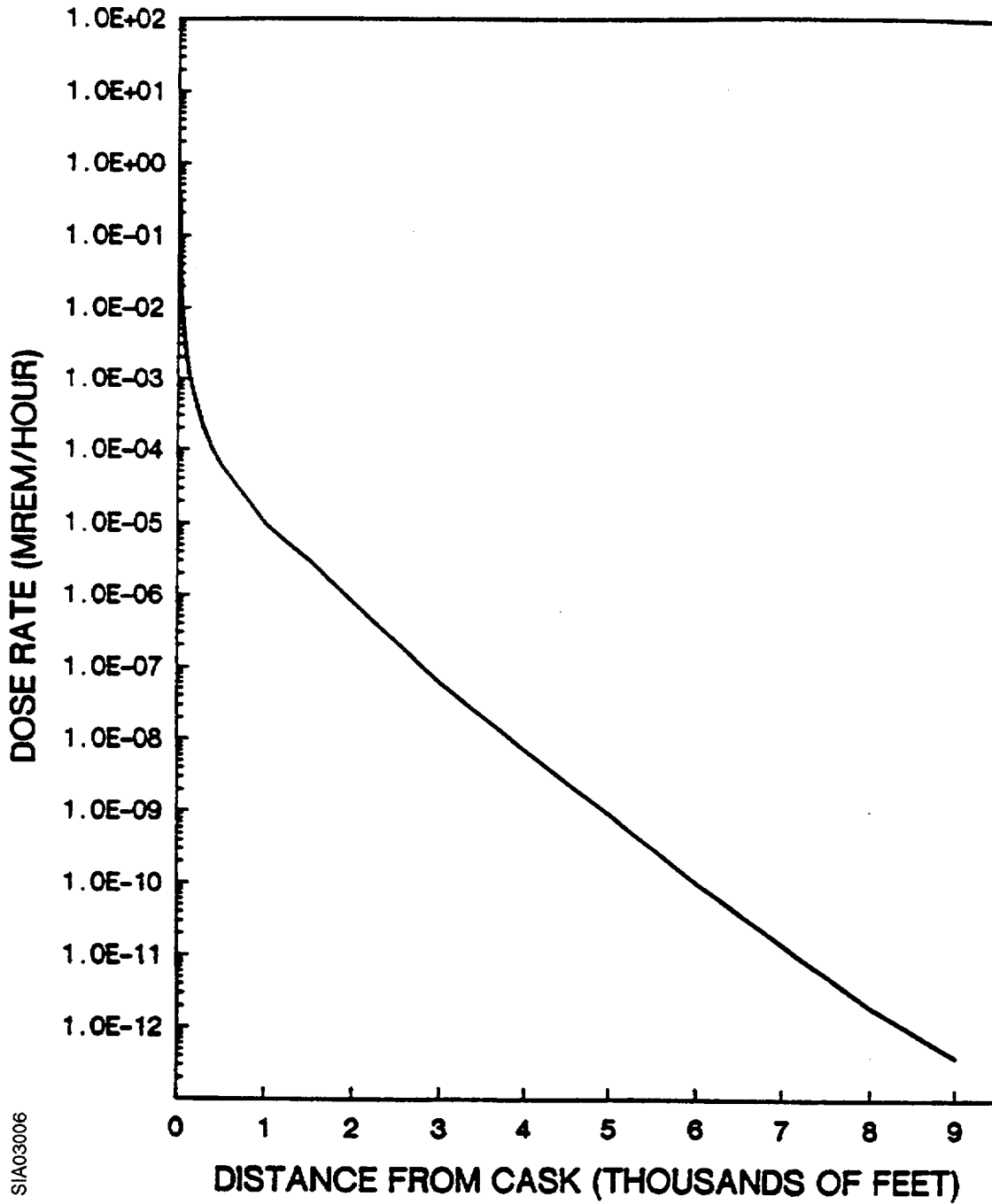
SIA03004

Figure A.3/7.3-4b  
NAC-I28 S/T  
GAMMA DOSE RATE FROM ONE CASK  
VERSUS DISTANCE  
(0-700 FEET)



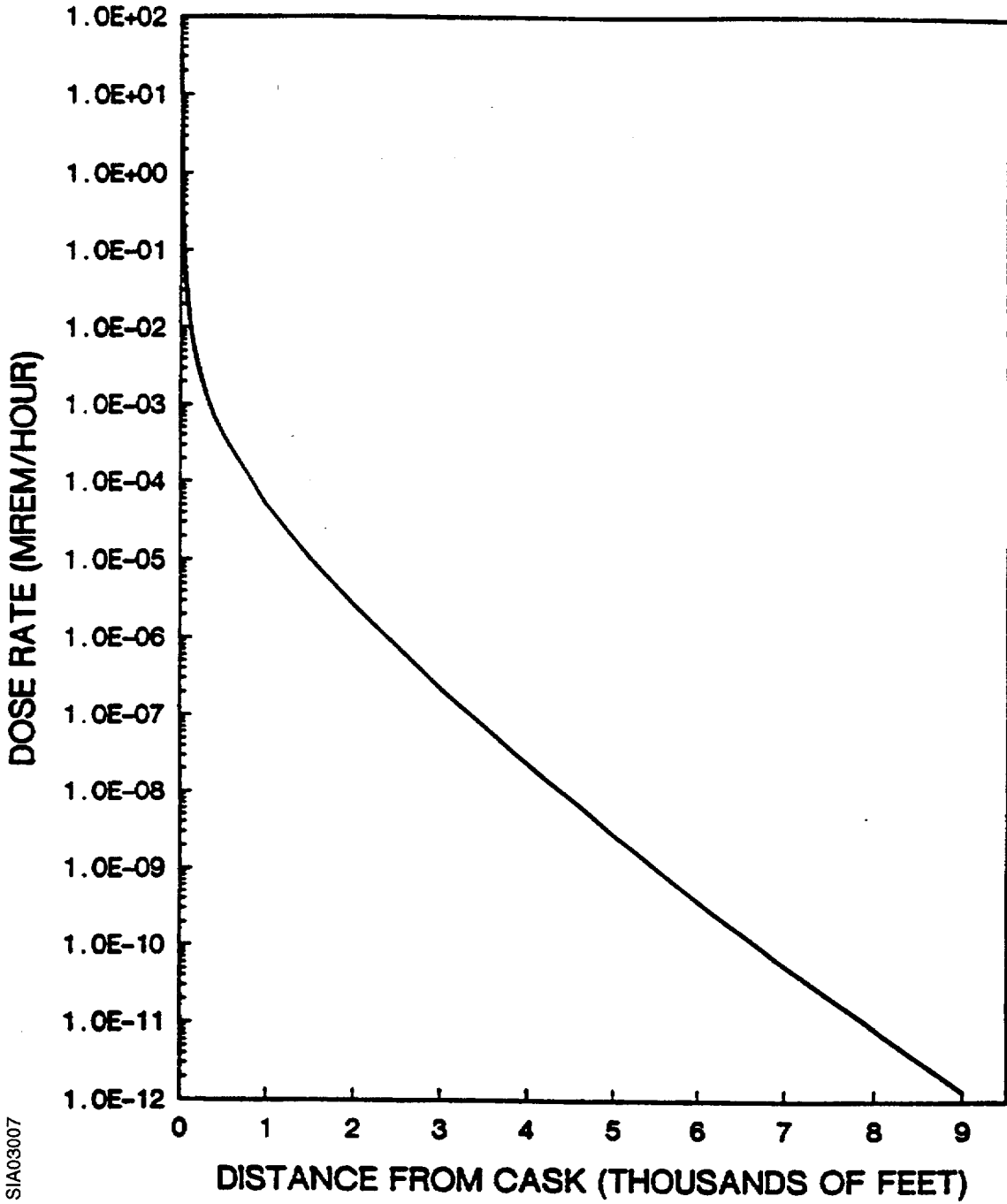
SIA03005

Figure A.3/7.3-5a  
NAC-I28 S/T  
NEUTRON DOSE RATE FROM ONE CASK  
VERSUS DISTANCE  
(0-9000 FEET)



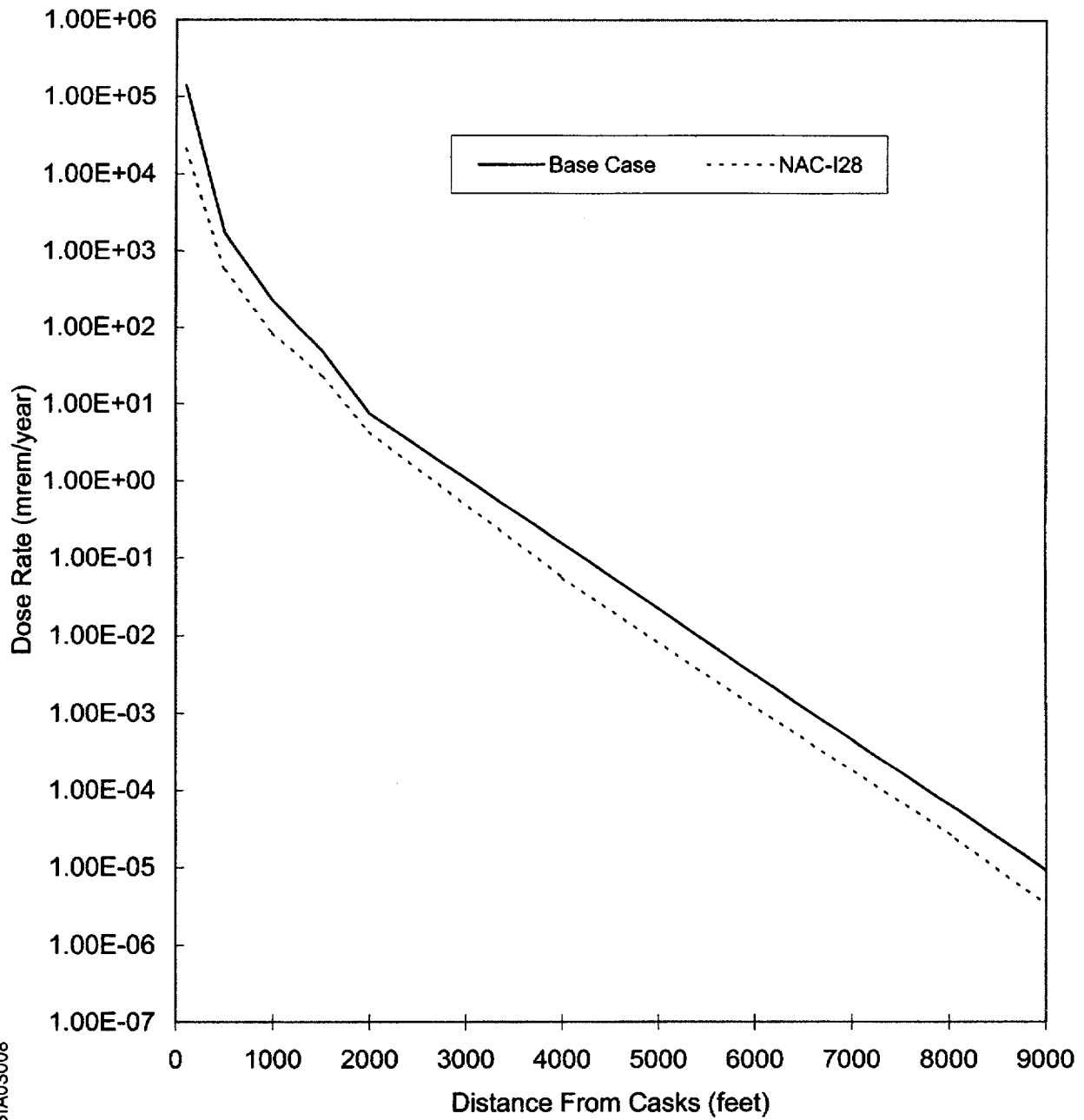
SIA03006

Figure A.3/7.3-5b  
NAC-I28 S/T  
GAMMA DOSE RATE FROM ONE CASK  
VERSUS DISTANCE  
(0-9000 FEET)



SIA03007

Figure A.3/7.3-6  
DOSE RATE FOR 63 NAC-I/28 CASKS  
VERSUS DISTANCE COMPARED TO ISFSI DESIGN  
BASIS BASE CASE VERSUS DISTANCE



SIA03008

**A.3/8.2.2 Extreme Wind**

The effects and consequences of extreme winds on the NAC-I28 S/T cask are presented in Section 8.2.7 of the NAC Topical Report. The NAC analysis demonstrates that extreme winds are not capable of overturning their cask nor of producing leakage from it. Since no radioactivity would be released, no resultant doses would occur.

**A.3/8.2.5 Fire**

The ability of the NAC-I28 S/T cask to withstand postulated fires is presented in Section 8.2.2 of the NAC Topical Report. As concluded in Surry ISFSI SAR Section 8.2.5, no fires other than small electrical fires are credible at the ISFSI slab. Therefore, consistent with Section 8.2.2.2 of the NAC Topical Report, a total loss of the cask neutron shield due to fire exposure is not a credible event for the Surry ISFSI. See also Section A.3/8.2.8 of this Appendix.

**A.3/8.2.8 Loss of Neutron Shield**

As discussed in Section 1.2.4 of the NAC Topical Report, the NAC-I28 S/T cask features an outer shell which contains a 7-inch thickness of borated solid shield material. Sections 8.2.1 and 8.2.2 of the NAC Topical Report postulate a loss of this outer neutron shielding due to fire. However, no fires other than small electrical fires are credible at the ISFSI slab based on Section 8.2.5 of the Surry ISFSI SAR. Therefore, consistent with the NAC evaluation of this event, a total loss of the cask neutron shield due to fire exposure is not a credible event for the Surry ISFSI.

Should the outer neutron shield be damaged from a postulated fire, cask tip-over, or cask drop event, temporary shielding could be placed external to the cask (e.g., high temperature polyethylene sheets or concrete blocks) until the cask shielding could be repaired. Depending on the extent of damage, Section 8.2.10 of the Surry ISFSI SAR outlines the steps that would be taken to return the cask to the spent fuel pool to facilitate the repair or replacement of the portion of the neutron shield that was damaged. See also the discussion in Section 5.1.3.5 of the NAC Topical Report.

**Intentionally Blank**

*Appendix A.4*  
*CASTOR X/33 Cask*

## **Appendix A.4**

### **CASTOR X/33 CASK**

#### **GENERAL DESCRIPTION**

The GNSI CASTOR X/33 cask is a thick-walled ductile cast iron cylinder that is approximately 15.8 feet high, 7.8 feet in diameter, and weighs (empty) approximately 94.5 tons. The cask has a cylindrical cavity which holds a fuel basket designed to accommodate 33 PWR fuel assemblies. The loaded weight of the cask is approximately 118.3 tons. Four trunnions are bolted on, two at the head end and two at the bottom end of the body.

The cask is sealed with two stainless steel lids installed one on top of the other and bolted to the cask body. The primary lid is 10.2 inches thick and is secured to the cask body with 44 bolts. The secondary lid is 3.2 inches thick and is secured to the cask body with 70 bolts. Both lids are sealed with multiple seals consisting of metal seals and elastomer o-rings.

For improved neutron shielding, one row of axial holes in the wall of the cask body are filled with polyethylene rods. The cast iron wall of the cask provides gamma radiation shielding.

A tipover impact limiter is attached to the top of the cask after the cask is placed at the ISFSI. This impact limiter consists of an annular ring of aluminum honeycomb material enclosed in a stainless steel shell. The impact limiter is attached to the cask using a trunnion support assembly bolted to the underside of the impact limiter.

#### **A.4/3.1.1 Materials To Be Stored**

Due to weight restrictions imposed for handling of the CASTOR X/33 by the 125-ton cask crane, no fuel insert components of any kind may be stored in this cask.

#### **A.4/7.3.2.1 Cask Surface Dose Rates**

The assumptions used in calculating the GNSI CASTOR X/33 cask surface dose rates and energy spectra are provided in Sections 3.3.5 and 7.3.2.2 of the GNSI Topical Safety Analysis Report (Reference 1).

Neutron and gamma source terms for the stored spent fuel were generated using OREST (ORIGEN II). Typical results from these runs are shown in Surry ISFSI SAR Tables 7.2-1, 7.2-2, 7.2-3, and 7.2-4. ANISN (Reference 4) and DOT (Reference 10) were used by GNSI to calculate the cask surface fluxes. Flux-to-dose rate conversion factors, as shown in Tables 7.2-2 and 7.2-3 of the GNSI CASTOR X/33 Topical Safety Analysis Report (Reference 1), were then used to obtain the surface dose rates for the cask. The GNSI cask average surface dose rates for 10-year-old fuel are 18.1 mrem/hour neutron and 51.2 mrem/hour gamma for the side and 47.4 mrem/hour neutron and 0.7 mrem/hour gamma for the top. When these dose rates are combined, the side and top average surface dose rates are 69.3 mrem/hour and 48.1 mrem/hour, respectively. These dose rates are bounded by the total average surface dose rates of

224 mrem/hour for the side and 76 mrem/hour for the top reported in the Surry ISFSI SAR, Section 7.3.2.1.

Figure A.4/7.3-2 shows the normalized surface dose rates on the GNSI CASTOR X/33 cask versus age of spent fuel for both gamma and neutron radiation.

#### **A.4/7.3.2.2 Dose Rate Versus Distance**

The cask surface dose rates discussed in Section A.4/7.3.2.1 result in the dose rates at various distances as shown on Figures A.4/7.3-3a through A.4/7.3-6. The neutron transport results shown on these figures were generated using a series of adjoint (References 2 & 3) ANISN (Reference 4) runs. These calculations were performed with a BUGLE-80 (Reference 5) cross-section set for an infinite-air medium. As explained in References 2 and 3, the adjoint method is the preferred analytical technique when more than one set of sources must be evaluated at a given detector location for a response of interest. For the adjoint analyses reported here, the adjoint source is the flux-to-dose conversion factor reported in Reference 9. Four separate ANISN analyses were performed at distances of 50, 460, 1500, and 2460 meters. The resulting adjoint fluxes are presented in Table A.1/7.3-3. These adjoint fluxes were then folded with the cask surface leakage spectra supplied by GNSI over the area of the cask's top and side. Cask surface neutron leakage data are provided in Table A.4/7.3-2.

The resultant neutron dose rates were then used to construct the dose rate versus distance curves presented on Figures A.4/7.3-3a, A.4/7.3-4a, and A.4/7.3-5a.

For the gamma-ray transport, simple point kernel calculations using infinite medium dose rate buildup factors in dry air were performed. Using a point source model and References 6 and 7, air-to-void correction factors were developed and applied to the gamma dose rates in void based on Reference 8. The gamma dose rates for the casks are shown on Figures A.4/7.3-3b, A.4/7.3-4b, and A.4/7.3-5b.

For Figure A.4/7.3-6, decay factors have been used assuming that three casks are placed in the ISFSI each year for 18 years and each new group of three casks has a minimum of 10 years decay of the fuel. As shown on Figure A.4/7.3-6, the design basis dose rate for the ISFSI bounds the dose rate for the ISFSI filled to capacity with 54 GNSI CASTOR X/33 casks.

#### **A.4/7.3.5 References**

1. *Topical Safety Analysis Report for the GNSI CASTOR X Cask for an Independent Spent Fuel Storage Installation (Dry Storage)*, General Nuclear Systems, Inc., June 1988.
2. V. R. Cain, The Use of Discrete Ordinates Adjoint Calculations, *A Review of the Discrete Ordinates 5 Method for Radiation Transport Calculations*, ORNL-RSIC-19, March 1968, pp. 85-94.
3. G. I. Bell, S. Glasstone, *Nuclear Reactor Theory*, Chapter 6.1 - The Adjoint Function and Its Applications, Van Nostrand Reinhold Company, New York, 1970.

4. W. W. Engle, Jr., *A User's Manual for ANISN, A One-Dimensional Discrete Ordinates Transport Code with Anisotropic Scattering*, K-1643, Union Carbide Corporation, Nuclear Division, June 1973.
5. *BUGLE-80, Coupled 47-Neutron, 20-Gamma-Ray, P3, Cross-Section Library for LWR Shielding Calculations*, DLC-75, R. W. Roussin, ORNL, June 1980.
6. Warkentin, J. K., *Polynomial Coefficients for Dose Buildup in Air*, Radiation Research Associates, Inc., August 15, 1975, RRA-N7511.
7. Hubbell, L. H., *Photon Cross-Sections, Attenuation Coefficients, and Energy Absorption Coefficients from 10 KeV to 100 GeV*, National Bureau of Standards, August 1969, NSRDS-NBS29.
8. *Spacetrans II, Dose Calculations at Detectors at Various Distances from the Surface of a Cylinder*, Neutron Physics Division of Oak Ridge National Laboratory, September 1973, ORNL-TM-2592.
9. ANSI/ANS-6.1.1-1977, *American National Standard-Neutron and Gamma Ray Flux to Dose Rate Factors*, American Nuclear Society, March 17, 1977.
10. Mynatt, F. R., Rhodes, W. A., et al., *The DOT-II Two Dimensional Discrete Ordinates Transport Code*, ORNL-TM-4280.

Table A.4/7.3-2  
 CASTOR X/33 CASK SURFACE NEUTRON LEAKAGES

| Neutron Group | Upper <sup>a</sup> Energy (ev) | Cask Surface<br>Leakage Spectra<br>(n/cm <sup>2</sup> - sec) |          |
|---------------|--------------------------------|--|----------|
|               |                                | Side   | Top      |
| 1             | 1.7E+07                        | 2.10E-03   | 2.41E-04 |
| 2             | 1.4E+07                        | 5.84E-03   | 6.70E-04 |
| 3             | 1.2E+07                        | 2.85E-02   | 3.14E-03 |
| 4             | 1.0E+07                        | 5.16E-02   | 4.98E-03 |
| 5             | 8.6E+06                        | 1.13E-01   | 9.65E-03 |
| 6             | 7.4E+06                        | 1.19E-01   | 1.03E-02 |
| 7             | 6.1E+06                        | 2.52E-01   | 2.26E-02 |
| 8             | 5.0E+06                        | 6.41E-01   | 3.83E-02 |
| 9             | 3.7E+06                        | 5.44E-01   | 6.77E-02 |
| 10            | 3.0E+06                        | 6.26E-01   | 9.58E-02 |
| 11            | 2.7E+06                        | 5.62E-01   | 8.58E-02 |
| 12            | 2.5E+06                        | 2.43E-01   | 5.22E-02 |
| 13            | 2.4E+06                        | 5.40E-01   | 1.16E-02 |
| 14            | 2.3E+06                        | 6.85E-01   | 1.31E-01 |
| 15            | 2.2E+06                        | 1.77E+00   | 3.38E-01 |
| 16            | 1.9E+06                        | 1.71E+00   | 4.51E-01 |
| 17            | 1.6E+06                        | 5.16E+00   | 1.51E+00 |
| 18            | 1.4E+06                        | 1.13E+01   | 7.30E+00 |
| 19            | 1.0E+06                        | 1.63E+01   | 1.71E+01 |
| 20            | 8.2E+05                        | 7.08E+00   | 7.44E+01 |
| 21            | 7.4E+05                        | 1.23E+01   | 1.29E+01 |
| 22            | 6.1E+05                        | 2.86E+01   | 6.16E+01 |
| 23            | 5.0E+05                        | 4.63E+01   | 1.27E+02 |
| 24            | 3.7E+05                        | 2.58E+01   | 7.10E+01 |
| 25            | 3.0E+05                        | 4.10E+01   | 1.13E+02 |
| 26            | 1.8E+05                        | 2.58E+01   | 7.10E+01 |
| 27            | 1.1E+05                        | 3.94E+01   | 6.83E+01 |
| 28            | 6.7E+04                        | 2.39E+01   | 4.15E+01 |
| 29            | 5.0E+04                        | 8.27E+00   | 1.43E+01 |
| 30            | 3.2E+04                        | 5.16E+00   | 8.98E+00 |
| 31            | 2.6E+04                        | 1.75E+00   | 3.04E+00 |
| 32            | 2.4E+04                        | 2.04E+00   | 3.54E+00 |
| 33            | 2.2E+04                        | 6.23E+00   | 1.08E+01 |
| 34            | 1.5E+04                        | 7.10E+00   | 1.23E+01 |
| 35            | 7.1E+03                        | 3.41E+00   | 5.91E+00 |

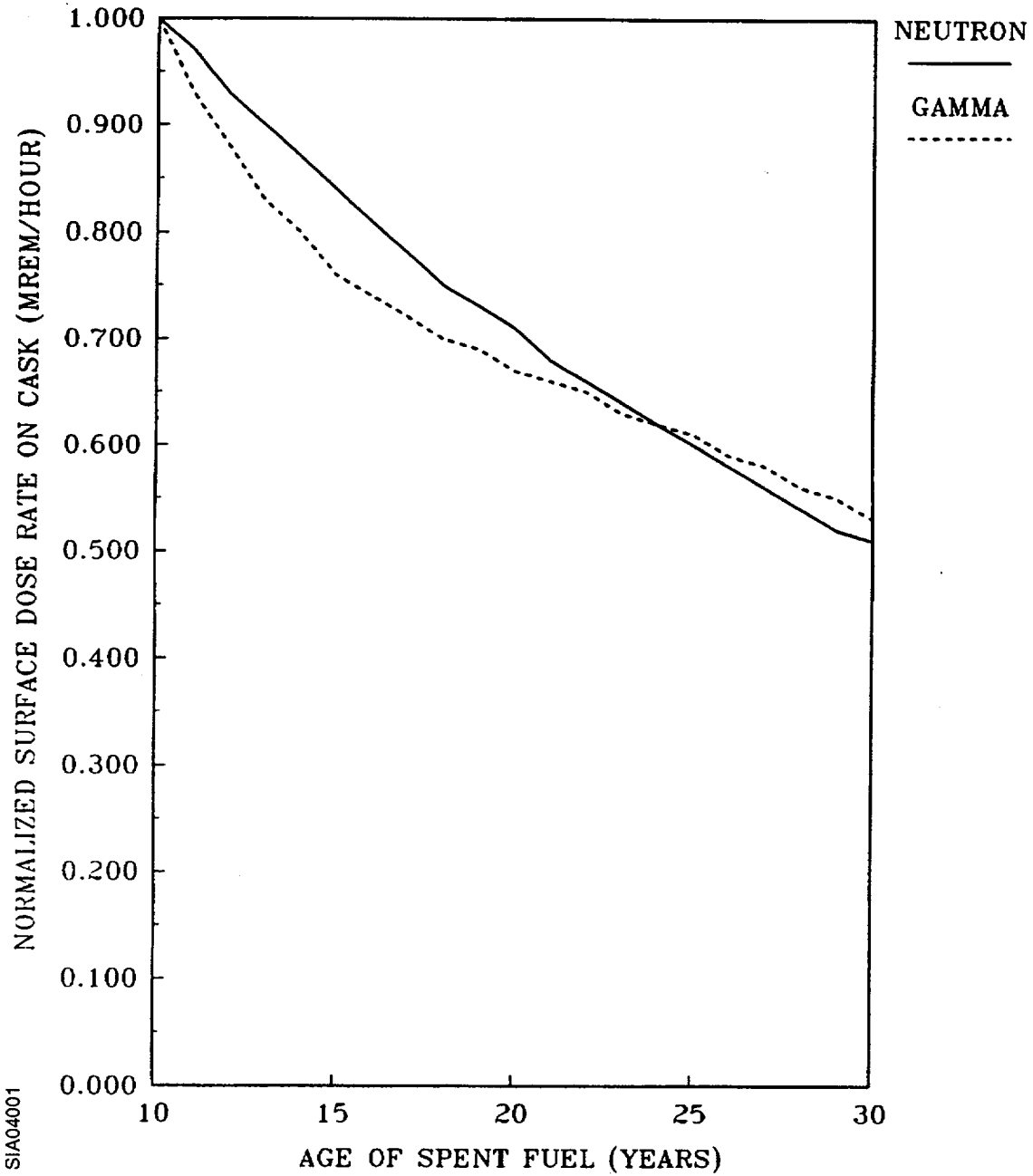
Table A.4/7.3-2  
 CASTOR X/33 CASK SURFACE NEUTRON LEAKAGES

| Neutron Group | Upper <sup>a</sup> Energy (ev) | Cask Surface<br>Leakage Spectra<br>(n/cm <sup>2</sup> - sec) |          |
|---------------|--------------------------------|--|----------|
|               |                                | Side   | Top      |
| 36            | 3.4E+03                        | 1.39E+01   | 1.65E+01 |
| 37            | 1.6E+03                        | 1.55E+01   | 1.63E+01 |
| 38            | 4.5E+02                        | 1.07E+01   | 9.05E+00 |
| 39            | 2.1E+02                        | 5.14E+00   | 4.31E+00 |
| 40            | 1.0E+02                        | 1.53E+01   | 9.38E+00 |
| 41            | 3.7E+01                        | 1.01E+01   | 5.96E+00 |
| 42            | 1.1E+01                        | 1.33E+01   | 6.40E+00 |
| 43            | 5.0E+00                        | 6.16E+00   | 2.30E+00 |
| 44            | 1.8E+00                        | 5.38E+00   | 1.61E+00 |
| 45            | 8.8E-01                        | 3.01E+00   | 7.10E-01 |
| 46            | 4.1E-01                        | 8.27E-01   | 1.33E-02 |
| 47            | 1.0E-01                        | 2.37E-01   | 3.80E-02 |

Note: CASTOR X/33 Cask Surface Area: 360,549 cm<sup>2</sup> (side),  
 44,676 cm<sup>2</sup> (top).

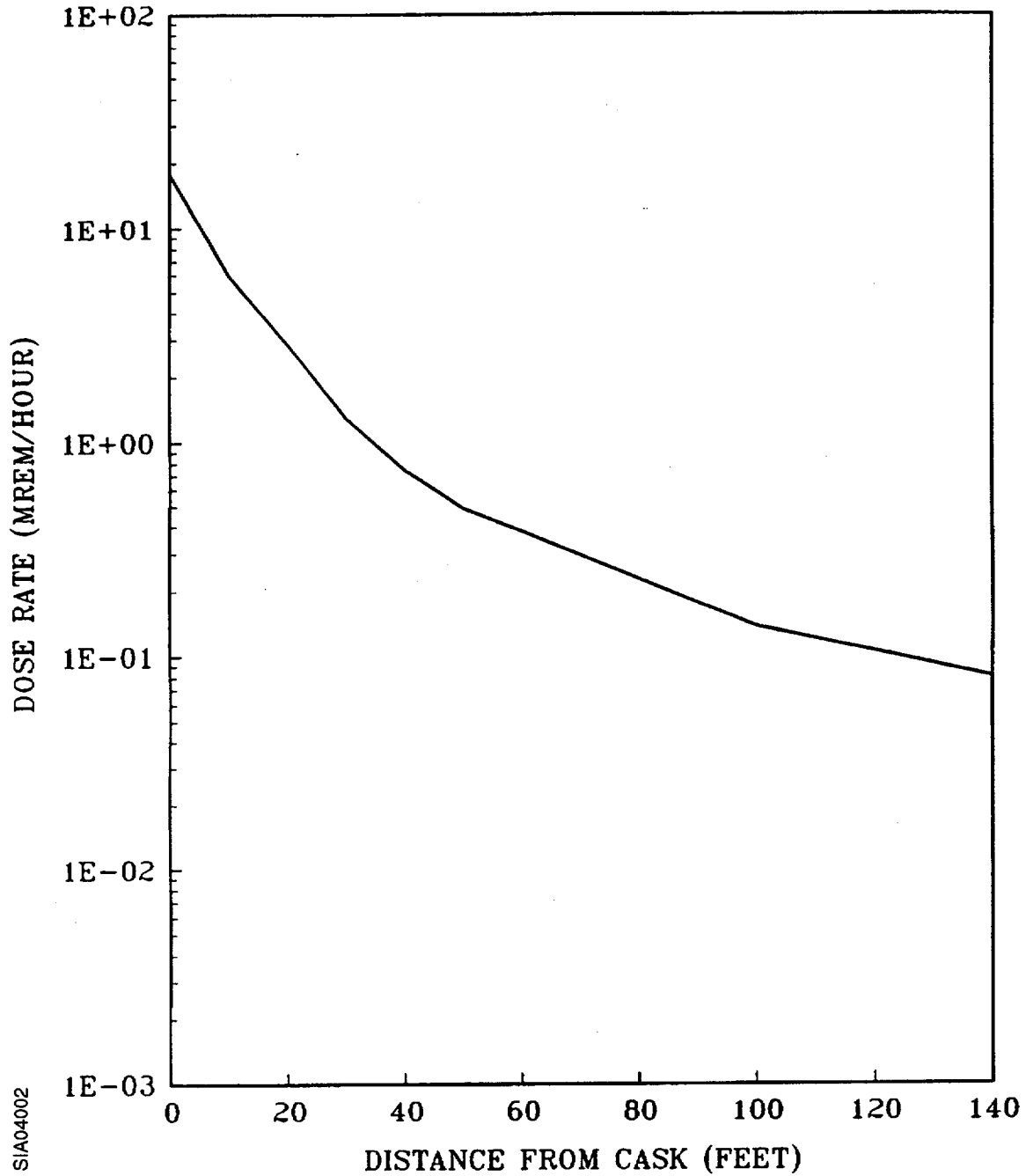
a. Reference 5.

Figure A.4/7.3-2  
NORMALIZED SURFACE DOSE RATE ON  
GNSI CASTOR X/33 CASK  
VERSUS AGE OF SPENT FUEL



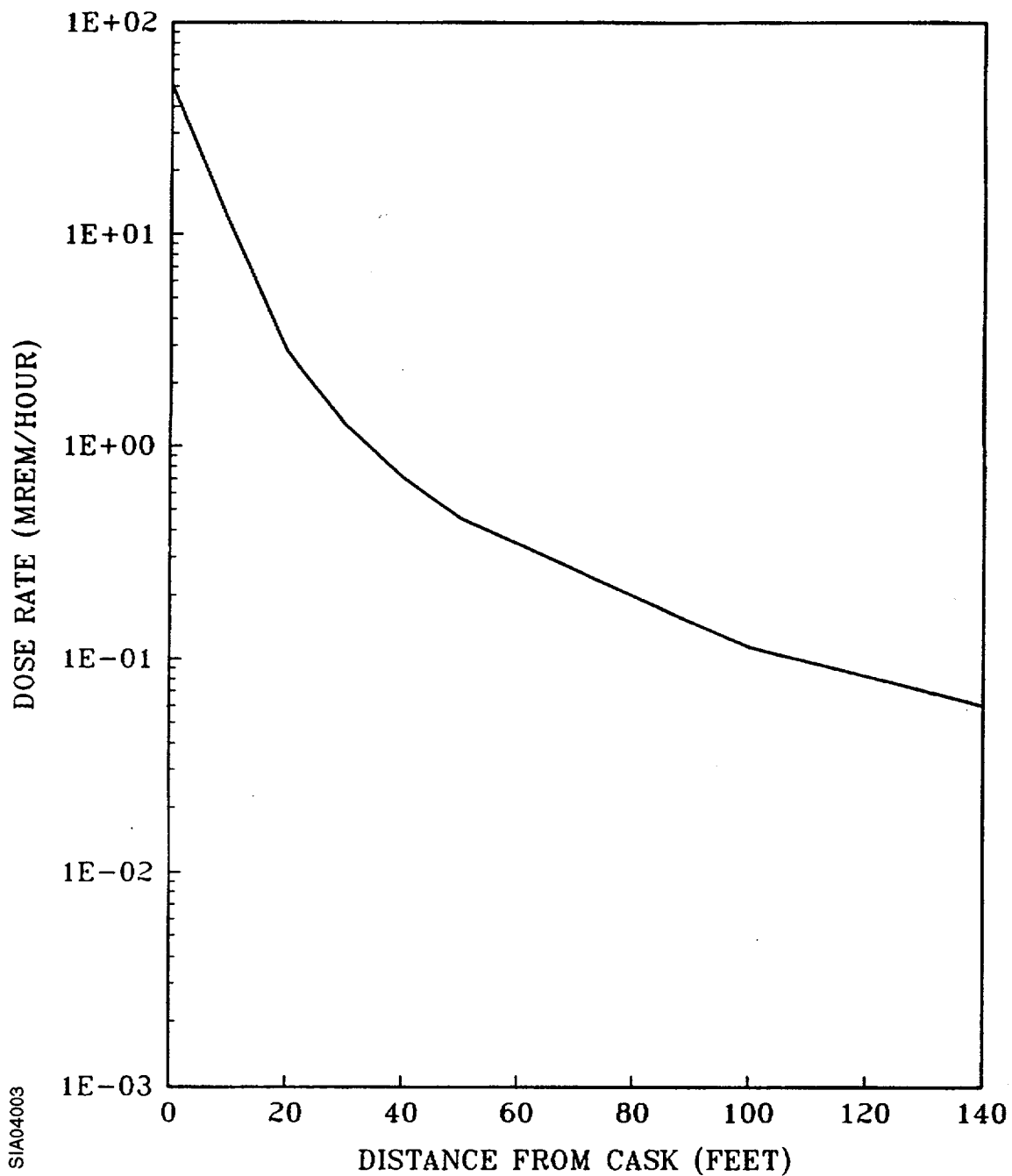
SIA04001

Figure A.4/7.3-3a  
GNSI CASTOR X/33  
NEUTRON DOSE RATE FROM ONE CASK  
VERSUS DISTANCE  
(0-140 FEET)



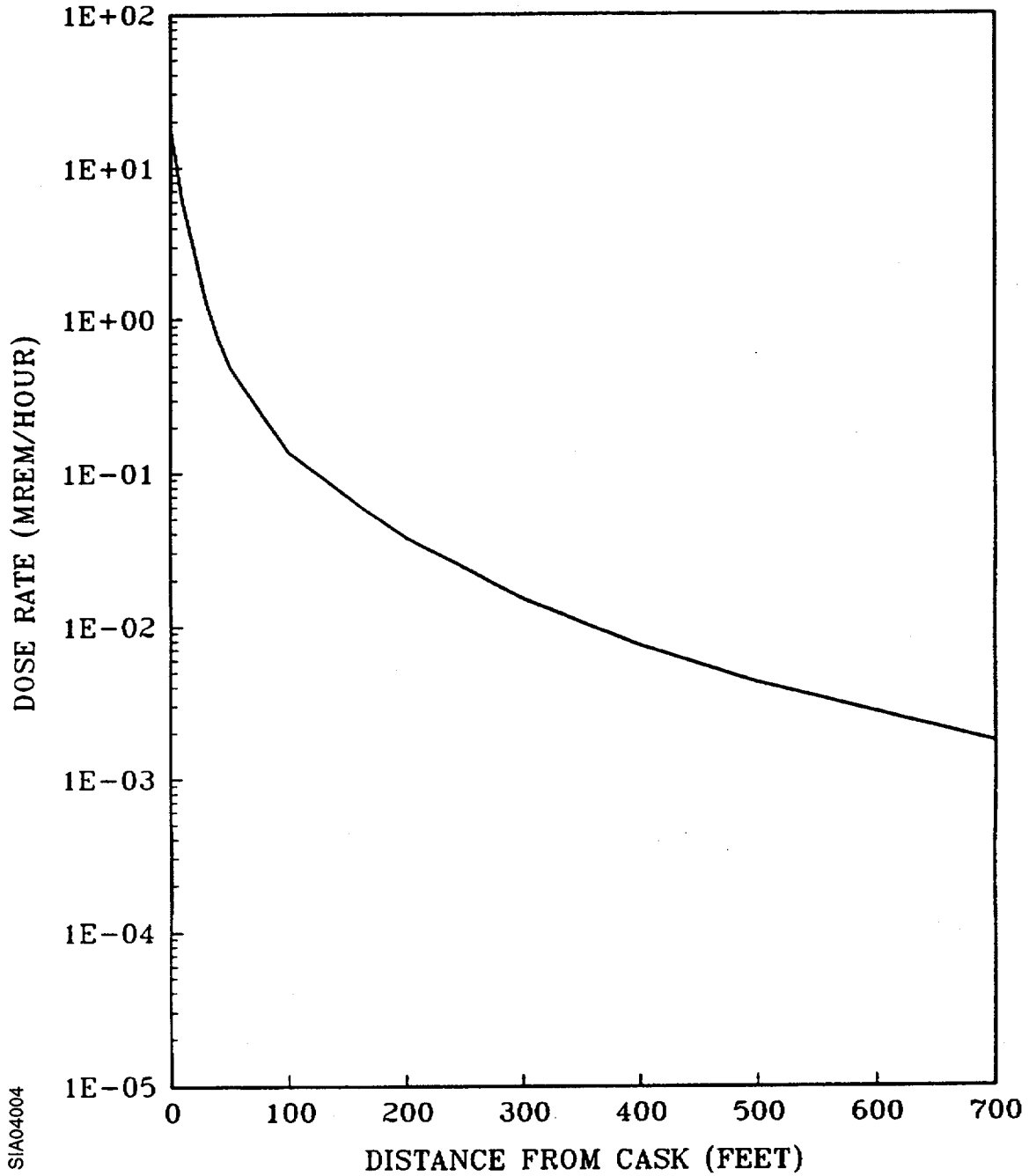
S/A04002

Figure A.4/7.3-3b  
GNSI CASTOR X/33  
GAMMA DOSE RATE FROM ONE CASK  
VERSUS DISTANCE  
(0-140 FEET)



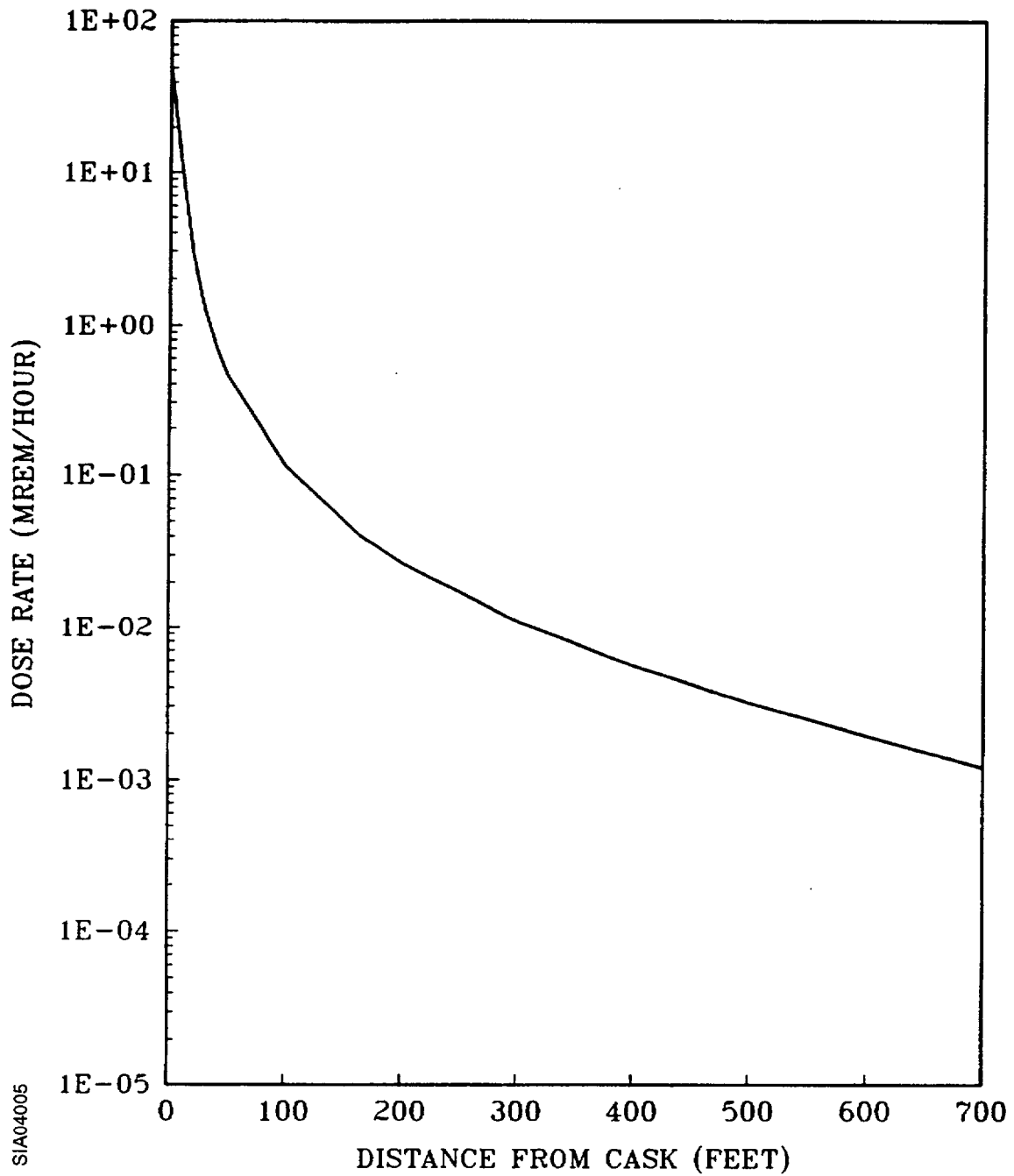
SIA04003

Figure A.4/7.3-4a  
GNSI CASTOR X/33  
NEUTRON DOSE RATE FROM ONE CASK  
VERSUS DISTANCE  
(0-700 FEET)



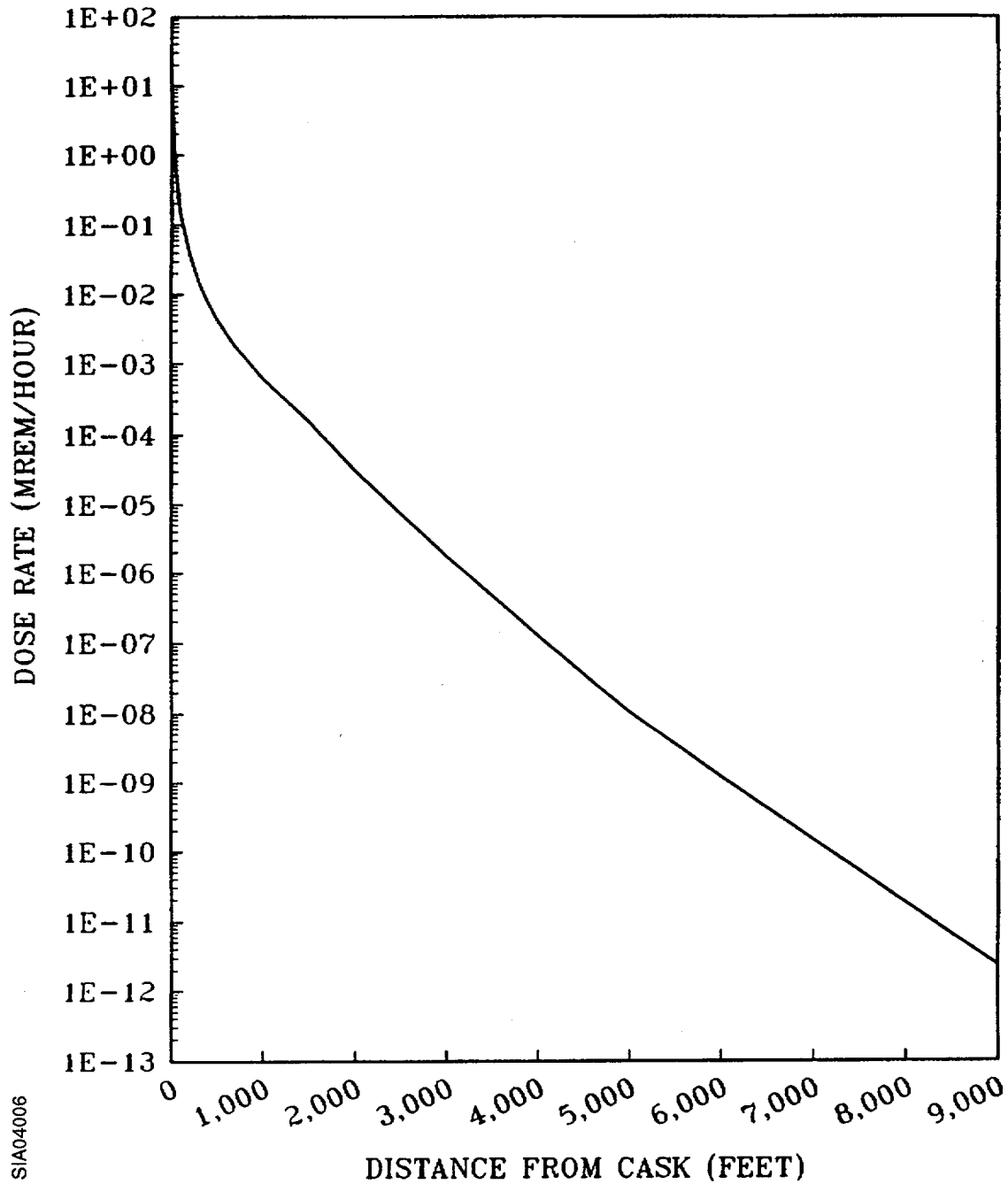
SIA04004

Figure A.4/7.3-4b  
GNSI CASTOR X/33  
GAMMA DOSE RATE FROM ONE CASK  
VERSUS DISTANCE  
(0-700 FEET)



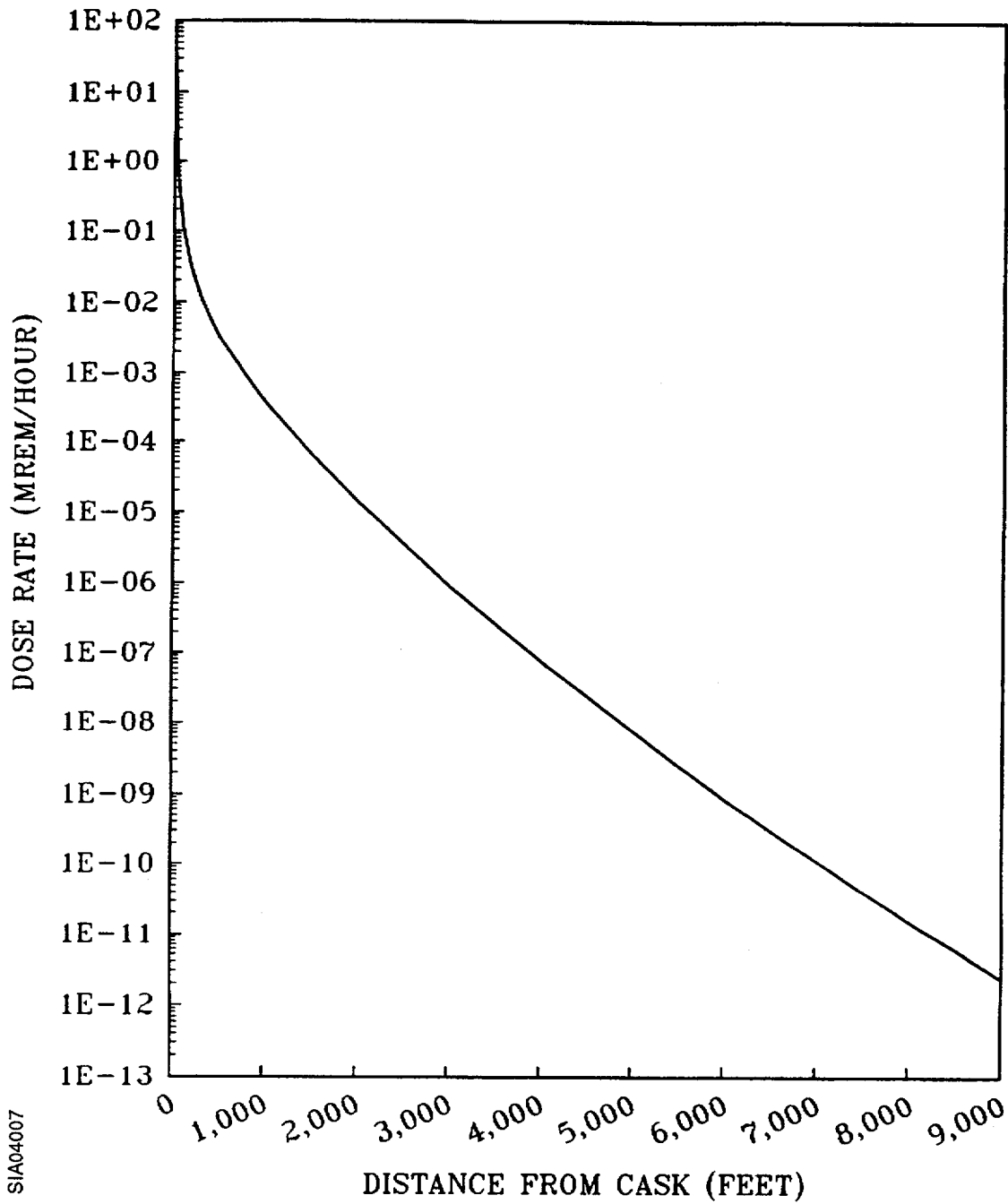
SIA04005

Figure A.4/7.3-5a  
GNSI CASTOR X/33  
NEUTRON DOSE RATE FROM ONE CASK  
VERSUS DISTANCE  
(0-9000 FEET)



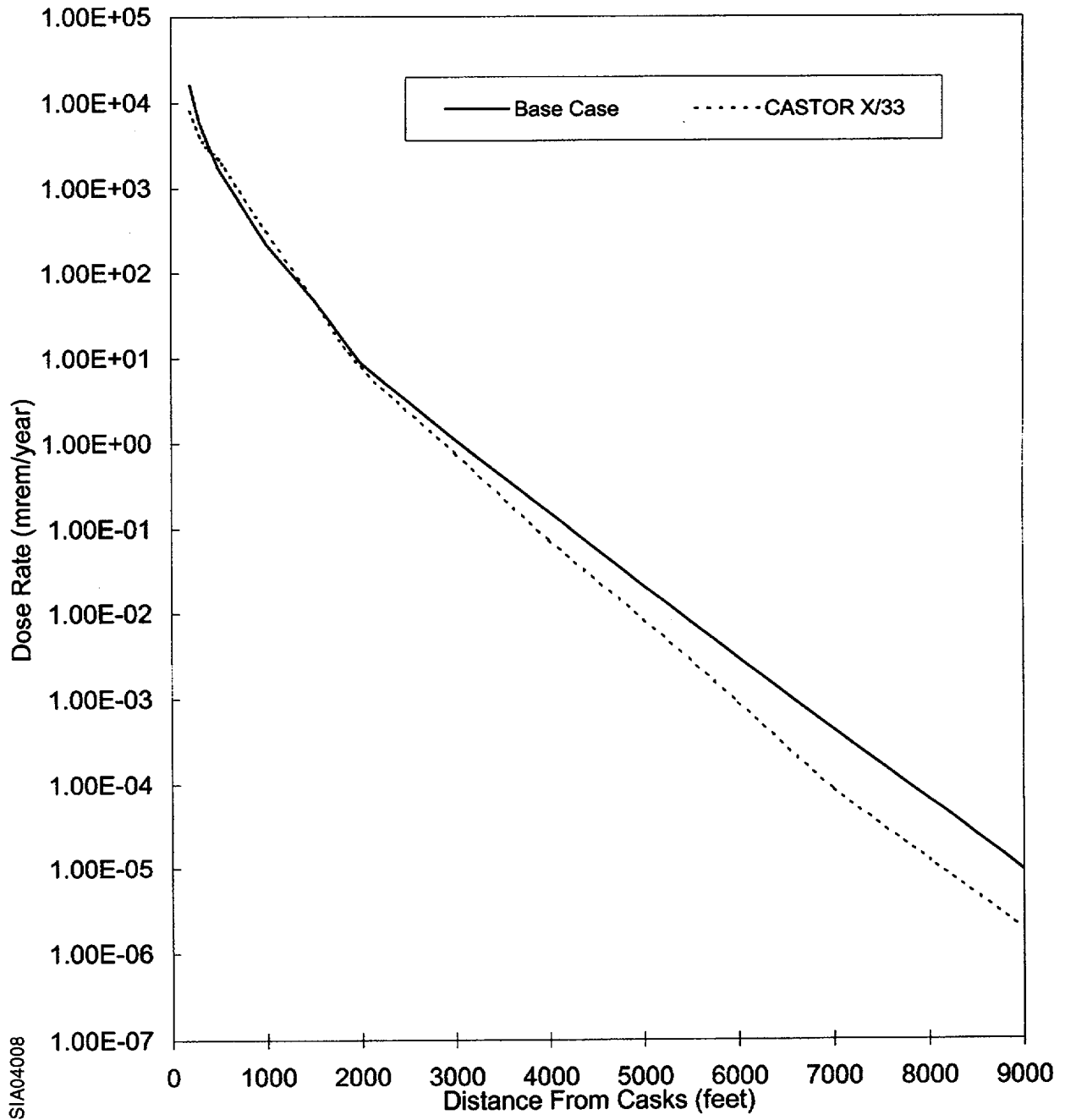
SIA04006

Figure A.4/7.3-5b  
GNSI CASTOR X/33  
GAMMA DOSE RATE FROM ONE CASK  
VERSUS DISTANCE  
(0-9000 FEET)



SIA04007

Figure A.4/7.3-6  
DOSE RATE FOR 54 CASTOR X/33 CASKS  
VERSUS DISTANCE COMPARED TO ISFSI BASE CASE DOSE RATE  
VERSUS DISTANCE



**A.4/8.2.2 Extreme Wind**

The effects and consequences of extreme winds on the GNSI CASTOR X/33 cask are presented in Section 8.2.1.2.1 of the GNSI Topical Safety Analysis Report. The GNSI analysis demonstrates that extreme winds are not capable of overturning their cask nor of producing leakage from it. Since no radioactivity would be released, no resultant doses would occur.

**A.4/8.2.5 Fire**

The ability of the GNSI CASTOR X/33 cask to withstand postulated fires is presented in Section 8.2.1.2.7 of the GNSI Topical Safety Analysis Report. As concluded in Surry ISFSI SAR Section 8.2.5, no fires other than small electrical fires are credible at the ISFSI slab. Based on the GNSI analyses referenced above, since no radioactivity would be released, no resultant doses would occur.

**A.4/8.2.8 Loss of Neutron Shield**

As discussed in Section 1.2.4 of the GNSI Topical Safety Analysis Report, the neutron absorbing material for the GNSI CASTOR X/33 cask includes polyethylene rods inserted into the cask wall. Thus, no loss of neutron shield is postulated.

*Appendix A.5*  
*TN-32 Cask*

## Appendix A.5 TN-32 CASK

### GENERAL DESCRIPTION

The TN-32 cask is a smooth right circular cylinder of multi-wall construction that is approximately 16.8 feet high, 8.1 feet in diameter and weighs (empty) approximately 91.0 tons. The cask inner shell and containment vessel is a welded, carbon steel cylinder that is 1.5 inches thick and has a sprayed metallic aluminum coating for corrosion protection. Surrounding the outside of the containment vessel wall is a steel gamma shield with a wall thickness of 8.0 inches. The bottom end of the gamma shield has a thickness of 8.75 inches. The cask has a cylindrical cavity which holds a fuel basket designed to accommodate 32 PWR fuel assemblies. The loaded weight of the cask is approximately 115.5 tons. Four trunnions are welded on, two at the top end and two at the bottom end of the body.

During fabrication of the TN-32 cask, the inner containment vessel and the gamma shielding are fit together by a shrink-fit procedure. The gamma shielding is heated so that the inner containment vessel, with the flange attached, can be inserted into the outer gamma shielding vessel. This allows a close fit between the two cylindrical shells for good heat transfer. During the shrink fit operation, a small circumferential gap between the flange of the inner vessel and the gamma shielding forms as the heated gamma shield cools. Prior to welding the flange to the gamma shield, the gap is filled with shims made of one of the materials specified in the TN-32 TSAR for the gamma shield shell.

The cask is sealed with one carbon steel lid bolted to the top flange of the containment vessel. The lid is 10.5 inches thick and is secured to the cask body with 48 bolts. The lid and lid penetration covers are sealed with metallic o-ring seals.

Neutron shielding is provided by a 4.5-inch thick resin compound enclosed in long aluminum boxes that surround the gamma shield. The neutron shield boxes are enclosed by a painted carbon steel shell that is 0.50 inches thick.

In Chapter 1 of the TN-32 Topical Safety Analysis Report (Rev. 9A, 12/96), drawing 1049-70-2, Rev. 2, includes a view of a cask trunnion (item 6). The back side of the trunnion (weld prep) is shown at a 30 degree angle. This angle should actually be shown as 45 to 50 degrees.

Section 3.1.1, Paragraph 3 of the TN-32 Topical Safety Analysis Report (Rev. 9A, 12/96) states that "Other structural and structural attachment welds are examined by the liquid penetrant or the magnetic particle method in accordance with Section V, Article 6 of the ASME Code. Acceptance standards are in accordance with Section III, Subsection NF, Paragraph NF-5350." However, Paragraph NF-5350 only pertains to liquid penetrant inspection. Paragraph NF-5340 pertains to magnetic particle inspection. Section 3.1.1, Paragraph 3 of the TN-32 Topical Safety

Analysis Report (Rev. 9A, 12/96) should read “Other structural and structural attachment welds are examined by the liquid penetrant or the magnetic particle method in accordance with Section V, Article 6 of the ASME Code. Acceptance standards are in accordance with Section III, Subsection NF, Paragraphs NF-5340 and NF-5350.”

In Chapter 5 of the TN-32 Topical Safety Analysis Report (Rev. 9A, 12/96), Table 5.1-2 provides a summary of maximum calculated dose rates which are used to estimate personnel exposure from cask loading activities. In order to provide consistency with the NRC SER, the total (neutron plus gamma) side dose rates under normal conditions at the cask surface and at one meter from the cask surface are rounded up from 86.2 mrem/hr to 90 mrem/hr and from 46 mrem/hr to 50 mrem/hr, respectively. In Chapter 10 of the TN-32 TSAR, Table 10.3-1 provides an estimate of occupational exposures for cask loading, transport and emplacement. The dose rate of 46 mrem/hr used in this table is rounded up to 50 mrem/hr, and the total estimated dose is changed from 3.06 man-rem to 3.3 man-rem. These dose rates and estimated doses remain bounded by ISFSI Technical Specification dose limits and dose estimates for cask loading provided in the ISFSI SAR.

The weld between the aluminum plates separating the fuel storage tubes and the outer aluminum plates at twenty-four locations around the periphery of the fuel basket is shown on TN-32 TSAR drawing 1049-70-6, rev. 3 as a 0.25 inch groove weld. In order to provide consistency with as-built conditions, this weld may alternatively be a 0.25 inch fillet weld.

The weld creating the longitudinal seam of the neutron shield outer shell is shown on TN-32 TSAR drawing 1049-70-2, revision 2 as a full penetration weld. In order to provide improved heat transfer between the outer shell and the neutron shield tubes, this weld may alternatively be a partial penetration weld.

TN-32 TSAR Revision 9A drawing 1049-70-5 specifies that the top of borated aluminum plates in the fuel basket be placed nominally 11.88 inches from the top of the basket assembly. Revision 11 of the TN-32 TSAR, which contains analyses to support loading of fuel with higher burnup and enrichment, specifies that the top of the borated aluminum plates be placed nominally 12.00 inches from the top of the basket assembly. Since Revision 9A is the TN-32 TSAR of record for the Surry ISFSI, the dimensions must be reconciled in order to facilitate future loading of TN-32 casks with Surry fuel of higher burnup and enrichment. Therefore, the nominal dimension may be either 11.88 inches or 12.00 inches without any impact to cask criticality evaluations.

Structural analyses for Missile Types B and C contained in sections 2.2.1.3.1 and 2.2.1.3.3 of the TN-32 TSAR include the protective cover. Transnuclear has revised those analyses and the protective cover is no longer used in the model. The revised TSAR pages are included as Attachment 2 to this appendix. The revised analyses conclude that the code allowable stresses on

the lid are not exceeded during a missile impact event. Sections 2.2.1.3.2 and 2.2.1.3.3 in the TN-32 TSAR, Rev. 9A are replaced by the attached sections 2.2.1.3.2 and 2.2.1.3.3.

The lid bolt analysis presented in Appendix 3A.3 of the TN-32 TSAR has been updated to allow for torque in the range of 880 ft-lb to 1230 ft-lb, to incorporate High Purity Loctite N-5000 Antiseize lubricant, and to allow the use of silver-jacketed O-rings. In addition, the summary of bolt stresses presented in Table 3.4-7 of the TN-32 TSAR has been corrected. The updated analysis, figures, and tables are included as Attachment 1 to this appendix. The revised analysis concludes that the code allowable stresses on the bolts are not exceeded for both normal and accident conditions. Pages 3A.3-1 through 3A.3-13, Figures 3A.3-1, 3A.3-2, 3A.3-4, 3A.3-5 and 3A.3-6, and Table 3.4.7 in the TN-32 TSAR Revision 9A are replaced by the attached pages 3A.3-1 through 3A.3-15, Figures 3A.3-1, 3A.3-2, 3A.3-4, 3A.3-5 and 3A.3-6, and Table 3.4.7.

TN-32 TSAR Revision 9A drawing 1049-70-1, drawing 1049-70-4, Figure 1.2-1, and Figure 2.3-1 show that the overpressure system is completely contained under the protective cover. Figure 2.3-1 also shows wiring penetrating the top of the cover and running down the side of the cask. In order to make the pressure switches/transducers more accessible and eliminate the connector at the top of the cover, an alternative design is shown in the revised TSAR pages included as Attachment 3 to this appendix. For this design, the protective cover includes a sealable bolt-on access plate that is both airtight and watertight. The access plate has a through-wall fitting that connects to the OP system on the inside of the protective cover and connects to tubing on the outside of the protective cover. This tubing runs down the side of the cask to an instrumentation box in which the pressure switches/transducers are located. In addition, another connection is located at the access plate which openly communicates to the atmosphere within the protective cover. The external connection to this fitting will connect to tubing that also is mounted along the side of the cask.

Drawings 1049-70-1 and 1049-70-4 of the TN-32 TSAR show the cask with the unmodified protective cover and overpressure switches. The corresponding configuration with modifications is shown in drawing SK-VP-SAR-1 in Attachment 3. Similarly, Figures 1.2-1 and 2.3-1 illustrate the confinement boundary components and pressure monitoring system. The corresponding drawings with modifications are Figures VP1.2-1 and VP2.3-1, respectively, and are contained in Attachment 3. The confinement boundary components shown in Figures 1.2-1 and VP1.2-1 are:

1. Inner shell and bottom closure
2. Flanged and bolted lid
3. Flange
4. Vent cover
5. Drain cover

It should be noted that the confinement boundary components are not changed with the alternative design.

Table 8.1-1 of the TN-32 TSAR describes the sequence of operations associated with the TN-32 cask. For a modified cask, step 13 for installing the protective cover will be performed prior to step 11 for checking the function of the overpressure system transducers or switches. Also, step 11 will not include instructions to check the function of the transducers or switches before the protective cover is installed.

TN-32 casks used at the Surry ISFSI are fabricated to the requirements of the TN-32 Topical Safety Analysis Report (TSAR), Revision 9A or the TN-32 Final Safety Analysis Report (FSAR), Revision 0. TN-32 casks fabricated to the requirements of the TN-32 FSAR, Revision 0 have been evaluated with respect to the design bases for the TN-32 TSAR, Revision 9A, and have been found to be acceptable. Analyses included in the TN-32 FSAR, Revision 0 may not be credited in the use of TN-32 casks unless they have been added to the ISFSI SAR. The analyses in Chapters 4 and 6 of the TN-32 FSAR, Revision 0 have been added to this Appendix A.5.

The only physical difference between TN-32 TSAR, Rev. 9A casks and TN-32 FSAR, Rev. 0 casks is the design of the non-safety related overpressure system. TN-32 TSAR, Rev. 9A casks use an overpressure system with two pressure switches located under the protective cover and wiring through the protective cover that connects to the facility alarm panel. TN-32 FSAR, Rev. 0 casks use tubing through the protective cover to the pressure switches/transducers in a box on the side of the cask near ground level. An evaluation has shown that either overpressure system configuration is acceptable for use at the Surry ISFSI.

The fabrication of TN-32 FSAR, Rev. 0 casks differs in the following two ways from the fabrication of TN-32 TSAR, Rev. 9A casks.

1. The nil ductility transition temperature (NDTT) required for containment material is minus 80°F. The TN-32 TSAR, Rev. 9A cask containment materials have a specified NDTT of no more than minus 40°F.
2. Progressive PT and MT inspections are required of the bottom to gamma shield weld and the lid to lid shield weld. Progressive inspections were not required in the TN-32 TSAR, Rev. 9A.

These two changes provide additional margin in the structural evaluation performed for the TN-32 FSAR, Rev. 0 cask; however, this evaluation is not approved for use at the Surry ISFSI. The TN-32 FSAR, Rev. 0 cask meets the structural design criteria for casks to be used at the Surry ISFSI. The design and fabrication changes described above will be in effect for TN-32 casks number TN-32.32 and higher.

The US NRC has approved the generic use of TN-32 casks by 10 CFR Part 50 licensees. The TN-32 FSAR, Rev. 0 provides the licensing basis for this use and includes Technical Specifications. The Surry ISFSI Technical Specifications, and the TSAR, Rev. 9A, however, will

govern the use of TN-32 Rev. 0 casks at the Surry ISFSI, except to the extent that specific analyses (e.g., criticality or thermal performance) from the FSAR, Rev. 0 have been added to the ISFSI SAR.

#### **A.5/3.1.1 Materials to be Stored**

The structural evaluations of the TN-32 cask are provided in Chapters 3 and 11 of the Topical Report. These evaluations used a fuel weight of 1533 lb, which bounds all possible combinations of Surry Units 1 and 2 fuel assemblers containing a burnable poison rod assembly (BPRA) or thimble plugging device (TPD).

An evaluation has also been performed on the effect to the cask surface dose rates as a result of placing BPRAs or TPDs in the fuel stored in the TN-32. This evaluation confirmed that the calculated surface dose rates for the TN-32 remained less than the design basis dose rates used to calculate doses at the ISFSI perimeter and to the nearest resident.

An evaluation has been performed on the effect on criticality control from the storage of BPRAs and/or TPDs in the fuel stored in the TN-32. The criticality control analysis in the TN-32 TSAR assumes that water borated to 2000 ppm is present in the cask cavity. This analysis was redone assuming that the borated water in the fuel assembly thimble tubes was replaced with aluminum rods, which have lower neutron cross sections than a fully depleted BPRA. The results show a slight decrease in reactivity. TPDs are short and do not displace water in the thimble tubes, therefore, their use will not affect reactivity.

The TN-32 is designed for a maximum internal pressure under accident conditions, and helium buildup of pre-pressurization in BPRAs will affect this analysis. The confinement analysis for the TN-32 has been reanalyzed for thirty-two 20-finger BPRAs, and this reanalysis shows that the maximum pressure under accident conditions would be 69.4 psig, when the design basis for this cask is 100 psig. The impact of TPDs on the confinement analysis is bounded by the impact of BPRAs.

To account for the additional decay heat from BPRAs and TPDs, fuel assembly decay heat estimates must include an estimate for the decay heat from the actual component in each fuel assembly. Therefore, the combined decay heat from the fuel assembly and its components must be less than the limit for a fuel assembly in the TN-32.

Based on these evaluations, the storage of fuel assemblies with BPRAs or TPDs is acceptable for the TN-32.

#### **A.5/3.1.2 Thermal Evaluation**

Chapter 4 of the TN-32 Final Safety Analysis Report, Revision 0 (Reference 2) includes a thermal evaluation for normal conditions that was based on the following inputs.

1. A maximum heat load of 32.7 kilowatts from 32 fuel assemblies with BPRAs or TPDs, or 1.02 kilowatt/fuel assembly.

2. An ambient temperature range of -30 to 115°F. The temperature range was averaged over 24 hours and a maximum daily averaged ambient temperature of 100°F was used for the maximum cask temperature evaluation.
3. A total solar heat load for a 12-hour period of 1475 Btu/ft<sup>2</sup> for curved surfaces and 2950 Btu/ft<sup>2</sup> for flat surfaces, per 10 CFR 71.71(c). Since the cask has a large thermal inertia, the total insolation was averaged over a 24-hour period.

Using these inputs, the thermal analysis for normal storage concluded that the TN-32 design meets all applicable requirements. The maximum temperature of any confinement structure component was less than 315°F, which has an insignificant effect on the mechanical properties of the confinement materials used. The predicted maximum fuel cladding temperature was 565°F, which is well below the allowable fuel temperature limit of 622°F.

### **Thermal Evaluation - Loading/Unloading Conditions**

All fuel transfer operations occur when the cask is in the spent fuel pool with the cask lid removed. The fuel is always submerged in free-flowing water, permitting heat dissipation. After fuel loading is complete, the cask is removed from the pool, drained and the cavity is dried.

The loading condition evaluated for the TN-32 would be the heatup of the cask before its cavity can be backfilled with helium. This occurs during the vacuum drying operation of the cask cavity. Transient thermal analyses are provided in Reference 2 to predict the heatup time history for the cask components assuming air is in the cask cavity.

The results of the transient thermal analysis for the maximum heat load of 32.7 kw predicted that the fuel cladding reaches a maximum temperature of 935°F, which was well below the loading or unloading temperature limit of 1058°F. Therefore, the duration of the cask drying procedure is not constrained by the fuel cladding temperature limit. However, transient analyses showed that in order to prevent cask component peak temperatures from exceeding their analyzed temperature range, in particular the basket, the time before backfilling the cask with helium must be limited to less than 36 hours for the new design heat load.

Unloading of a cask would require the flooding of the cask prior to the removal of the fuel. A quench analysis of the fuel is provided in Reference 2, and concluded that the total stress on the fuel cladding was below the cladding material's minimum yield stress. In addition, by limiting the water flow rate into the cask and monitoring the pressure of the air/steam outflow mixture, the buildup of steam pressure in the cavity was limited to less than the cask design pressure.

### **Thermal Evaluation - Conclusions**

The thermal design of the TN-32 cask is in compliance with 10 CFR 72 and the applicable design and acceptance criteria have been satisfied. The evaluation of the thermal design provides reasonable assurance that the TN-32 will allow the safe storage of spent fuel for 20 years.

The temperatures determined by the evaluation of the cask systems, structures and components important to safety will remain within their operating temperature ranges, and cask internal pressures under normal conditions were acceptable. The TN-32 cask is designed with a heat removal capability having testability and reliability consistent with its importance to safety.

The TN-32 cask provides adequate heat removal capacity without active cooling systems. Spent fuel cladding will be protected against degradation that leads to significant fuel failures by maintaining the clad temperature below maximum allowable limits and by providing an inert environment in the cask cavity.

#### **A.5/3.3.4 Criticality Evaluation**

Chapter 6 of Reference 2 includes an evaluation of the storage of the Westinghouse 15 x 15 Standard Fuel design. This evaluation is summarized below.

Criticality control in the TN-32 is provided by the basket structural components, which maintain the relative position of the spent fuel assemblies under normal and accident conditions, by the neutron absorbing plates between the basket compartments, and by dissolved boron in the spent fuel pool water.

The contents of a TN-32 cask at the Surry ISFSI will be limited to the Westinghouse 15 x 15 Standard Fuel and Surry Improved Fuel (SIF) designs with a maximum enrichment of 4.05 weight percent U-235. The SIF design envelope has dimensions identical to the Standard Fuel design, but several structural elements are made of different materials. These material differences do not affect the criticality analyses, however, and so the criticality evaluations for these fuel types were equivalent.

The fuel assemblies were evaluated with and without BPRAs. BPRAs were modeled using aluminum rods containing no boron. This displaces the borated water and bounds the effect of depleted BPRAs. The criticality evaluations did not rely on any special loading patterns or special orientation of the fuel assemblies. However, a boron concentration of 2300 ppm in the water used in the cask was assumed in the analysis.

The evaluations assumed that each fuel assembly design contained a certain amount of uranium. In the case of the Westinghouse 15 x 15 Standard Fuel design, this content was 467.1 kgU per fuel assembly.

The criticality evaluations were performed by Transnuclear using the CSAS25 sequence from the SCALE4.3 code system with the SCALE 27-group ENDF/B-IV cross section library. Within this sequence, resonance correction based on the fuel pin cell description was provided by NITAWL using the Nordheim Integral method, and  $k_{\text{eff}}$  was determined by the KENO-Va code. A sufficiently large number of neutron histories were run so that the standard deviation was below 0.0020 for all calculations.

The TN-32 cask was evaluated for a variety of configurations intended to bound normal, off-normal, and accident conditions. The following conditions were evaluated individually.

1. Baseline: Most reactive TN-32 design basis fuel configuration, 100% borated water density. The fuel assemblies are shifted toward the cask vertical axis until the outer pin cells contact the basket compartment wall. This condition bounds all possibilities of fuel assemblies positioned off-center in the compartment.
2. The neutron absorber plates and the active fuel zone are offset by two inches axially. This condition might occur due to fuel design differences in the distance from the bottom of the fuel assembly to the beginning of the active fuel, or due to fuel pins slipping in the spacer grids during handling.
3. The inside dimension of the compartment is increased and decreased by 0.06 inches. All compartments move correspondingly further apart or closer together. This condition bounds the dimensional tolerance on the basket tubes.
4. The width of the neutron poison plate is reduced by 0.06 inches, corresponding to its dimensional tolerance. It is not necessary to evaluate the tolerance in length because it is bounded by the two-inch axial offset condition above.
5. Fresh water is placed in the gap of all fuel rods. Although a fuel rod that develops a cladding breach during reactor operations could be saturated with unborated water at the end of its operating cycle, it is unlikely that the water in the fuel rod would remain unborated after years of storage in borated water.
6. The borated water density is varied, except in the homogenized basket rail/borated water zone, to simulated the reduction in density that might occur during unloading operations.
7. Borated water is drained down to the top of the active fuel, except in the basket rail zone. This was the most reactive configuration expected during loading and unloading operations, because it reduces the boron capture of reflected neutrons.

As expected, reduction of the neutron absorber plate width, reduction of compartment size, borated water drain-down, and inclusion of fresh water in the fuel rod gap all caused a slight increase in  $k_{\text{eff}}$ . The optimal borated water density was found at about 95%.

These conditions were combined for a worst case normal condition, and the borated water density was again varied from 85% to 100%, resulting in a maximum  $k_{\text{eff}} = 0.9264 \pm 0.0009$  at 90% borated water density.

To evaluate accident conditions, the worst case normal model was re-run with a single fuel assembly with enrichment of 5 weight percent U-235, and this fuel assembly was placed in one of the four center basket locations. This case demonstrated compliance with the requirement of 10 CFR 72.124 by combining at least two unlikely, independent, and concurrent changes in the conditions essential to nuclear criticality safety: worst case geometry and accidental loading of a fuel assembly outside the design basis. The result was  $k_{\text{eff}} = 0.9315 \pm 0.0009$ .

#### **A.5/3.3.4.1 Neutron Absorber Tests**

Effective boron-10 content of the borated aluminum fuel basket neutron absorber sheets is verified by neutron transmission testing of coupons taken from each sheet. The transmission through the coupons is compared with transmission through calibrated standards composed of a homogeneous boron compound without other significant neutron absorbers, for example zirconium diboride or titanium diboride. These standards are paired with aluminum shims sized to match the scattering by aluminum in the neutron absorber sheets. The effective boron-10 content of each coupon, minus  $3\sigma$  based on the neutron counting statistics for that coupon, must be  $\geq 10$  mg boron-10/cm<sup>2</sup>.

In the event that a coupon fails the single neutron transmission measurement, four additional measurements may be made on the coupon, and the average of the 5 measurements, less  $3\sigma$  based on the counting statistics, must be  $\geq 10$  mg boron-10/cm<sup>2</sup>.

Macroscopic uniformity of boron-10 distribution is verified by neutron radioscopy or radiography of the coupons. The acceptance criterion is that there be uniform luminance across the coupon. This inspection shall cover the entire coupon.

Normal sampling of coupons for neutron transmission measurements and radiography/radioscopy shall be 100%. Rejection of a given coupon shall result in rejection of the associated sheet. Reduced sampling (50% - every other coupon) may be introduced based upon acceptance of all coupons in the first 25% of the lot. A rejection during reduced inspection will require a return to 100% inspection of the lot. A lot is defined as all the sheets rolled from a single casting.

#### **Criticality Evaluation - Conclusions**

The TN-32 cask is designed to be substantially subcritical under all credible conditions. The criticality design is based on favorable geometry, fixed neutron poisons, and soluble poisons in the spent fuel pool. An appraisal of the fixed neutron poisons has shown that they will remain effective for the 20-year storage period, and there is no credible way to lose them. The analysis and evaluation of the criticality design and performance have demonstrated that the cask will provide for the safe storage of spent fuel for a minimum of 20 years with an adequate margin of safety.

The criticality design features for the TN-32 are in compliance with 10 CFR 72, and the applicable design and acceptance criteria have been satisfied. The evaluation of the criticality design provides reasonable assurance that the TN-32 will allow the safe storage of spent fuel.

#### **A.5/4.2.1 Structural Specifications**

As noted in Section 4.2.1, the concrete pads used to support the casks stored at the Surry ISFSI are approximately three feet thick and are constructed with reinforced concrete with a nominal design concrete compressive strength of 3000 psi at 28 days. In the Safety Evaluation

Report for the TN-32, the NRC stated that it had evaluated the cask drop and tipover analyses in the TN-32 Topical Report and that “cask confinement and spent fuel retrievability from the basket will be assured if the concrete storage pad 1) is not more than 3 feet thick, 2) the concrete strength is not greater than 4000 psi, and 3) the soil modulus of elasticity is not greater than 40 ksi.” The as-built conditions for the second pad at the Surry ISFSI meet these requirements. The 3000 psi nominal design strength for the Surry ISFSI is less than the 4000 psi nominal compressive strength limit. The average measured 28-day climate controlled compressive strength for the second pad is within the range expected for concrete construction in accordance with applicable American Concrete Institute codes and standards for a 4000 psi nominal concrete strength. Therefore, the as-built conditions of the second pad at the Surry ISFSI are acceptable for storage of TN-32 casks.

#### **A.5/4.2.3.3 Codes and Standards**

The TN-32 cask is designed and fabricated in accordance with Section III of the 1992 edition of the ASME Code. Exceptions to the Code are listed in Table A.5/4.2-1.

Changes to Table A.5/4.2-1 or ASME Code exceptions not included in the Table shall be reviewed in accordance with 10 CFR 72.48. This review should demonstrate that:

1. The changes or exceptions would provide an acceptable level of quality and safety, or
2. Compliance with the specified requirements of Section III of the 1992 edition of the ASME Code would result in hardship or unusual difficulty without a compensating increase in the level of quality and safety.

Table A.5/4.2-1  
TN-32 ASME CODE EXCEPTIONS

List of ASME Code Exceptions for TN-32 Dry Storage Cask Confinement Boundary/Gamma Shielding/Basket

The cask confinement boundary is designed in accordance with the 1992 edition of the ASME Code, Section III, Subsection NB. The basket was designed in accordance with the 1992 edition of the ASME Code, Section III, Subsection NF. The gamma shielding, which is primarily for shielding, but also provides structural support to the confinement boundary during drop accidents, was analyzed in accordance with Subsection NB. Inspections of the gamma shielding are performed in accordance with the 1992 edition of the ASME Code as delineated in the TN-32 Topical Safety Analysis Report, Rev. 9A, December 1996 (the TSAR).

| Component                                 | Reference ASME Code/Section | Code Requirement   | Exception, Justification & Compensatory Measures  |
|---|-----------------------------|--|---|
| TN-32 Cask                                | NB-1100                     | Stamping and preparation of reports by Certificate Holder                    | The TN-32 cask is not N stamped, nor is there a code design specification generated. A design criteria document was generated in accordance with TN's QA Program and the design and analysis is provided in the TSAR.   |
| TN-32 Cask                                | NCA-3800                    | Quality Assurance Requirements   | The Quality assurance requirements of NQA-1 or 10 CFR 72 Subpart G are imposed in lieu of NCA-3800 requirements.  |
| Lid Bolts                                 | NB-3232.3                   | Fatigue analysis of bolts  | A fatigue analysis of the bolts is not performed for storage, since the bolts are not subject to significant cyclical loads.  |
| Gamma Shielding                           | NB-1132.2                   | Non-pressure retaining structural attachments shall conform to Subsection NF | The primary function of the gamma shield is shielding, although credit is taken for the gamma shielding in the structural analysis. A surface examination of the welds is performed in accordance with the requirements of Subsection NF.   |
| Pressure test of the confinement boundary | NB-6110                     | All pressure retaining components shall be pressure tested                   | The TN-32 cask is not pressure limited. All confinement welds are fully radiographed. In addition, the gamma shielding supports the confinement boundary under all conditions, so a pressure test of the confinement vessel separately will not simulate actual loading conditions. If the pressure test is performed with the confinement vessel inside the gamma shield, the confinement boundary welds cannot be examined. |

Table A.5/4.2-1  
 TN-32 ASME CODE EXCEPTIONS

| Component                   | Reference ASME Code/Section | Code Requirement                                  | Exception, Justification & Compensatory Measures   |
|-----------------------------|-----------------------------|---|--|
| Confinement Vessel Material | NB-2120                     | Requirement materials to be ASME Class 1 material | <p>Standard Review Plan, NUREG-1536 has accepted the use of either Subsection NB (Class 1) or NC (Class 2 or 3) of the Code for the confinement. SA-203 Gr. D is similar to SA-203 Gr. E, which is a Class 1 material. The chemical content of the two grades are identical, except that Gr. E restricts the carbon to 0.20 max., while Gr. D further restricts the carbon content to 0.17 max. Gr. D is acceptable as a Class 2 material up to 500°F. SA-350, Gr. LF3 is the same material as the SA-203, Gr. D, except in a forged condition. SA-350, Gr. LF3 is a Class 1 material in the 1995 edition of the ASME Code, and a Class 2 material in the 1992 Code.</p> <p>Gr. D was selected because of its ductility, since the higher strength is not required. SA-203 Gr. D has better elongation than Gr. E and due to its lower strength is more likely to have the good fracture toughness at low temperatures.</p> <p>In selecting materials for storage and transport casks, one of the major selection criteria is fracture toughness at low temperatures. SA-203, Gr. D and SA-350 Gr. LF3 were selected on this basis. There is no similar requirement for pressure vessels, as they are used at much higher temperatures. For the SA-203 Gr. D and SA-350, Gr. LF3 materials, the allowable stress was based on <math>S</math>, the allowable stress for Class 2 components. This is conservative, since NB is based on <math>S_m</math>, which is 1/3 the tensile strength, while <math>S</math> is 1/4 the tensile strength. Thus there is additional margin over and above the margin required by the code for Class 1 materials.</p> |

Table A.5/4.2-1  
TN-32 ASME CODE EXCEPTIONS

| Component                       | Reference ASME Code/Section | Code Requirement  | Exception, Justification & Compensatory Measures   |
|---------------------------------|-----------------------------|---|--|
| Weld of Lid Shield Plate to Lid | NB-4335                     | Impact testing of weld and heat affected zone of lid to shield plate  | If two different materials are joined, the fracture toughness requirements of either may be used for the weld metal. There are no fracture toughness requirements on the shield plate, and therefore none are performed on the base metal or the heat affected zones. This weld is not subject to low temperatures, as it is inside the cask cavity. |
| Gamma Shielding                 | NB-2190                     | Material in the component support load path and not performing a pressure retaining function welded to pressure retaining material shall meet the requirements of NF-2000 | The gamma shielding materials were procured to ASTM or ASME material specifications. Material testing is performed in accordance with the applicable specification. Impact testing is not performed on the gamma shielding materials (including welding materials).  |
| Confinement Vessel              | NB-7000                     | Vessels are required to have overpressure protection  | No overpressure protection is provided. Function of confinement vessel is to contain radioactive contents under normal, off normal, and accident conditions of storage. Confinement vessel is designed to withstand maximum internal pressure considering 100% fuel rod failure and maximum accident temperatures.                                   |
| Confinement Vessel              | NB-8000                     | States requirements for nameplates, stamping and reports per NCA-8000   | TN-32 cask to be marked and identified in accordance with 10 CFR 72 requirements. Code stamping is not required. QA data package to be in accordance with Transnuclear approved QA program.  |
| Confinement Vessel material     | NB-2000                     | Requires materials to be supplied by ASME approved material supplier; Quality assurance to meet NCA requirements  | Material will be supplied by Transnuclear approved suppliers with Certified Material Test reports (CMTR) in accordance with NB-2000 requirements. The cask is not code stamped. The quality assurance requirements of NQA-1 or 10 CFR 72 Subpart G may be imposed in lieu of the requirements of NCA-3800.   |

Table A.5/4.2-1  
TN-32 ASME CODE EXCEPTIONS

| Component   | Reference ASME Code/Section | Code Requirement   | Exception, Justification & Compensatory Measures  |
|---|-----------------------------|--|---|
| Corner weld between bottom inner plate to inner shell | NB-5231                     | Full penetration corner welded joints require the fusion zone and the parent metal beneath the attachment surface to be UT inspected after welding | In lieu of the UT inspection, the joint will be examined by RT and either PT or MT methods in accordance with ASME Subsection NB requirements.  |
| Boundary of Jurisdiction                              | NB-1131                     | The design specification shall define the boundary of a component to which another component is attached   | A code design specification was not prepared for the TN-32 cask. A TN design criteria was prepared in accordance with TN's QA program. The containment boundary is specified in Chapter 1 of the TSAR.  |
| PT/MT inspection of plates                            | NB-5130                     | Weld preparations in plates 2 inches and over are required to be surface examined by PT or MT  | The final thickness of the shell is 1.5 inches, and therefore this requirement was not imposed. However, the confinement shells may be made from shells with original thickness greater than 1.5 inches. We interpret the code to mean the final thickness of the pressure vessel. The weld prep on one side of the wall is performed by back gouging after the opposite side is welded. An MT examination of this back gouged surface before welding is performed. A UT examination is performed on the plate material when purchased. This examination is intended to discover indications, both laminar and nonlaminar imperfections. Therefore the UT examination of the plate prior to welding can be expected to reveal any indications or imperfections that exist in the plate. |

Table A.5/4.2-1  
TN-32 ASME CODE EXCEPTIONS

| Component   | Reference ASME Code/Section | Code Requirement  | Exception, Justification & Compensatory Measures   |
|---|-----------------------------|---|--|
| Surface examination after machining                       | NB-4121.3                   | If more than 1/8 inch of material is removed, a surface examination is required of components which have been previously surface examined | The containment flanges and the lids are procured with both a UT and MT examination. More than 1/8 inch of material may be removed during processing, and no additional surface examinations are performed.  |
| Aluminum basket plate and rail, neutron absorber plates   | NF-2120                     | Materials to be ASME Class 1 material   | The aluminum plate strength is not used for structural analysis under normal operating loads nor the 50g accident end drop load. The aluminum plate strength is only assumed to be effective for the short duration dynamic loading from a tipover accident and for secondary thermal stress calculations. 6061-T6 is ASME code material (Class 2 or 3). The strength of the neutron absorber plates are not considered in any analysis. |
| Basket  | NF-4000/<br>NF-5000         | Welding/NDE Inspections   | Basket welding procedures are qualified in accordance with ASME Section IX. Due to this unique nature of these welds, special inspections and tests were developed for these welds.  |
| Components other than the containment boundary and basket | Subsection NB               |   | The code does not apply to components other than the containment boundary and basket. The gamma shielding has been analyzed and inspected in accordance with Subsection NB as defined at the beginning of this table.  |

Table A.5/4.2-1  
TN-32 ASME CODE EXCEPTIONS

| Component | Reference ASME Code/Section | Code Requirement   | Exception, Justification & Compensatory Measures  |
|-----------|-----------------------------|--------------------|---|
| Basket    | NF-3000                     | Allowable Stresses | The ASME Code gives stress values up to 400°F. Stress values above 400°F are taken from "Aluminum Standards and Data," 1990. The allowable stresses used for the aluminum basket plate and rail are based on S, the allowable stress for a Class 2 or 3 component. This is conservative, since the analyses of the basket and rail are performed in accordance with the rules of Subsection NF. Subsection NF allowables are based on $S_m$ which is 1/3 the ultimate strength, while S is 1/4 the ultimate strength. Thus there is additional margin built into the analysis of the basket and rail over and above the margin required by Subsection NF for Class 1 materials. |

### A.5/7.3.2.1 Cask Surface Dose Rates

The TN-32 shielding and dose analyses were based on spent fuel with an initial enrichment of 3.5 weight percent U-235, burnup of 45,000 MWD/MTU and cooling time of 7 years (Reference 2). Using an enrichment lower than the 4.05 weight percent U-235 approved for the TN-32 yields a bounding isotope inventory, and is in accordance with NUREG-1536 and NRC Interim Staff Guidance.

Source terms for the fuel were calculated using the SAS2H/ORIGEN-S module of SCALE4.3 as described in Section 5.1 of Reference 2. These source terms are then passed through a SAS2H cask shield model for a 1-dimensional dose assessment. Section 5.2 (Reference 2) describes the source specification and Section 5.3 (Reference 2) describes the shielding analyses performed for the TN-32 cask.

In addition to the spent fuel, the TN-32 is capable of storing BPRAs and TPAs. BPRAs and TPAs with combinations of cumulative exposures and cooling times are permissible for storage in the TN-32 cask. The source evaluation of the BPRAs and TPAs is described in Section 5.2 (Reference 2).

Virginia Power conducted an independent analysis of the TN-32 surface dose rate. This analysis was used to form the basis for the cask surface dose rate limit in the ISFSI Technical Specifications. The surface dose rates calculated for the TN-32 base case cask were 224 mrem/hr (neutron and gamma) for the side surface and 76 mrem/hr (neutron and gamma) for the top surface.

The average side surface dose rate will be determined by averaging dose rate measurements separately, above the radial neutron shield, along the radial neutron shield, and below the neutron shield. Area weighting will be applied in the proportions of 10% for both the average above and below the neutron shield, and 80% for the average along the neutron shield. The average side surface dose rate limit was calculated as follows:

| <u>Location</u>      | <u>Gamma<br/>(mrem/hr)</u> | <u>Neutron<br/>(mrem/hr)</u> | <u>Total<br/>(mrem/hr)</u> | <u>Weight<br/>Factor</u> | <u>Total*Facto<br/>r (mrem/hr)</u> |
|----------------------|----------------------------|------------------------------|----------------------------|--------------------------|------------------------------------|
| Above Neutron Shield | 352                        | 140                          | 492                        | 0.1                      | 49.2                               |
| Along Neutron Shield | 149                        | 20                           | 169                        | 0.8                      | 135.2                              |
| Below Neutron Shield | 191                        | 200                          | 391                        | 0.1                      | 39.1                               |
|                      |                            |                              |                            | <u>Total</u>             | <u>224</u>                         |

Surface gamma and neutron dose rates will be measured separately and separate limits for the average side surface gamma and neutron dose rates were calculated as follows:

| <u>Location</u>      | <u>Gamma<br/>(mrem/hr)</u> | <u>Weight<br/>Factor</u> | <u>Gamma*Factor<br/>(mrem/hr)</u> |
|----------------------|----------------------------|--------------------------|-----------------------------------|
| Above Neutron Shield | 352                        | 0.1                      | 35.2                              |
| Along Neutron Shield | 149                        | 0.8                      | 119.2                             |
| Below Neutron Shield | 191                        | 0.1                      | 19.1                              |
|                      |                            | Total                    | 174                               |

| <u>Location</u>      | <u>Neutron<br/>(mrem/hr)</u> | <u>Weight<br/>Factor</u> | <u>Neutron*Factor<br/>(mrem/hr)</u> |
|----------------------|------------------------------|--------------------------|-------------------------------------|
| Above Neutron Shield | 140                          | 0.1                      | 14.0                                |
| Along Neutron Shield | 20                           | 0.8                      | 16.0                                |
| Below Neutron Shield | 200                          | 0.1                      | 20.0                                |
|                      |                              | Total                    | 50                                  |

The average side gamma dose rate limit (174 mrem/hr) or the average side neutron dose rate limit (50 mrem/hr) may be exceeded as long as the total average side dose rate limit (224 mrem/hr) is not exceeded.

The average top surface dose rate will be determined by averaging nine dose rate measurements from the protective cover. One measurement will be made at the center of the cover, four midway between the center and edge of the cover, and four along the edge of the cover. An area-weighted average will not be used for the top surface dose rate, and separate gamma and neutron surface dose rate limits are not used.

#### **A.5/7.3.2.1.1 Cask Surface Dose Rate Measurement**

Beginning with the issuance of the license amendment to permit the storage of fuel assemblies having an initial enrichment of 4.05 weight percent U-235 and an average fuel assembly burnup of 45,000 MWD/MTU, the following method will be used to determine the average surface dose rates of TN-32 casks to compare with Technical Specifications limits.

##### **Side Surface Dose Rate**

The surface dose rates shall be measured at approximately the following points (see also Figure A.5/7.3-7). Obtain separate measurements for gamma and neutron dose rates.

- a. Above the Radial Neutron Shield (Map location A)

Obtain four measurements, equally spaced circumferentially, midway between the top of the cask body flange and the top of the radial neutron shield. Do not obtain measurements over or in the immediate vicinity of the cask trunnions.

Add the measurements together and divide by the number of measurements obtained in this area. The result is the average dose rate above the neutron shield.

b. Sides of Radial Neutron Shield (Map locations B, C, and D)

Obtain four measurements, equally spaced circumferentially, at each of the following approximate elevations: one sixth, one half and five sixths along the axial span of the radial neutron shield. Do not obtain measurements over or in the immediate vicinity of the cask trunnions.

Add the measurements together and divide by the number of measurements obtained over the neutron shield. The result is the average dose rate over the radial neutron shield.

c. Below Radial Neutron Shield (Map location E)

Obtain four measurements, equally spaced circumferentially, midway between the bottom of the radial neutron shield and the bottom of the cask. Do not obtain measurements over or in the immediate vicinity of the cask trunnions. Also, it may not be possible for a neutron dose rate meter to access the surface at location E. If so, the neutron dose rate meter may be located as much as one foot away from the cask surface to obtain measurements.

Add the measurements together and divide by the number of measurements obtained in this area. The result is the average dose rate below the neutron shield.

### Top Surface Dose Rate

d. Top of Cask (Map locations F, G, and H)

Obtain one measurement at the center of the protective cover (F). Obtain four measurements equally spaced circumferentially half way between the center and the knuckle (G). Obtain four measurements equally spaced circumferentially at the knuckle (H).

Add the measurements together and divide by the number of measurements obtained over the protective cover. The result is the average dose rate over the top surface of the cask.

### Final Average Surface Dose Rate

The average surface gamma and neutron dose rates shall be determined by the following formulae. Note that A, B, C, and D refer to the average values obtained in steps A, B, C, and D above, respectively. The 0.1 and 0.8 multipliers are area weighting factors.

$$\text{Average Side Surface Gamma Dose Rate} = (0.1 \times A_\gamma) + (0.8 \times B_\gamma) + (0.1 \times C_\gamma)$$

$$\text{Average Side Surface Neutron Dose Rate} = (0.1 \times A_n) + (0.8 \times B_n) + (0.1 \times C_n)$$

$$\text{Average Top Surface Gamma Dose Rate} = D_\gamma$$

$$\text{Average Top Surface Neutron Dose Rate} = D_n$$

#### A.5/7.3.2.2 Dose Rate Versus Distance

Analyses were completed to determine dose rates at the ISFSI perimeter fence, the site boundary and the nearest permanent resident. These analyses were performed using the MCNP Monte Carlo transport code and the following conservative inputs.

1. Isotope inventories were based on 32 fuel assemblies with enrichment of 3.5 weight percent U-235, burnup of 45,000 MWD/MTU and seven years decay.
2. The three storage pads were filled with 84 base case TN-32 casks, each pad having 28 casks. This input is conservative, since the first storage pad is filled with CASTOR V/21, CASTOR X/33, MC-10 and NAC-I28 storage casks, all of which have maximum surface dose rates that are lower than the base case TN-32. In addition, using 84 TN-32 casks results in an amount of fuel stored on the pads which exceeds the current licensed limit of 811.44 TeU, providing additional conservatism to the analysis.
3. The analyses assume no decrease in the gamma and neutron emission rates as a result of decay beyond the initial seven-year requirement. That is, all 84 casks were assumed to be placed simultaneously at the ISFSI.
4. The effects of irradiated insert components were included in the MCNP analyses. Each cask was assumed to contain 32 irradiated insert components with the source spectrum and source strength identified in Reference 1.

The MCNP analysis of the dose rate at the ISFSI perimeter fence using base case TN-32 casks resulted in peak dose rates that range from 2.9 to 12.2 mrem/hr when all three pads were full. Dose rate measurements at the ISFSI perimeter fence will be used to ensure that the requirements of 10 CFR 20 are met.

The MCNP analysis for the nearest site boundary indicated that the maximum dose rate at this location was less than 100 mrem/yr, which meets the requirements of 10 CFR 20.1301.

The licensing basis for the annual dose to the nearest permanent resident was based on 84 GNSI CASTOR V/21 casks, adjusted for decay, and air and distance attenuation of neutron and gamma rays. The annual dose to the nearest permanent resident (1.53 miles away) for this case was  $6.0E-05$  mrem, based on Section 2.3 of the NRC's Safety Evaluation Report for the Surry Dry Cask Independent Spent Fuel Storage Installation and Section 6.2 of the NRC's Environmental Assessment Related to the Construction and Operation of the Surry Dry Cask Independent Spent Fuel Storage Installation. The MCNP analysis using 84 base case TN-32 casks resulted in an annual dose to the nearest permanent resident from normal ISFSI operation that is bounded by the ISFSI licensing basis.

**A.5/7.3.5 References**

1. *TN-32 Dry Storage Cask Safety Analysis Report*, Revision 9A, Transnuclear Inc., December 1996.
2. *TN-32 Final Safety Analysis Report*, Revision 0, Transnuclear Inc., January 2000.
3. *SCALE4.3, A Modular Code System for Performing Standardized Computer Analyses for Licensing Evaluation for Workstations and Personal Computers*, CCC-545, Oak Ridge National Laboratory.
4. *MCNP Version P01.3, Monte Carlo N-Particle Transport Code System*, CCC-660, Los Alamos National Laboratory.
5. [Deleted]
6. [Deleted]
7. [Deleted]
8. [Deleted]
9. [Deleted]
10. [Deleted]
11. [Deleted]

Table A.5/7.3-2  
[DELETED]

|

Figure A.5/7.3-2  
[DELETED]

|

Figure A.5/7.3-3  
[DELETED]

|

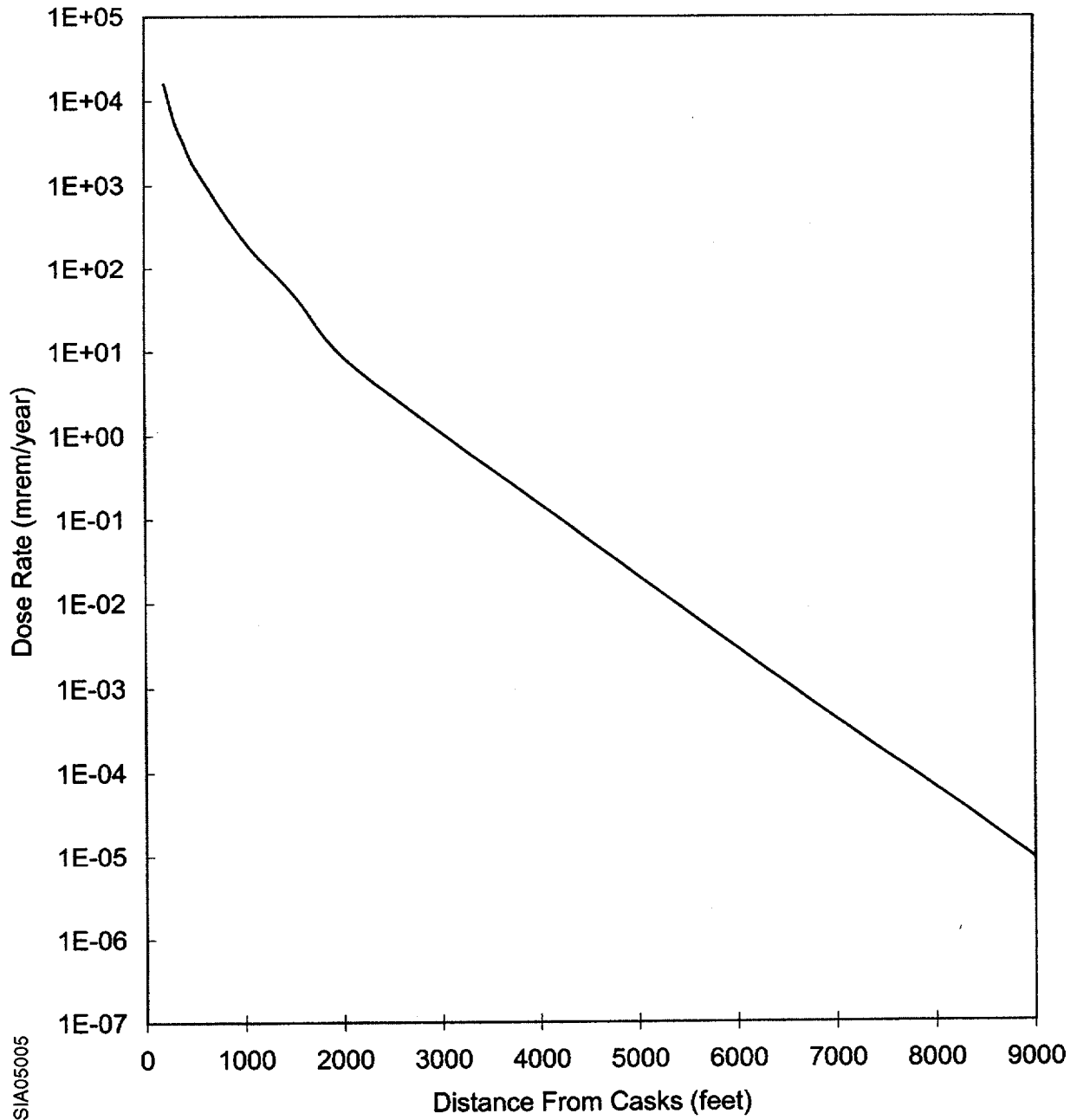
Figure A.5/7.3-4  
[DELETED]

|

Figure A.5/7.3-5  
[DELETED]

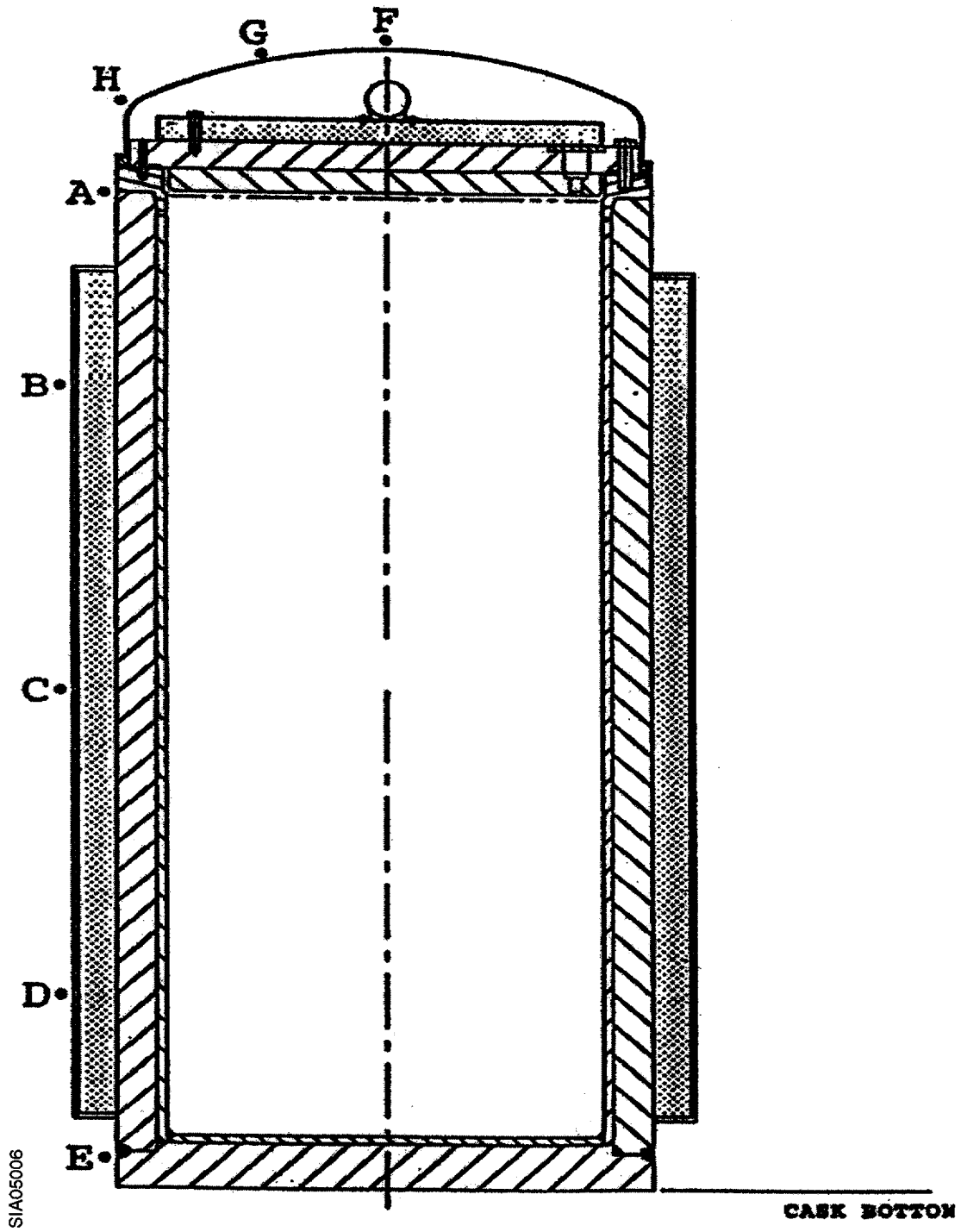
|

Figure A.5/7.3-6  
DOSE RATE FOR 84 BASE CASE TN-32 CASKS VERSUS DISTANCE



SIA05005

Figure A.5/7.3-7  
TN-32 SURFACE DOSE RATE MEASUREMENT LOCATIONS



### **A.5/8.2.2 Extreme Wind**

The effects and consequences of extreme winds on the TN-32 cask are presented in Section 2.2.1 of the TN-32 Topical Report. The Transnuclear analysis demonstrates that extreme winds are not capable of overturning the TN-32 cask nor of producing leakage from it. Since no radioactive material would be released, no resultant doses would occur.

### **A.5/8.2.5 Fire**

The ability of the TN-32 cask to withstand postulated fires is presented in Section 11.2.5 of the TN-32 Topical Report. As concluded in Surry ISFSI SAR Section 8.2.5, no fires other than small electrical fires are credible at the ISFSI slab. Consistent with the Transnuclear analyses referenced above, a total loss of the cask neutron shield due to fire exposure is not a credible event for the Surry ISFSI, nor would radioactive material be released. See Section A.5/8.2.8 below.

### **A.5/8.2.8 Loss of Neutron Shield**

As discussed in Section 1.2 of the TN-32 Topical Report, the TN-32 cask features an outer shell which contains a 4.5-inch thickness of resin material. Section 11.2.5 of the TN-32 Topical Report postulates a loss of this outer neutron shielding due to fire. However, no fires other than small electrical fires are credible at the ISFSI slab, based on Section 8.2.5 of the Surry ISFSI SAR. Therefore, consistent with the Transnuclear evaluation of this event, a total loss of the cask neutron shield due to fire exposure is not a credible event for the Surry ISFSI.

Should the neutron shield be damaged from a postulated fire, cask tipover, or cask drop event, temporary shielding could be placed external to the cask (e.g. high temperature polyethylene sheets or concrete blocks) until the cask shield could be repaired. Depending on the extent of the damage, Section 8.2.10 of the Surry ISFSI SAR outlines the steps that would be taken to return a cask to the spent fuel pool to repair or replace the damaged portion of the neutron shield.

### **A.5/8.2.9 Cask Seal Leakage**

An accident analysis using a TN-32 cask with the fuel limits in Reference 2 was performed based on the requirements of NUREG-1536, NRC Interim Staff Guidance, and the following inputs:

1. Isotope inventories were based on 32 fuel assemblies with an enrichment of 3.3 weight percent U-235, burnup of 45,000 MWD/MTU and seven years decay. This enrichment was selected after reviewing the enrichment and burnup of all Surry spent fuel to ensure that this enrichment is bounding. Using a lower enrichment than that approved for the cask yielded a bounding isotope inventory, and is in accordance with NRC Interim Staff Guidance.
2. The Co-60 source was calculated based on the surface area of a 17 x 17 fuel assembly and a seven-year decay time from discharge. This was a conservative assumption for Surry as a 17 x 17 fuel assembly has a larger surface area than a 15 x 15 fuel assembly does.

3. A cask seal leak rate was calculated in the Reference 2, however, the analysis assumed a leak rate 1.5 times greater to provide additional conservatism.
4. A conservative 500-meter dispersion factor ( $\chi/Q$ ) for accident conditions was used in the analysis.
5. The breathing rate identified in Reference 2 was used in the analysis.
6. The bounding dose conversion factors in EPA Guidance Report No. 11 were used to calculate the whole body, critical organ, and thyroid dose from inhalation.
7. The bounding dose conversion factors in EPA Guidance Report No. 12 were used to calculate the whole body, critical organ, thyroid, and skin dose from immersion.

The isotopes used in the analysis were based on the selection criteria in the NRC Interim Staff Guidance, and included Co-60 in the fuel rod crud, iodine-129, tritium, metastable tellurium-125, fission products that contributed greater than 0.1% of activity, and actinides that contributed greater than 0.01% of activity. The isotope concentrations were used with the release fractions, the free volume in the cavity of the TN-32 cask (5.39 cubic meters), and the cask seal leak rate to calculate the isotope release rate ( $\mu\text{Ci}/\text{sec}$ ) from the cask. The isotope release rate was used over a 30-day period to calculate a release inventory in curies.

Using this release inventory, the bounding dose conversion factors from EPA Guidance Report No. 11, a 500 meter dispersion factor ( $\chi/Q$ ), and the breathing rate, the site boundary inhalation dose for each isotope was calculated. Similarly, using this release inventory, the bounding dose conversion factors from EPA Guidance Report No. 12, and a conservative 500-meter dispersion factor ( $\chi/Q$ ), the site boundary immersion dose for each isotope was calculated.

This accident evaluation resulted in a deep dose plus committed dose equivalent to the worst organ (bone marrow) that is less than the licensing basis of 84 mrem identified in Section 8.2.

## **Appendix A.5**

### **Attachment 1**

#### **Revision of Lid Bolt Analysis**

**Supplants the Analyses in TN-32 TSAR, Revision 9A, Section 3A.3  
and TN-32 FSAR, Revision 0, Section 3A.3**

**Intentionally Blank**

### 3A.3 Lid Bolt Analyses

The lid bolt analysis presented below is performed using the weight of the TN-32A lid (including top neutron shield) since it is slightly heavier than the standard TN-32 lid assembly (with top neutron shield). The use of either aluminum or silver metallic o-ring seals is discussed in the analysis below. Both are acceptable for use in a TN-32 cask lid system. O-ring parameters from either an aluminum or silver o-ring are used interchangeably in the following analyses, depending on which of the parameters from a particular o-ring provides the more limiting result.

#### 3A.3.1 Normal Conditions

##### 3A.3.1.1 Bolt Preload

The lid is secured to the cask body by forty-eight 1.5-in. diameter bolts. The selected bolt preload is such that the metallic confinement seals are properly compressed and the lid is seated against the flange with sufficient force to resist the maximum cavity internal pressure and any dead weight loads acting to unseat the lid. The maximum corresponding tensile preload stress in the bolts at temperature is 51,930 psi (corresponding to a maximum applied torque during cask loading of 1230 ft-lb. with lubrication) which is less than the stress allowable for the bolt material for Normal (Level A) Conditions. The minimum tensile preload stress in the bolts at temperature is 37,150 psi (corresponding to a minimum applied torque of 880 ft-lb. with lubrication) The load per bolt is:

$$\begin{aligned} \text{Maximum: } F_b &= A_b \times 51,930 \\ &= 1.492 \times 51,930 = 77,480 \text{ lb./bolt} \\ \text{Minimum: } F_b &= A_b \times 37,150 \\ &= 1.492 \times 39,260 = 55,430 \text{ lb./bolt} \end{aligned}$$

Since we have 48 bolts, the maximum total seating force of all 48 bolts is  $48 F_b = 3,719,000$  lb. and the minimum total seating force is 2,661,000 lb.

The force required to seat the metallic O-rings (also referred to as seals), from Reference 1, is a line load of 1399 pounds per inch of seal circumference for aluminum seals, or 2284 pounds per inch of seal circumference for silver seals. The diameter of the outer seal is 72.65 in. and the diameter of the inner seal 71.05 in. The seal seating force is then:

$$F_{\text{seating}} = 1399 \pi (72.65 + 71.05) = 631,570 \text{ lb. (aluminum)}$$

$$F_{\text{seating}} = 2284 \pi(72.65 + 71.05) = 1,031,000 \text{ lb. (silver)}$$

The maximum cask cavity internal pressure is the Design Pressure of 100 psi. The force required to react the pressure load (conservatively assuming the pressure is applied over the outer seal diameter) is:

$$F_{\text{Pressure}} = 100 \left( \frac{\pi}{4} \right) (72.65)^2 = 414,500 \text{ lbs.}$$

The TN-32 cask is always oriented vertical during loading, during transfer to the ISFSI and during storage on the pad. Dead weight of the lid and cask contents does not actually load the lid bolts. In fact the lid weight (and external pressure) helps to seat the lid. However, it is conservative to require that the bolt preload maintain lid seating in any cask orientation. The weights of the lid, fuel and basket are:

|                     |   |            |
|---------------------|---|------------|
| Lid Assembly Weight | = | 14,480 lb. |
| Fuel Weight         | = | 49,060 lb. |
| Basket Weight       | = | 16,900 lb. |
| $W_{\text{Total}}$  | = | 80,440 lb. |

The total of the seal seating force (conservatively assuming silver seals are used), pressure load and dead weight loads is:

|                       |   |               |
|-----------------------|---|---------------|
| $F_{\text{seating}}$  | = | 1,031,000 lb. |
| $F_{\text{pressure}}$ | = | 414,500       |
| $W_{\text{total}}$    | = | 80,440        |
|                       |   | 1,525,940 lb. |

This force is less than the preload stresses achieved for the torque value range of 880 to 1230 ft-lbs. and shows that ample lid seating force is provided under Normal Conditions. Furthermore, the range of preload stresses is well below the limiting value of  $2S_u$  (63,800 psi) for the bolt material at 300°F.

#### 3A.3.1.2 Differential Thermal Expansion

The 48 lid bolts preload the outer rim of the closure lid against the cask body flange. The 1.5 in. diameter bolts are installed through 1.56 in. diameter clearance holes in the 4.50 in. thick lid periphery. Preloading of the bolts against the lid is accomplished by tightening the bolts so that the shank

portions of the bolts within the clearance holes are stretched elastically. The bolt loads will therefore change from the initial installed values if any thermal expansion differences should occur between the lid (through thickness direction) and the bolts.

The bolt material is SA 320 Grade L43 (1 3/4 Ni 3/4 Cr 1/4 Mo). The lid and body flange are both SA 350 Grade LF3 (3 1/2 Ni). The Section III Code Appendices specify the same coefficient of thermal expansion for these materials. The bolts are in intimate contact with the lid and flange and will therefore operate at the same temperature as these components. Therefore there will be no thermal expansion differences between the lid and bolts, and the assembly preload will be maintained under all temperatures.

### 3A.3.1.3 Bolt Torsion

The torque required to preload the bolt is:

$$T = K D_N F_B \quad (\text{Reference 2})$$

Where

$$T_{\max} = 0.127(1.5)(77,480) = 14,760 \text{ in-lb.} = 1,230 \text{ ft-lb.}$$

$$T_{\min} = 0.127(1.5)(55,430) = 10,560 \text{ in-lb.} = 880 \text{ ft-lb.}$$

$$K = \text{Nut Factor} = 0.127 \text{ for N-5000 lubricant (as determined experimentally on a TN-32 cask)}$$

$$A_b = \text{Bolt stress area} = 1.492 \text{ in.}^2$$

$$D_N = \text{Bolt nominal diameter} = 1.5 \text{ in.}$$

$$F_{B\max} = 51,930 \text{ psi preload stress} \times A_b = 77,480 \text{ lb.}$$

$$F_{B\min} = 37,150 \text{ psi preload stress} \times A_b = 55,130 \text{ lb.}$$

The maximum residual torque in the bolt corresponds to the maximum applied torque and is:

$$T_R = 0.5625T = 0.5625 \times 14,760 = 8,303 \text{ in-lb.}$$

The minimum residual torque in the bolt corresponds to the minimum applied torque and is:

$$T_R = 0.5625T = 0.5625 \times 10,560 = 5,940 \text{ in-lb.}$$

The shear stress in the bolt due to the residual torque from the maximum preload given by Reference 3:

$$\tau_{\text{torsion}} = \frac{T_R r}{J}$$

where  $r$  and  $J$  are based on the bolt effective radius for the above stress area.

$r = 0.689$  in. effective bolt radius

$J =$  torsional moment of inertia of threaded bolt

$$J = \frac{\pi r^4}{2} = 0.354 \text{ inch}^4$$

$$\tau_{\text{torsion}} = 8,303(0.689)/0.354 = 16,160 \text{ psi (Torsional Shear Maximum)}$$

$$\tau_{\text{torsion}} = 5,940(0.689)/0.354 = 11,560 \text{ psi (Torsional Shear Minimum)}$$

#### 3A.3.1.4 Bolt Bending

It is assumed that bolt bending does not occur during seating of the lid against the cask body during assembly. The bolts are rotated as they are torqued so any slight relative movements between lid and body flange during preloading will not result in a net offset between the bolt head and tapped flange holes. In addition, since the lid, flange and bolt materials have the same coefficient of thermal expansion and will operate at essentially the same temperature, differential expansion between components will not produce bolt bending.

As internal pressure is applied to the cask cavity, the lid will bulge slightly and its edge will rotate. In addition, the body cylinder radius will increase slightly due to the internal pressure resulting in outward radial movement of the tapped bolt holes in the body flange. Since no net membrane stress is developed in the lid, the lid bolt holes (at the mid surface) will remain at the original location. Rotation of the edge of the lid will, however, produce radial movement of the outer surface of the lid at the bolt head location.

The hoop stress in the cask body cylinder is:

$$S_{\text{hoop}} = \frac{P R_i}{t}$$

Where  $P = 100$  psi Design Pressure  
 $R_i = 34.375$  in. inside radius  
 $T = 9.5$  in. thickness

$$S_{hoop} = \frac{100 \times 34.375}{9.5} = 361.8 \text{ psi}$$

The radial deflection at the bolt circle is:

$$\delta_{b.c.} = R_{bc} \times \frac{S_{hoop}}{E}$$

$R_{bc} = 38.03$  in. bolt circle radius

$$\delta_{b.c.} = \frac{38.03 \times 361.8}{28 \times 10^6} = 0.0004914 \text{ inches outward}$$

When pressure is applied to the lid, the edge rotation can be calculated assuming the lid is simply supported. From Reference 4, Table 24 case 10:

$$\theta = \frac{3W(1-\nu)R^3}{2Et^3}$$

Where

|          |                                      |
|----------|--------------------------------------|
| $\theta$ | = edge rotation, radians             |
| $W$      | = total applied load = 100 psi       |
| $\nu$    | = Poisson's ratio = 0.3              |
| $R$      | = 36.35 in. outer seal radius        |
| $T$      | = 4.5 in. lid thickness              |
| $E$      | = Young's modulus = $28 \times 10^6$ |

$$\theta = \frac{3 \times 100 \times (1-0.3) \times (36.35)^3}{2 \times 28 \times 10^6 \times (4.5)^3} = 0.00198 \text{ radians}$$

Figure 3A.3-1 shows the net movement of the threaded hole and the Point on the lid under the bolt head.

If it is assumed that the bolt head doesn't slide on the lid surface, the head will be forced from position a to a' as the lid deflects. Point a' under the bolt head moves outward 0.00445 in. while the threaded hole moves only 0.0004914 in. outward. The bolt head will be bent laterally by 0.00445 - 0.0004914 in. or 0.00396 in. from the threaded end.

The bending model of the bolt is shown in Figure 3A.3-2. The moment on the bolt is calculated assuming the bolt is

subjected to affect bending with the head and threaded end prevented from rotating. For a cantilevered bolt free to rotate at the head, the bending moment would be reduced by one half. Therefore the assumption of fixed ends is the most conservative and results in the highest stress.

The shear force, P, and bending moment, M, for a beam subjected to offset bending with ends prevented from rotating are:

$$P = \frac{12EI \delta}{L^3}$$

$$M = \frac{6EI \delta}{L^2}$$

Where

- P = lateral load to deflect the bolt distance  $\delta$ , lb.  
 $\delta$  = lateral displacement  
 = 0.00396 in.  
 E = Young's modulus,  $28 \times 10^6$  psi @300°F  
 L = bolt length in bending  
 = 4.625 in. (including tapped hole chamfer)  
 I =  $\pi r^4/4$   
 = 0.177 in.<sup>4</sup> (r=0.689 in. based on stress area of 1.492 in.<sup>2</sup>)

Therefore

$$M_B = \frac{6 \times 28 \times 10^6 \times 0.177 \times 0.00396}{4.625^2}$$

$$= 5,500 \text{ in-lb.}$$

$$P = \frac{12 \times 28 \times 10^6 \times 0.177 \times 0.00396}{4.625^3}$$

$$= 2,380 \text{ lb.}$$

The bending stress in the bolt is

$$\sigma_b = \frac{Mr}{I} = \frac{5,500 \times 0.689}{0.177}$$

$$= 21,430 \text{ psi}$$

The shear stress due to the lateral force is

$$\tau_p = P/A = 2,380/1.492 = 1,595 \text{ psi}$$

### 3A.3.1.5 Combined Stresses

The total shear stress for the maximum preload stress (51,930 psi corresponding to a torque of 1230 ft-lbs.) is then equal to the residual torsional shear stress plus that due to force P.

$$\begin{aligned}\tau_{\text{total}} &= \tau_{\text{torsion}} + \tau_p \\ &= 16,160 + 1,595 \\ &= 17,755 \text{ psi}\end{aligned}$$

The total shear stress for the minimum preload (torque of 880 ft-lbs.) equals:

$$\tau_{\text{total}} = 11,560 + 1,595 = 13,155$$

The average tensile stress is the bolt preload stress:

$$\sigma_{\text{average}} = 51,930 \text{ psi}$$

The maximum tensile stress at two locations in the bolt is the preload stress plus the bending stress.

$$\sigma_{\text{max}} = 51,930 + 21,430 = 73,360 \text{ psi}$$

Therefore, the average combined stress intensity is:

$$\begin{aligned}SI_{\text{average}} &= (\sigma_{\text{average}}^2 + 4 (\tau_{\text{total}})^2)^{1/2} \\ &= (51,930^2 + 4 \times 17,755^2)^{1/2} \\ &= 62,910 \text{ psi (62.9 ksi)} < 2S_m = 63.8 \text{ ksi}\end{aligned}$$

The maximum combined stress intensity is:

$$\begin{aligned}SI_{\text{max.}} &= (\sigma_{\text{max}}^2 + 4 (\tau_{\text{total}})^2)^{1/2} \\ &= (73,360^2 + 4 \times 17,755^2)^{1/2} \\ &= 81,500 \text{ psi} = 81.5 \text{ ksi} < 3S_m = 95.7 \text{ ksi}\end{aligned}$$

For Level A conditions, the average bolt stress is limited to  $2 S_m$  or  $2 \times 31.9 = 63.8$  ksi. The maximum bolt stress is limited to  $3 S_m$  or 95.7 ksi. The analyzed stresses are within

these limits as well as the yield strength of the bolt material (also 95.7 ksi).

### 3A.3.2 Accident Conditions

The lid bolts are analyzed in this section under the loadings selected to bound those for the hypothetical bottom end drop and tipover onto the concrete storage pad.

#### 3A.3.2.1 Bottom End Drop

The bottom end drop from a height of 5 feet onto the concrete storage pad is analyzed in Section 3A.2.3.2. That section indicates that the cask deceleration may reach 42 g. This analysis conservatively examines the effects (if any) of a 50 g quasistatic loading on the lid bolts.

During a bottom end drop, the rim of the lid is forced against the flange of the cask body. The lid is initially seated against the flange by preloading (torquing) the bolts. The bolt preload will not be affected if compressive yielding of the contact bearing area does not occur.

The contact force on the bearing area, conservatively neglecting internal pressure, is the bolt preload force less the seal compression force plus the 50 g inertial force of the lid system. The maximum preload force, from Section 3A.3.1, is 3,719,000 lb. The seal seating force is 631,570 lb. for the aluminum seal and 1,031,000 for the silver seal. The weight of the lid system (weight of lid plus weight of top neutron shield assembly, 11560 + 2960 = 14,480 lbs., the highest weight among TN-32, TN-32A and TN-32B casks) is 14,480 lb.

Therefore, during a 50 g deceleration in the axial direction, and conservatively assuming an aluminum seal is used (i.e., an aluminum seal has a lower seating force compared to the silver seal thus resulting in a greater contact force), the contact force between lid and cask body is:

$$\begin{aligned} F_{\text{contact}} &= F_{\text{Bolt Preload}} - F_{\text{seal seating}} + 50 (W_{\text{lid system}}) \\ &= 3,719,000 - 631,570 + 50(14,480) \\ &= 3,811,000 \text{ lb.} \end{aligned}$$

Figure 3A.3-3 illustrates the bearing interface between lid edge and body flange. The bearing area equals the area within the diameter of the lid raised section (74.0 in.) less the outside of the body chamber (70.22 in.) less the area of the seal groove.

$$A_{\text{bearing}} = \frac{\pi}{4} (74^2 - 72.95^2 + 70.75^2 - 70.22^2) = 180 \text{ in}^2$$

3A.3-8

The bearing stress during impact is then equal to:

$$S_{\text{bearing}} = 3,811,000 / 180 = 21,170 \text{ psi (21.2 ksi)}$$

This contact stress is below the 33.2 ksi yield strength of the lid and flange material at 300°F. The bolt preload will not be affected by the bottom drop. Therefore, this hypothetical accident case will not affect the bolt stresses.

#### 3A.3.2.2 Tipover

The tipover onto the concrete storage pad is analyzed in Appendix 3A.2.3.2 of Revision 9A of the TN-32 TSAR and Appendix 3D.2.5 of Revision 0 of the TN-32 FSAR. The tipover scenario is summarized in Figure 3A.3-4. The peak deceleration occurs at the top of the cask. The deceleration is much less at the center of gravity and essentially zero at the bottom corner pivot point. For this analysis the lateral deceleration at the lid end of the body is conservatively taken as 67g and that at the pivot point is zero.

There are two dynamic loadings acting on the lid tending to push or throw it off of the cask body (i.e. producing tensile forces in the lid bolts). There is a small axial (parallel to cask longitudinal axis) centrifugal inertia load due to the internals acting on the lid and the lid weight itself while the cask is rotating.

For the evaluation of the lid bolts it is assumed herein that the cask impacts on the corner at the lid end. There is no accident condition postulated that would cause greater load on the lid bolts. The cask orientation for the analysis is shown in Figure 3A.3-5. The axis of the cask is 30° from horizontal with the lid down. Note that this orientation is well beyond that predicted in the tipover analyses. If the lateral load,  $G_L$ , is 67g, then the axial load used is  $67 \times \tan 30^\circ$  or 38.7g.

The loads acting on the cask are shown in Figure 3A.3-5. The loads acting on the lid are shown in Figure 3A.3-6. Also shown is the reaction load at the cask interface and the pivot point, O, for analysis of lid rotation. Figure 3A.3-7 shows the lid bolt loads resisting rotation of the lid about pivot point O. The increase in bolt load beyond the preload varies uniformly from pivot point, O, to the bolt farthest from O.

The moment acting on the lid about pivot point, O, due to the inertia load is calculated as follows:

$$M_T = W_I \times 38.7 \times R_T + W_L \times 38.7 \times R_T + W_L \times 67 \times a + P_A \times R_T$$

Where  $M_T$  = Total moment about pivot point, in-lb.

$$W_I = \text{Weight of internals} \\ = 16,900 + 49,060 = 65,960 \text{ lb.}$$

and  $W_L$  = Weight of lid system (including shield plate resin disk), 14,480 lb.

$$P_A = \text{Internal pressure load} \\ = 414,500 \text{ lb.}$$

$$R_T = \text{Distance from center of lid to pivot point} \\ = 39.75 \text{ in.}$$

$$a = \text{Moment arm of lid inertia load, } W_L, \text{ in.} \\ = 2.25 \text{ in. (very conservative since shield weight effect moves CG toward 0)}$$

Therefore:

$$M_T = (65,960 \times 38.7 \times 39.75) + (14,480 \times 38.7 \times 39.75) \\ + (14,480 \times 67 \times 2.25) + (414,500 \times 39.75) \\ = 142.4 \times 10^6 \text{ in-lb.}$$

This moment is resisted by the effect of the preload on the lid bolts. The moment due to preload is calculated as follows:

$$M_p = N \times F_B \times R_T$$

Where

$$M_p = \text{moment due to bolt preload, in-lb.} \\ N = \text{number of bolts, 48} \\ F_B = \text{preload per bolt} \\ = A_b \times \text{preload stress} \\ = \text{stress area bolt} \times \text{preload stress} \\ = 1.492 \text{ in.}^2 \times 51,930 \text{ psi} = 77,480 \text{ lb. with 1230 ft-lbs. torque}$$

$$= 1.492 \text{ in.}^2 \times 37,150 \text{ psi} = 55,430 \text{ lb. with 880 ft-lbs. torque}$$

$R_T$  = distance from center of lid to pivot point, 39.75 in.

Therefore:

$$\begin{aligned} \text{Torque} &= 1230 \text{ ft-lbs.:} \\ M_p &= 48 \times 77,480 \times 39.75 \\ &= 147.8 \times 10^6 \text{ in-lb.} > 142.4 \times 10^6 \text{ in-lb.} \end{aligned}$$

$$\begin{aligned} \text{Torque} &= 880 \text{ ft-lbs.:} \\ M_p &= 48 \times 55,430 \times 39.75 \\ &= 105.8 \times 10^6 \text{ in-lb.} < 142.4 \times 10^6 \text{ in-lb.} \end{aligned}$$

Since the bolt preload moment,  $M_p$ , corresponding to the maximum torque value is higher than the moment due to inertial load,  $M_T$ , there will not be any additional load due to a tipover accident. However, the bolt preload moment corresponding to the minimum torque value is less than the moment due to inertial load. In this case, the inertial moment is partially resisted by the effect of the preload on the bolts. The increase in bolt load beyond the preload due to the inertia g loads created by the difference between  $M_T$  and  $M_p$  which is:

$$\begin{aligned} M_T &= M_T - M_p \\ M_T &= 142.4 \times 10^6 - 105.8 \times 10^6 \\ M_T &= 36.6 \times 10^6 \text{ in-lbs.} \end{aligned}$$

The lid bolts resist the above moment which tends to unseat the lid. The increase in lid bolt load ( $\Delta F_{Bo}$ ) beyond the preload is proportional to the distance from the pivot point O. The additional resisting moment,  $M_R$ , applied by the bolts about point O is obtained from the following expressions. Refer to Figure 3A.3-8 of Revision 9A of the TN-32 TSAR for terminology.

$$\Delta \text{Bolt Force} = \Delta F_{Bo} \times \frac{[R + R \cos(n\theta) + B]}{2R + B}$$

$$\Delta \text{Moment for a given bolt} = \Delta \text{Bolt Force} \times [R + R \cos(n\theta) + B]$$

Therefore, the additional moment,  $M_R$ , can be expressed in general terms as follows:

$$M_R = \frac{\Delta F_{B0} \left[ (2R+B)^2 + B^2 + 2 \sum_{n=1}^{n=23} (R + R \cos(n\Theta) + B)^2 \right]}{(2R+B)}$$

$$R = 39.75 \text{ in.}$$

$$B = 1.72 \text{ in.}$$

$$\Theta = 7.5^\circ$$

Substituting yields:

$$M_R = 1421.7 \times \Delta F_{B0}$$

$$\text{Therefore, } \Delta F_{B0} = 36.6 \times 10^6 / 1421.7 = 25,740 \text{ lb.}$$

The increase in tensile stress in the bolt beyond the preload is

$\Delta F_{B0} / A_B$  where:

$$A_B = \text{bolt area, } 1.492 \text{ in.}^2$$

The increased stress is then:

$$\Delta F_{B0} / A_B = 25,740 / 1.492 = 17,250 \text{ psi.}$$

The total tensile stress in Bolt 0 is  $37,150 + 17,250 = 54,400$  psi. Therefore, the total tensile stress for a bolt subjected to cask tipover is greater for a bolt torqued to 880 ft-lbs. than for a bolt torqued to 1230 ft-lbs. The remainder of this tipover analysis will evaluate both the 880 ft-lbs. torque and the 1230 ft-lbs. torque scenarios.

When the tensile stress is combined with the bolt bending stress due to the lid edge rotation under internal pressure calculated in Section 3A.3.1, the maximum tensile plus bending stress is  $54,450$  psi plus  $21,430$  psi (bending) =  $75,830$  psi and the minimum is  $51,930$  psi +  $21,430$  psi =  $73,360$  psi. The total shear stress due to torquing and lid deformation from Section 3A.3.1.5 is  $17,755$  psi for the 1230 ft-lbs. case and  $13,155$  psi for 880 ft-lbs. The combined stress intensity is then:

The average combined stress intensity is:

$$SI_{\text{average}} = (\sigma_{\text{average}}^2 + 4(\tau_{\text{total}})^2)^{1/2}$$

$$1230 \text{ ft-lbs. torque: } SI_{\text{average}} = (51,930^2 + 4 \times 17,755^2)^{1/2}$$

$$SI_{\text{average}} = 62,910 \text{ psi} < S_y = 95,700 \text{ psi}$$

$$880 \text{ ft-lbs. torque: } SI_{\text{average}} = (54,400^2 + 4 \times 13,155^2)^{1/2}$$

$$SI_{\text{average}} = 60,430 \text{ psi} < S_y = 95,700 \text{ psi}$$

The maximum combined stress intensity is:

$$SI_{\text{max}} = (\sigma_{\text{max}}^2 + 4(\tau_{\text{total}})^2)^{1/2}$$

$$1230 \text{ ft-lbs. torque: } SI_{\text{max}} = (73,360^2 + 4 \times 17,755^2)^{1/2}$$

$$SI_{\text{max}} = 81,500 \text{ psi} < S_u = 113,930 \text{ psi}$$

$$880 \text{ ft-lbs. torque: } SI_{\text{max}} = (75,830^2 + 4 \times 13,155^2)^{1/2}$$

$$SI_{\text{max}} = 80,260 \text{ psi} < S_u = 113,930 \text{ psi}$$

In addition to the above calculations, the lid bolts are evaluated based on the interaction formula from Appendix F of the ASME Code (Reference 5) for tension and shear:

$$\frac{(f_t)^2}{(F_{tb})^2} + \frac{(f_v)^2}{(F_{vb})^2} \leq 1$$

Where:

$f_t$  and  $f_v$  are the applied tensile and shear stresses

$F_{tb}$  = allowable tensile stress, smaller of  $(0.7S_u)$  or  $S_y$  (TSAR Table 3.1-3) =  $0.7 \times 113,930 = 79,750 \text{ psi}$

$F_{vb}$  = allowable shear stress, smaller of  $(0.42S_u)$  or  $0.6S_y$  (SAR Table 3.1-3) =  $0.42 \times 113,930 = 47,850 \text{ psi}$

1230 ft-lbs. torque:

$$\frac{51,930^2}{79,750^2} + \frac{17,755^2}{47,850^2} = 0.56 < 1$$

880 ft-lbs. torque:

$$\frac{54,400^2}{79,750^2} + \frac{13,155^2}{47,850^2} = 0.54 < 1$$

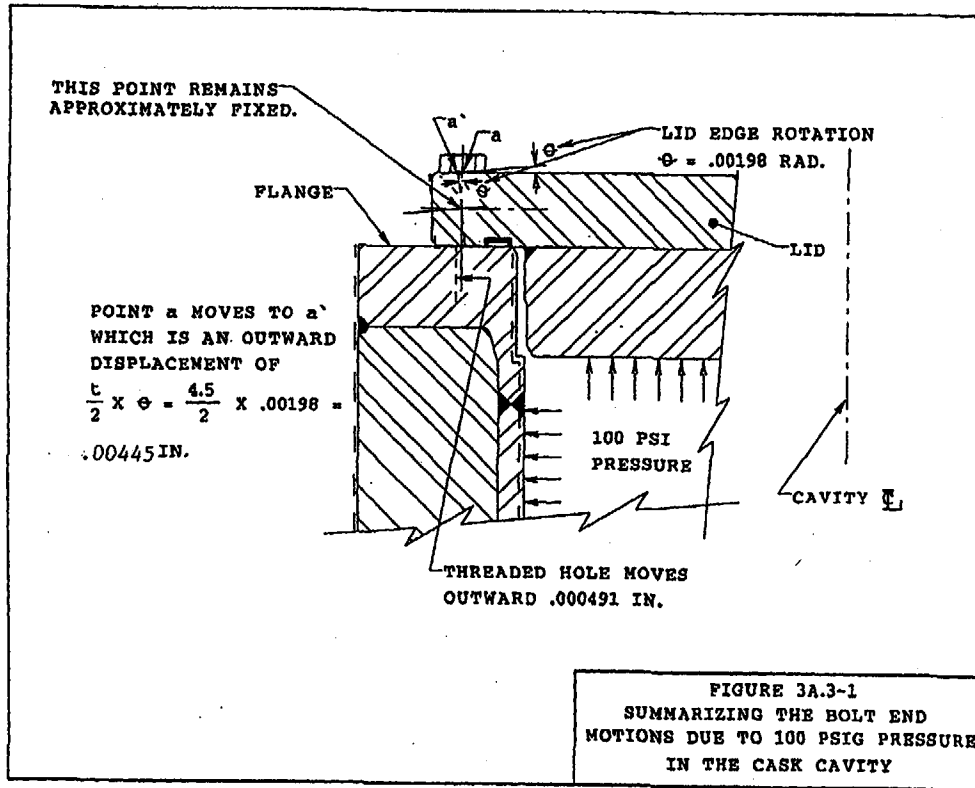
### 3A.3.3 Conclusions

Based on the above evaluation, it is concluded that:

1. The maximum normal and accident condition stresses in the lid bolts are acceptable.
2. A positive (compressive) load is maintained on seals during normal and accident condition loads as bolt preload is higher than the applied loads.

References

1. Resilient Metal Seals and Gaskets, Helicoflex Catalog H.001.002, Helicoflex Co., Boonton, N.J., 1983 pp.5-7.
2. NUREG/CR-6007, Stress Analysis of Closure Bolts for Shipping Casks, April 1992.
3. Hopper, A.G. and Thompson, G.V. "Stress in Preloaded Bolts," Product Engineering, 1964.
4. Roark, R.J.: "Formulas for Stress & Strain", 6th Edition, McGraw-Hill Book Co.
5. American Society of Mechanical Engineers, ASME Boiler and Pressure Vessel Code, Section III, Appendix F, 1992.



REV. 9A 12/96

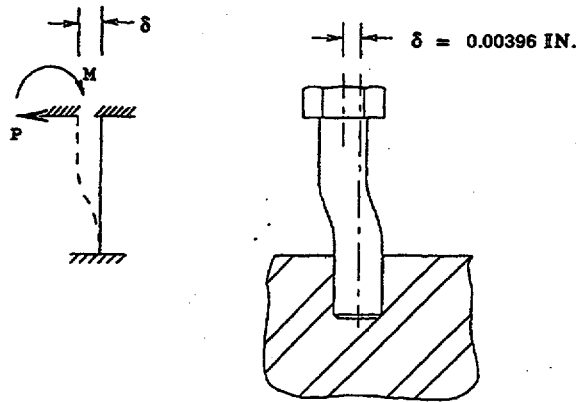
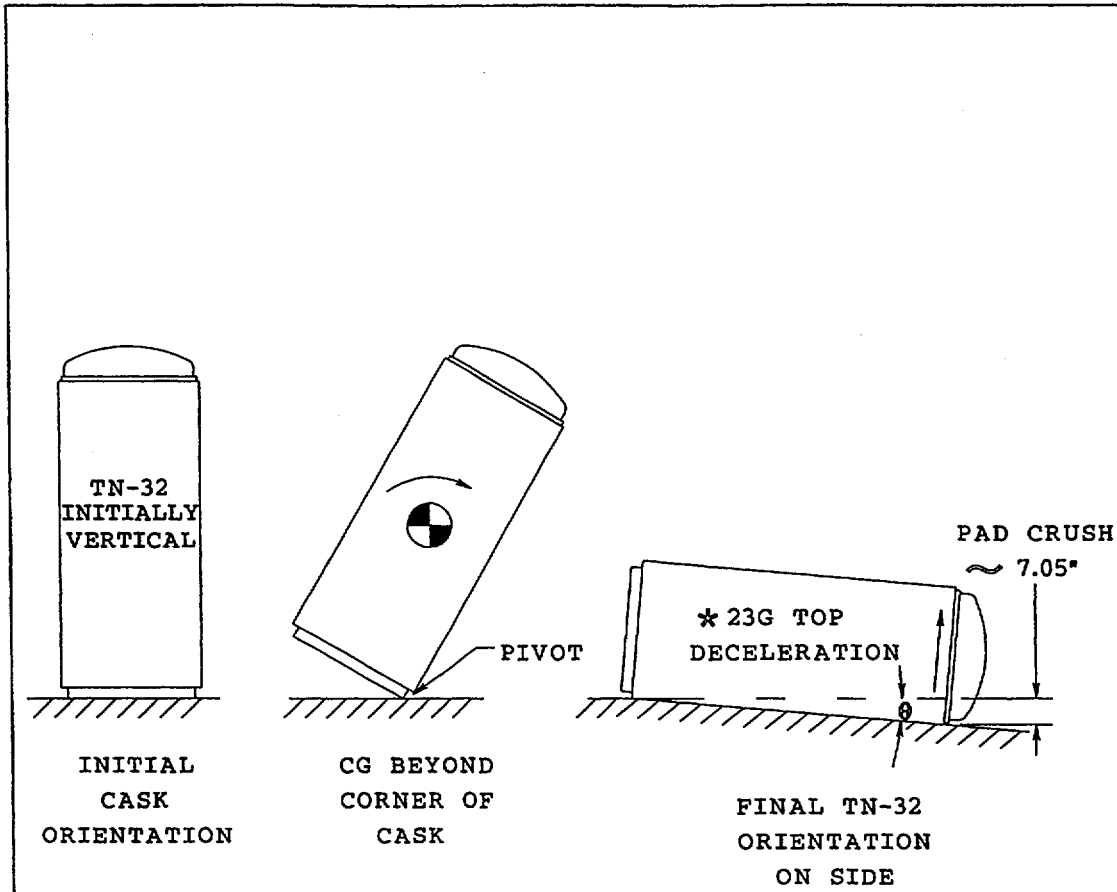


FIGURE 3A.3-2  
LID BOLT BENDING DUE TO LID EDGE  
ROTATION UNDER INTERNAL  
PRESSURE

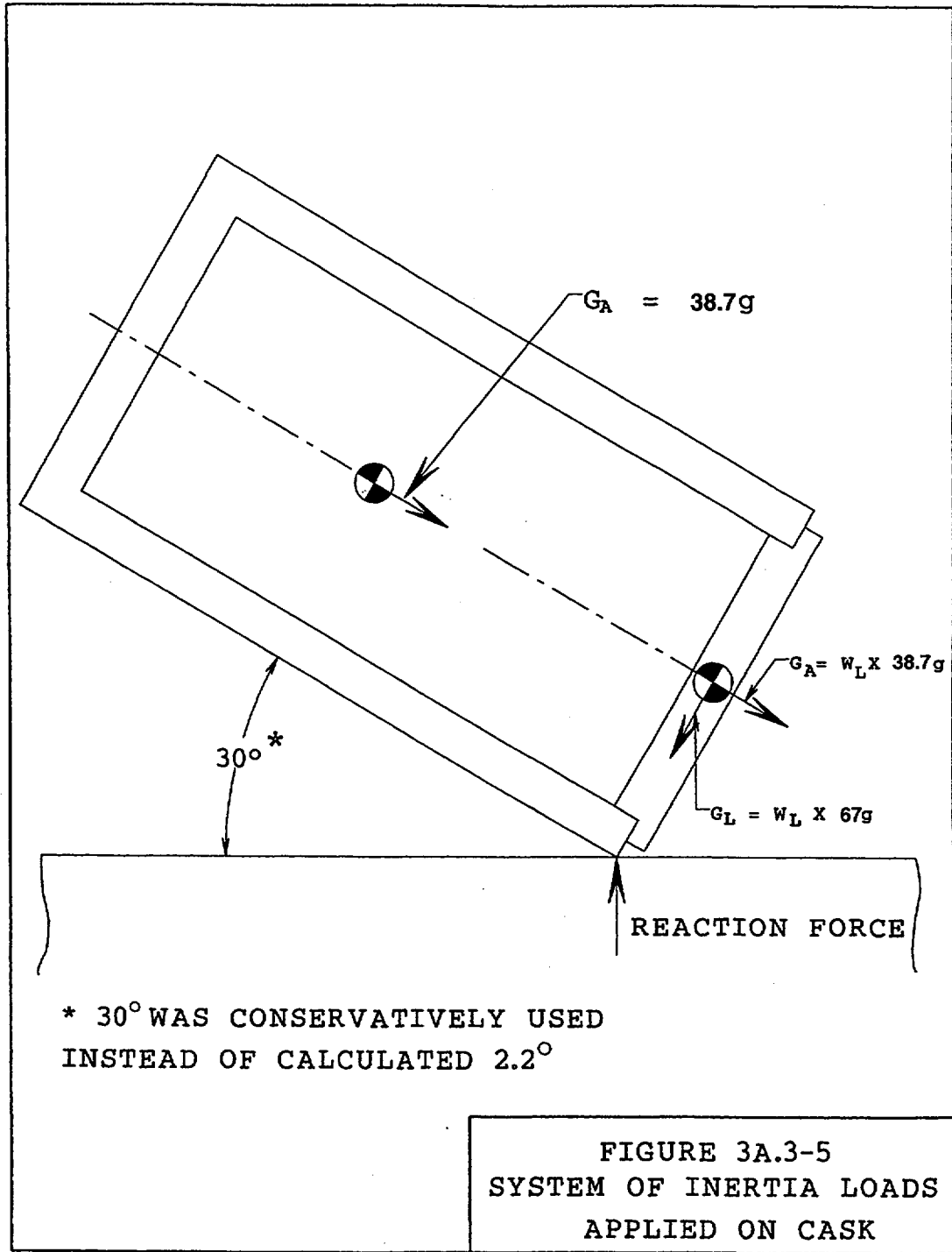
REV. 9A 12/96



$$\theta = \sin^{-1} \frac{7.05}{184} \approx 2.2^\circ$$

\* 67g IS CONSERVATIVELY USED FOR LID BOLT ANALYSIS

FIGURE 3A.3-4  
TIPOVER ONTO CONCRETE  
STORAGE PAD



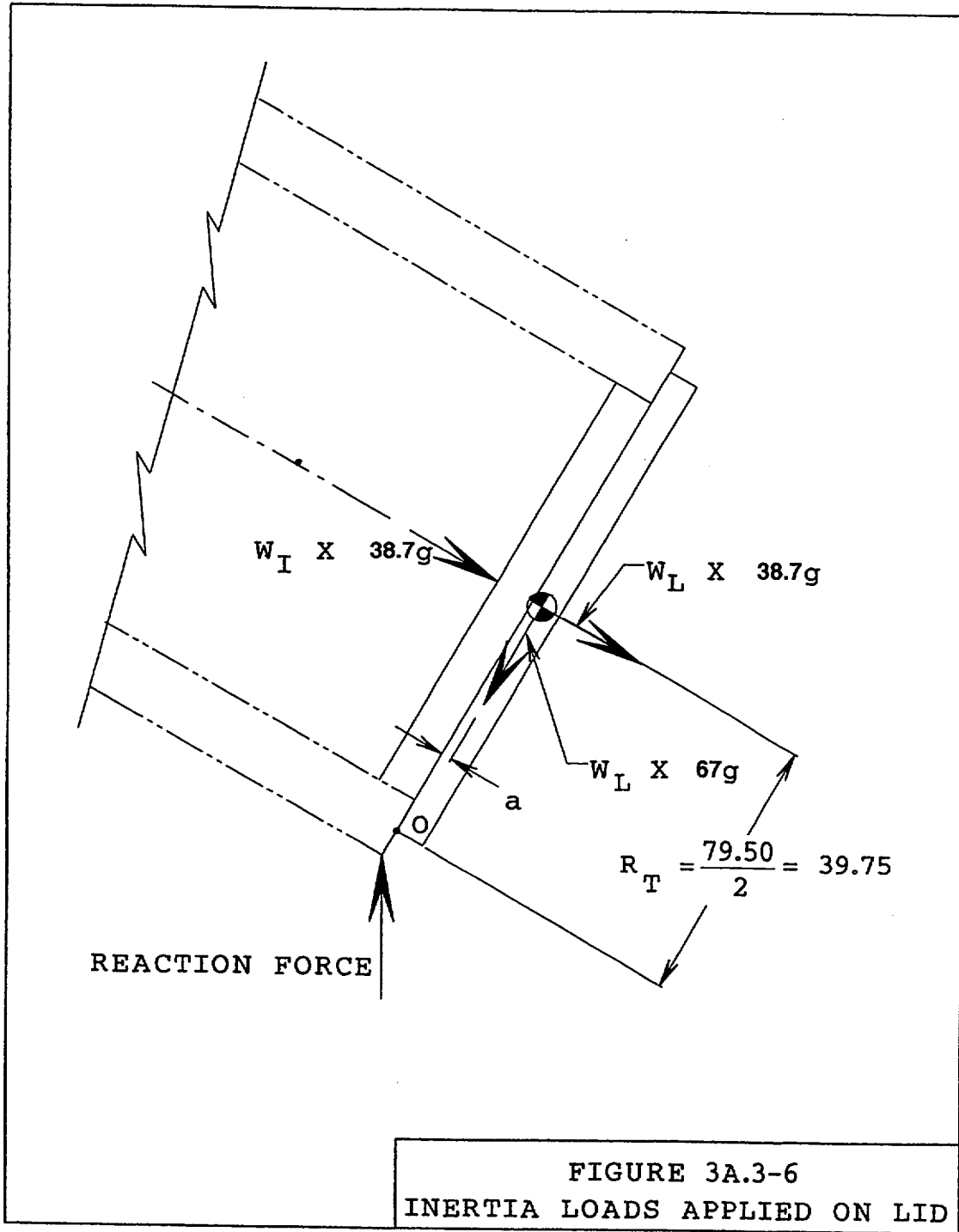


FIGURE 3A.3-6  
INERTIA LOADS APPLIED ON LID

**Table 3.4-7**  
**Summary of Maximum Stress Intensity and Allowable Stress Limits for Lid Bolts**

| <b>STRESS CATEGORY</b> | <b>SERVICE CONDITION</b> | <b>MAXIMUM CALCULATED STRESS (psi)</b> | <b>ALLOWABLE STRESS (psi)</b> | <b>SAFETY FACTOR</b> |
|------------------------|--------------------------|--|-------------------------------|----------------------|
| Tensile                | Level A                  | 51,930                                 | 63,800 ( $2S_m$ )             | 0.23                 |
|                        | Level D                  | 54,440                                 | 79,750 ( $0.7 S_u$ )          | 0.46                 |
| Tensile + Bending      | Level A                  | 73,360                                 | 95,700 ( $3 S_m$ )            | 0.30                 |
|                        | Level D                  | 75,830                                 | 113,930 ( $S_u$ )             | 0.50                 |
| Shear                  | Level A                  | 17,755                                 | 38,280 ( $0.4 S_u$ )          | 1.16                 |
|                        | Level D                  | 17,755                                 | 45,572 ( $0.4 S_u$ )          | 1.57                 |
| Combined S.I.          | Level A                  | 62,910                                 | 95,700 ( $3 S_m$ )            | 0.52                 |
|                        | Level D                  | 81,500                                 | 113,930 ( $S_u$ )             | 0.40                 |

**Intentionally Blank**

**Appendix A.5**

**Attachment 2**

**Revision of Tornado Missile Analysis  
Excerpt from TN-32 TSAR (Rev. 9A, 12/96)**

**Intentionally Blank**

### 2.2.1.3.2 Missile B

Missile B (rigid) partially penetrates the cask wall. The loss in kinetic energy is dissipated as strain energy in the cask wall. The force  $F_b$  developed by an 8 in. diameter missile penetrating the cask body is calculated below. With a yield strength of 31,900 psi at 300°F, used for the gamma shield material:

$$F_b = S_y \left( \frac{\pi}{4} \right) (8)^2 = 1.603 \times 10^6 \text{ lbs.}$$

From conservation of energy:

$$F_b x = \frac{1}{2} m_b v_o^2$$

For a given puncture force  $F_b$ :

$$x = \frac{m_b v_o^2}{2 F_b}$$

where  $x$  is the penetration distance.

The penetration distance is found to be 1.10 in. for a perpendicular impact of the missile.

When the impact angle is not 90 degrees, the missile will rotate during the impact limiting the energy available for penetration (conservatively neglected), since part of the energy will be transformed into rotational kinetic energy.

When hitting the weather protective cover, Missile B deforms the dished head before penetration begins. This will decrease the penetration distance from the above value.

If the missile were to impact the top of the cask in the vertical orientation, the missile velocity would be 88.2 mph (70% of the horizontal impact velocity of 126 mph). The kinetic energy would be:

$$\begin{aligned} \text{KE} &= 0.5 \times (276 \text{ lbs}/32.2 \text{ ft}/\text{sec}^2) \times (88.2 \text{ mph} \times 5280 \text{ ft}/\text{mi}/3600 \text{ sec}/\text{hr})^2 \times 12 \text{ in}/\text{ft} \\ &= 860,440 \text{ in lbs.} \end{aligned}$$

Ignoring the effect of the protective cover and the top neutron shield, the lid bending stresses under a top impact are evaluated. Reference 20 is used to evaluate the stresses for two boundary conditions:

1. Modeling the lid as a simply supported plate.
2. Modeling the lid as a plate with the edges fixed.

For edges simply supported, Table X, Case 2 of Reference 20 is used. The maximum stresses occur at the center, where the plate thickness is  $t = 10.5$  in. The impact force,  $F_b = 1.603 \times 10^6$  lbs.

The maximum stress at the center is calculated below:

$$S_r = S_t = 3W/(2\pi mt^2) \times [m + (m+1)\ln(a/r_o) - (m-1)r_o^2/4a^2]$$

Where  $r_o$  = uniform load radius = missile radius = 4 inches  
 $m = 3.33$   
 $t = 10.5$  inches  
 $a = 38.03$  inches (effective radius for a simply supported lid at the bolt circle)  
 $W = F_b = 1.603 \times 10^6$  lbs.

Therefore,  $S_r = S_t \approx 28.5$  ksi

This is well below the Level D allowable stress of 63,000 psi.

For the second case, with the lid edges fixed, Table X, case 7 of Reference 20 is used.

The maximum stress occurs at the edge, where the plate thickness,  $t = 4.5$  inches.

$$S_r = 3W/(2\pi t^2) (1 - r_o^2/2a^2)$$

Where  $W = F_b = 1.603 \times 10^6$  lbs.  
 $r_o$  = uniform load radius = missile radius = 4 inches  
 $t = 4.5$  inches  
 $a = 38.03$  inches

$S_r \approx 37.0$  ksi.

This is also well below the allowable Level D stress of 63,000 psi.

#### 2.2.1.3.3 Missile C (steel sphere 1" diameter)

The impact of the steel sphere can result in a local dent by penetrating into the cask surface at the yield strength,  $S_y$ , for a penetration depth,  $d$ . The contact area on the cask surface is:

$$A = \pi(2Rd - d^2)$$

Where:

$R$  is the radius of the sphere, 0.5 inches,  
and  $d$  is the penetration depth

The kinetic energy of the steel sphere is dissipated by displacing the cask surface material:

$$KE = \frac{1}{2}(m_c v_o^2) = S_y \int_0^d \pi(2Rd - d^2) \delta_d$$

Where  $m_c$  = sphere mass

$$KE = 0.5(4/3)(\pi)(0.5)^3(0.28)(1/32.2)(126 \times 5280/3600)^2 = 933 \text{ in-lbs}$$

$$S_y \int_0^d \pi(2Rd - d^2) \delta_d = S_y \pi(Rd^2 - d^3/3) = KE = 933 \text{ in-lbs}$$

For a yield strength of 31,900 psi, by trial and error:

$$d = 0.14 \text{ in.}$$

The area,  $A$ , is therefore 0.38 sq. inches. A maximum impact force of  $12.1 \times 10^3$  lb. ( $A \times S_y$ ) will be developed. It can be concluded that only local denting of the cask will result.

If the impact is at the top of the cask (ignoring the protective cover and the neutron shielding), Reference 20, Table X, Case 4 is used to determine the stresses. The impact force is assumed to act at the center of the lid, where  $p = 0$ ,  $r_o = 0.353$  in. and  $a = 38.03$  inches.

The maximum stress is:

$$S_r = S_t = 3W / (2\pi mt^2) \times [m + (m+1)\ln(a/r_o) - (m-1)r_o^2/4a^2] \approx 1.1 \text{ ksi.}$$

Since all penetrations are covered, the steel sphere will have a negligible effect on the cask.

**Intentionally Blank**